SPACE SCIENCES LABORATORY

ELECTRICAL PROPERTIES OF DRY ROCKS

FINAL REPORT NGR-05-003-447

JUNE 1973

PROFESSOR H.F. MORRISON

SPACE SCIENCES LABORATORY SERIES 14 ISSUE 34

UNIVERSITY OF CALIFORNIA, BERKELEY

ELECTRICAL PROPERTIES OF DRY ROCKS

FINAL REPORT NGR-05-003-447

JUNE 1973

PROFESSOR H.F. MORRISON

CONTENTS

CHAPTER 5

ELECTRICAL PROPERTIES OF DRY ROCKS

FINAL REPORT NGR-05-003-447

ABSTRACT

The mechanism by which atmospheric moisture affects the conductivity and dielectric constant of rock specimens is studied in time and frequency domains. It is suggested that adsorbed water molecules alter the surface conductivity in a manner similar to that observed in semiconductors and insulators. Powdered basalts show a low-frequency dispersion produced by the atmospheric moisture remaining in the pore system of the sample in a high vacuum; this effect is attributed to isolated adsorption centers of the type mentioned above.

Simulated lunar permafrost at 100°K and a vacuum of 10^{-8} torr together with data on lunar samples contaminated with atmospheric moisture and the dielectric properties of ice at various temperatures indicate that, if permafrost exists in the moon it should present a relaxation peak at approximately 300 Hz; for temperatures up to 263°K it may go up to 20 KHz.

The response of a lunar powder simulator between 100° and 373°K suggests that the dielectric properties of the uppermost layer of the lunar regolith undergo rapid changes during three tenths of a lunation while remaining approximately constant during the remaining seven tenths.

When a current flows through a rock, interfacial effects arise between adjoining mineral grains of different electrical properties; it is concluded that in order to have electrical steady state conditions in rock samples it is necessary to have volume charge accumulations at interfaces within the sample and at the electrode sample interface. A method for measuring heterogeneous dielectrics with non-negligible ohmic and dielectric conductivities is proposed and experimentally verified.

Evidence of electrical non-linear behavior in some dry resistive rocks is presented, showing the existence of a non-linear region followed by a linear one when the voltage, or current density, is increased. The effect is attributed to interfacial phenomena occurring at electrode-sample interfaces. A warning is made regarding the use of resistivity vs current density plots to decide on non-linear behavior. It is suggested that interfacial phenomena and non-linear effects may be common features in two-and four-electrode systems.

INTRODUCTION

The objective of the proposed study was to analyze the electrical conductivity and dielectric constant of rocks devoid of water, to evaluate the changes induced by atmospheric moisture on such properties, to reduce or avoid electrode contributions to dielectric permittivity measurements and to analyze electrical non-linear behavior in rocks.

This report is divided in five chapters, each one containing its own abstract, conclusions, references, and figures, and dealing with specific aspects of the research items mentioned above. Two chapters consist of reprints of material recently published and the others are either in press or being considered for publication.

Effects of Atmospheric Moisture on Rock Resistivity

ROMÁN ALVAREZ

Engineering Geoscience, University of California, Berkeley
Berkeley, California 94720

The role of water in the electrical resistivity of rocks has long been recognized as an important one This study examines the changes in resistivity of rock samples as induced by atmospheric moisture An analysis of the term dry rock leads to the conclusion that oven drying and evacuation are methods that yield only relative degrees of desiccation To obtain absolute values of the moisture present in a sample, one should probably use nuclear magnetic resonance and mass spectrometry Experiments were performed on samples of hematitic sandstone, pyrite, and galena The sandstone underwent a change in resistivity of 4 orders of magnitude when it was measured in a vacuum of 5×10^{-7} torr and in air of 37% relative humidity Pyrite and galena showed no variations in resistivity when they were measured under the same conditions These results, plus others obtained elsewhere, indicate that rocks of the resistive type are affected in their electrical properties by atmospheric moisture, whereas rocks of the conductive type are not The experimental evidence obtained is difficult to reconcile with a model of aqueous electrolytic conduction on the sample surface, it is instead suggested that adsorbed water molecules alter the surface resistivity in a manner similar to that observed in semiconductors and insulators

Natural state rocks are found in many regions to be saturated with aqueous solutions from the water table down to a depth of 4 or 5 km [*Brace*, 1971]. At greater depths it is still not known how common the pore fluids are in the crustal environment According to *Wyllie* [1971], the same mineral assemblages can exist with and without a pore fluid, thus the possibility of having some aqueous solutions in pores at great depths seems indeed to exist

Above the water table the amount of water present at a given time must be a function of the local rainfall regime and, to some extent, of the atmospheric conditions prevailing at the surface The presence of water in the uppermost crustal layers of the earth alters in various ways the electrical properties of the rocks in such regions

Many studies have been made analyzing from various points of view the influence of water in rock resistivity [*Hill and Milburn*, 1956, *Mandel et al*, 1957, *Keller and Licastro*, 1959, *Worz*, 1964, *Parkhomenko*, 1967, *Scott et al*, 1967, *Brace and Orange*, 1968], although few have dealt directly with atmospheric moisture effects Determining the magnitude of the alteration experienced by electrical rock properties as a function of moisture content is relevant to field measurements as well as to laboratory determinations The term moisture shall be understood to include any water molecules that do not form a part of the mineral constituents of a rock sample

There seems to be a central problem in trying to relate the amount of moisture present in a rock sample to the electrical effect it produces, the problem consists in precisely determining the amount of water in the sample The study reported by *Wu* [1964] in which, by means of nuclear magnetic resonance, he was able to detect three types of protons associated with water molecules corresponding to three different types of bonding in clay minerals is a good example, given the complexity of these minerals, of the nontriviality of the problem Although determination of the amount of moisture in rocks is mostly done by weighing, it has to be recognized that it is only a crude indicator of the presence of water in a sample

DRY ROCKS

When the label dry rock is applied to samples used in laboratory measurements, it usually has one of three operational meanings (1) water has not been intentionally added to the rock, (2) the rock has been subject to desicca-

tion by some heat treatment, or (3) the rock has been placed in an evacuated space The first two meanings are found most often, the second possibly being the most common Few instances of the third exist [*Keller and Licastro,* 1959, *Howell and Lacastro,* 1961, *Saint-Amant and Strangway,* 1970], and the vacuums involved have usually been low (i e , $\sim 10^{-3}$ torr) A brief discussion about the water content in each of these three cases shall be given

The sample in case 1 is exposed to atmospheric moisture, and therefore its surface will contain an amount of moisture proportional to the relative humidity of the air, the interior of the sample may present a different amount of water, depending on its size, porosity, and history

In case 2 *Worz* [1964] has arrived at the conclusion that samples of different thicknesses dry out differently in an oven, the thicker the sample, the less the loss of water in a given time at a given temperature Furthermore, this method of desiccation is clearly a relative one, since the criterion is usually that of observing the loss in weight of a sample, at a given temperature T_1, until no changes in it occur, but, if the temperature is changed to $T_2 > T_1$, it will generally be observed that the previously stabilized weight will be further decreased In Table 1 we show the results of such an experiment in five different rock samples at temperatures in the range of those usually reported The samples were kept immersed in tap water for 7 days, and thereby some degree of saturation is achieved, whether it was total was irrelevant to the purpose of our experiment The samples were allowed to dry (as visually estimated) at the surface before the first measurement (i e , $t = 0$) was performed The accuracy of the measurements is ± 0.0005 gram The oven used was of the forced air circulation type With the exception of the muscovite schist, all samples experienced an extra loss of weight when the temperature was raised from 106° to 186°C The difficulty in deciding at which temperature a particular sample will be considered completely dry is obvious Furthermore, if the temperature is raised sufficiently for a given sample, hydration water may begin to be lost from its mineral constituents

Finally, in case 3, moisture near the sample surface will be rapidly removed, but moisture

TABLE 1 Increased Loss in Weight Resulting from an Increase in Temperature

Heating Time, hours	Temperature, °C	Limestone		Hematitic Sandstone		Clay		Granite		Muscovite Schist	
		Weight, grams	Weight Loss, %	Weight, grams	Weight Loss, %	Weight, grams	Weight Loss, %	Weight, grams	Weight Loss, %	Weight, grams	Weight Loss, %
0	22	12 510		6 550		13 685		24 335		7 520	
6 5	106	12 450	0 478	6 380	2 596	12 340	9 829	24.255	0.329	7.495	0 333
22 5	106	12.445	0 520	6 380	2 596	12 340	9 829	24 255	0 329	7 495	0 333
31 0	106	12 445	0.520	6 380	2 596	12 337	9 851	24 255	0 329	7 495	0 333
53 0	106	12 445	0 520	6 380	2 596	12 335	9 865	24 255	0 329	7 495	0 333
78.0	106	12 445	0 520	6 378	2 626	12 335	9 865	24 255	0 329	7 495	0 333
78 + 18	186	12 438	0 576	6 375	2 672	12 325	9 938	24 250	0 350	7 495	0 333
78 + 42	186	12.435	0 600	6 372	2 718	12 320	9 975	24 250	0 350	7 495	0 333
78 + 97	186	12 435	0 600	6 372	2 718	12 320	9 975	24.250	0.350	7 495	0 333
78 + 105	186	12 435	0 600	6 372	2 718	12 325*	9 938	24 250	0 350	7 495	0 333

Accuracy of the measurements is ±0 0005 gram
*Although all measurements were completed in less than 2 min, the sample in this one was exposed to room conditions for 10 to 15 min before weighing It is likely that the sample absorbed 5 mg of atmospheric moisture in that time

in its interior may require long times of pumping owing to the effect of the pore system of the rock, and, if the pores do not interconnect, the water may never come out The question again is how much moisture is removed in a given time and a given vacuum As was pointed out above, this manner of desiccating has involved vacuums of the order of 10^{-3} torr, which are usually obtained with mechanical vacuum pumps and pumping times of around 10 hours In the experiment to be described, evidence is shown of water release from the sample occurring even after 50 hours of pumping at around 10^{-7} torr Therefore what may seem to be a dry rock in a low-vacuum system would appear as a strongly contaminated sample in a high-vacuum system This phenomenon indicates that evacuation is also a relative method of rock desiccation

The term dry rock used with the meanings described above could be used without complications in electrical studies if the effects of small amounts of water were in proportion to the amount of water present Unfortunately, very small amounts of water can have very large electrical effects Evidence will be presented suggesting that there is a large class of resistive rocks that are affected in such properties by quantities of water amounting possibly to a few monolayers of H_2O in the surfaces of the sample Consequently, a reconsideration of the term dry rock as well as a precise method of determining moisture content in rocks seems to be needed

EXPERIMENTAL METHOD AND RESULTS

To evaluate the effects of atmospheric moisture on rock resistivity, we used an experimental setup consisting of two electrometers, a dc regulated voltage supply, a chart recorder, a high-vacuum system, and a sample holder The electrometers were Keithley models 610B and 601 having input impedances of 10^{14} Ω, they were used in two measuring configurations In Figure 1*a* an electrometer is used to measure the total resistance of the sample, it was used to monitor the resistance for continuous periods of several hours each In Figure 1*b* the two electrometers measure voltage and current across the sample The responses of both configurations were recorded in a Brush Mark 200 recorder (not shown in the figures), model RF-

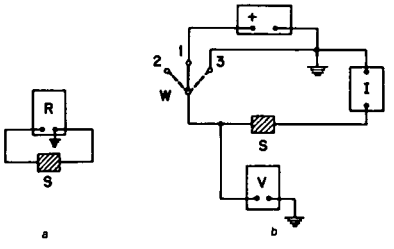

Fig 1. (*a*) An electrometer R measures the total resistance of sample S (*b*) Two electrometers, I and V, measure the current and voltage in sample S When switch W is in position 1, the plus terminal of the voltage source is connected to the sample, and dc current and voltage can be determined, if the switch is now connected to position 2, the sample terminals will be open, and a transient voltage decay, controlled by the sample properties, can be measured If the switch goes from position 1 to position 3, the sample terminals will be short circuited, and the internal current discharge in the sample can be determined

1783-60 These responses will be further discussed The regulated dc voltage source was a Princeton Applied Research model TC-602CR with a voltage range of 0–60 volts, a no-load to full-load regulation of better than 0 0001%, and a ripple of less than 50-μv rms at any load

The high-vacuum system consisted of a Davis and Wilder model 616 system with a diffusion pump capable of reaching a vacuum of $1\,0 \times 10^{-7}$ torr in 15 min starting from atmospheric pressure, the ultimate vacuum attainable by the system being in the lower range of 10^{-8} torr The low- and high-vacuum meters were those of a Granville-Phillips controller unit model 260016 with ranges 10^{3}–10^{-3} and 10^{-4}–10^{-9} torr, respectively The sample holder was of the simplest kind and is shown in Figure 2 Indium-mercury amalgam electrodes were used to ensure an intimate contact with the sample, connections to the sample electrodes were made through two copper screws mounted on acrylic blocks so that high insulation (i e, $>10^{15}$ Ω) between them and the base plate is achieved Electrical connections from atmospheric pressure to high vacuum were made by means of vacuum feedthroughs of the octal pin type, the resistance between the measuring pins, including as well that of the coaxial cables used, was found to be in the 10^{11}-Ω range, coaxial teflon-insulated cable was used for the connections inside the high-vacuum chamber

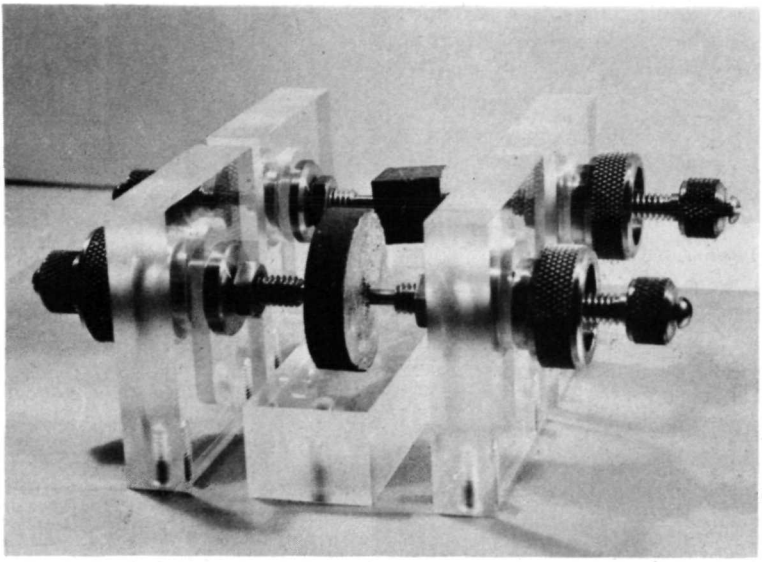

Fig. 2. The sample holder used in the measurements consisted simply of copper screws mounted on acrylic blocks. The electrical shield has been removed to show the arrangement of elements; two samples of different geometries are mounted in place. The copper screws make direct contacts with the indium-mercury amalgam electrodes.

The types of responses obtained by measuring with the configuration in Figure 1*b* are shown in Figure 3; 1 corresponds to position 1 of switch W indicated in Figure 1*b*, 2 indicates switching from 1 to 2, and 3 indicates switching from 1 to 3. Let us assume that the switch is placed in position 1; the voltage across the sample will be the voltage of the source (it was kept fixed at +5.000 volts throughout the experiments using the configuration in Figure 1*b*) less the voltage drop across the current meter I, which was kept, at all times, at less than 0.005 volt. The corresponding schematic response is shown in Figure 3; the response of the current to the step voltage applied indicates the presence of the Maxwell-Wagner effect in the electrode-sample system [*Alvarez,* 1972]. If the switch is now connected to position 2, the sample terminals will be open and the current will go to zero, whereas the voltage will decay in a way resembling an exponential function. If, instead of switching from 1 to 2, one switches from 1 to 3, the voltage will go to zero, since the sample terminals will be short circuited, and one will be able to measure the current flow across the sample; notice the current reversal and decay typical of the Maxwell-Wagner effect. The resistance value obtained directly with one electrometer was compared almost in every instance with the value of the ratio obtained with the second configuration. They agreed within 5% at all times. The readings in such cases were made when all transients had disappeared.

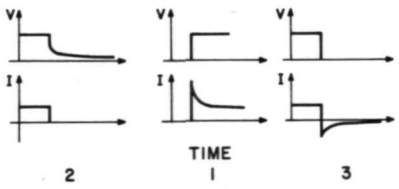

Fig. 3. Types of responses obtained for various positions of switch W in Figure 1*b*. Number 1 corresponds to position 1, 2 indicates switching from 1 to 2, and 3 indicates switching from 1 to 3.

A sample of hematitic sandstone (Table 2) from the core used in the desiccation experiment (Table 1) and having a porosity of approximately 2.6% was prepared with the indium-mercury electrodes; the sample had been at atmospheric conditions for more than a year. Equilibrium with atmospheric moisture throughout the interconnected pores of the sample at the time of measurement was assumed. The sample diameter was 3.22 cm, and its average

TABLE 2 Porosity, Resistivity, and Mineralogy of Rock Samples

Rock	Porosity, %	Resistivity, Ω m	Mineral Composition,* wt %	Comments
Hematitic sandstone	2 6	See text	53 8 SiO_2, 26 5 Fe_2O_3, 11 7 Al_2O_3, 6 8 TiO_2	Fine grained
Pyrite	0 7	1 11 x 10^{-2}	71 0 FeS_2, 25 2 $CuFeS_2$, 2 8 PbS, 1 2 SiO_2	FeS_2 crystal size $\leq$0 5 mm
Galena	0 4	3 22 x 10^{-2}	87 5 PbS, 12 5 SiO_2	Quartz inclusions in massive galena

Hematitic sandstone from Copper Mine River, Canada Pyrite and galena of unknown origin
*Determined by X ray analysis

thickness 8 21 mm, thus the electrodes covered an area of 8 13 cm^2

At the start of the experiment the sample resistance at atmospheric pressure was 3 7 × 10^5 Ω, corresponding to a resistivity of 3 6 × 10^4 Ω m The bell jar was located in place, and pumping started while the resistance was continuously recorded In Figure 4, trace 1 shows the sample resistance as a function of time, it is clearly seen that the effect of evacuation is immediately reflected in a change in resistance The initial rate of change of resistivity was about 2 1 × 10^4 Ω m/min Evacuation proceeded for 63 hours at pressures from 10^{-6} to 10^{-7} torr At around t = 50 hours a tendency of the resistance value to stabilize began to appear, to make sure that the readings were effectively stabilized, we kept monitoring for 13 hours more Various rates of resistance increase were observed while we pumped down to the final vacuum attained, toward the end of this part of the experiment, variations of 1% in resistance occurred in 2-hour periods

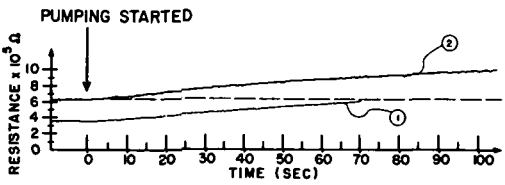

Fig 4 Trace 1 shows the increase in sample resistance when the initial evacuation started, the resistivity rate of change is about 2 1 × 10^4 Ω m/min After the initial evacuation, air was admitted into the high-vacuum chamber, in 23 hours of exposure to atmospheric moisture the sample reached a value of resistivity of 6.23 × 10^4 Ω m Trace 2 shows the resistance variation as the second evacuation started The resistivity rate of change is the same as that of the initial evacuation

At t = 63 hours, air of 37% relative humidity was admitted in the high-vacuum chamber, the response of the resistance variation is shown in Figure 5 Prior to air admission the resistance was stabilized at a value of 2 78 × 10^9 Ω with a corresponding resistivity of 2 75 × 10^8 Ω m at a pressure of 5 0 × 10^{-7} torr, therefore a change in resistivity of 4 orders of magnitude took place from initial to final conditions Figure 5 shows the immediate change in resistance when air was admitted, the irregular variation around 60 sec corresponds to the lifting of the bell jar, so that the sample is directly exposed to atmospheric conditions The initial air admission is made through a valve, and, once the inside pressure is stabilized with the atmospheric pressure, the bell jar can be lifted The transient behavior when the bell jar is lifted is systemically observed We believe that transient air currents are forced into the chamber at the time of lifting the bell jar and produce the

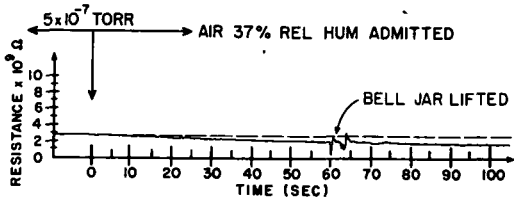

Fig 5. Prior to air admission (i e, t = 0) the resistance was stable at a value of 2 78 × 10^9 Ω, with a corresponding resistivity of 2 75 × 10^8 Ω m and a pressure of 5 0 × 10^{-7} torr, the sample had been in a vacuum for 63 hours At t = 0, air of 37% relative humidity was admitted, the sample resistance started decreasing within 1 sec at a rate of 1.21 × 10^7 Ω m/min The irregular variations around 60 sec correspond to lifting the bell jar to allow direct exposure of the sample to atmospheric conditions Before the bell jar was lifted, air was admitted through a valve to the high-vacuum chamber

observed response The behavior normalizes immediately afterward, and the downward trend of the resistivity value continues at a rate of 1.21×10^7 Ω m/min, after 23 hours of exposure to atmospheric moisture the sample attained a value of 6.23×10^4 Ω m in resistivity The small difference in resistivity between this value and the one obtained at $t = 0$ indicates that conditions at this time were very close to those at the time the experiment was initiated Exact reproduction of the initial resistivity value was not attained, probably owing to a 4% decrease in the room's relative humidity

To test whether the atmospheric moisture was, in effect, responsible for the variations observed, it was decided to repeat the cycle of evacuation and gas admission, except that this time dry nitrogen (i e , 99 99% N_2) would be admitted instead of air Reevacuation started at $t = 86$ hours, and, after 22 hours of pumping, the sample reached a value of resistivity of 1.03×10^8 Ω m at a pressure of 6.4×10^{-7} torr, the response of the rock resistance is shown as trace 2 in Figure 4 Notice the same rate of resistance increase as in the original pumping Further pumping might have taken the value of ρ closer to the one reported previously at this pressure range (i e , 2.75×10^8 Ω m), but it was not considered necessary to do so Notice that these values were attained in about one third of the time originally needed for reaching similar conditions, this reduction is possibly due to access paths for the gas/water molecules being left open after the first evacuation, but at present there is no way of verifying this assumption The nitrogen was admitted at this time until a pressure of 1 atm was reached inside the vacuum chamber The value of the resistance was monitored continuously for around 2 hours, in which time no significant changes of ρ were observed Finally, a new cycle of evacuation and air admission resulted in a response similar to the one in Figure 5

From the observations presented up to this point it is clearly established that the reported changes in resistivity are due to water effects, since, when dry nitrogen substitutes for air, no such changes occur Furthermore, we have often observed that variations in atmospheric moisture (e g , from 20 to 30% relative humidity) correspond to changes in ρ up to 1 order of magnitude

Our observations have been made on a sample of hematitic sandstone, but one can generalize the statement made above to a larger group of rocks, recalling the results of *Howell and Licastro* [1961] as well as those of *Worz* [1964], both sets of results have shown the variations of electrical properties of rocks as a function of moisture by comparing results obtained with atmospheric moisture present with those made at moderate vacuums (i e , $\sim 10^{-3}$ torr) The study of *Howell and Licastro* [1961] on 23 common minerals and 71 rock samples concludes that below 1 megacycle the presence of moisture in a rock plays a dominating role in determining its electrical properties, whereas the study of *Worz* [1964] on red sandstone concludes that there is a gradual decrease in the frequency dependence of ϵ with the decrease in water content, whereas for σ only a change of the absolute value is observed, the frequency dependence being largely constant *Brace et al* [1965] analyzed the electrical resistivity of rocks under pressure and suggested that even minute water films may cause the resistivity to remain below the dry values by orders of magnitude

Consequently, a large number of rocks are substantially affected by moisture, the magnitude of the change in electrical properties depending on the specific rock type considered There is, however, another group of rocks that do not seem to be affected in their resistivity by atmospheric moisture We have tried to detect changes in the resistivity of samples (Table 2) containing amounts of more than 50% pyrite and others containing more than 75% galena (presenting ρ values of 1.11×10^{-2} and 3.22×10^{-2} Ω m, respectively) when they are evacuated to 10^{-7} torr, and none have been observed *Brace and Orange* [1968] have observed a similar effect for a Nahant gabbro The fact that their resistivities show no change when they are measured from atmospheric moisture to such vacuums indicates that the mechanism of conduction responsible for their low resistivities (rocks are considered of low resistivity, or sometimes also called 'good conductors,' when $\rho \lesssim 1$ Ω m), whatever it may be, has to be considered as dominating over atmospheric moisture contributions to conduction

TRANSIENT RESPONSES

To gain more insight about how atmospheric moisture affects conduction in the hematitic sandstone sample studied, we shall next present the transient responses of current and voltage as measured with the arrangement shown in Figure 1*b* In Figure 6*a*, *b*, *c*, and *d* the current and voltage responses of the sample to the excitation voltage are shown The time scale in Figure 6*b* applies to Figure 6*a* and *c* as well The switching in Figure 6*b* was made by hand, and therefore the length of the pulses is not the same, this difference is of no consequence to our observations, and it is noted only to avoid confusing these dc excitations with a square wave excitation often used in rock measurements Furthermore, the applied voltage was always positive

Figure 6*a* shows the current response of the rock when it is in a vacuum of 5×10^{-7} torr or in an atmosphere of dry N_2 (after evacuation), whereas Figure 6*c* shows the current response when the sample was in air of 37% relative humidity for 22 hours after the first evacuation, this response and that obtained prior to evacuation were substantially the same

Comparing the current responses in Figure 6*a* and *c*, one can determine the change in the magnitude of the current flowing through the sample These results also suggest that there is a modification of the shape of the current transient, which is better manifested through the voltage decay curves shown in Figure 6*d* Curve 1 (Figure 6*d*) corresponds to the conditions specified for Figure 6*a*, and curve 2 to those of Figure 6*c*, they were obtained when switch W in Figure 1*b* was changed from position 1 to position 2 Clearly, the relaxation time involved in the high-vacuum or N_2 atmospheres is longer than the one obtained at atmospheric conditions, and the change in shape of the current transients is thereby confirmed Such

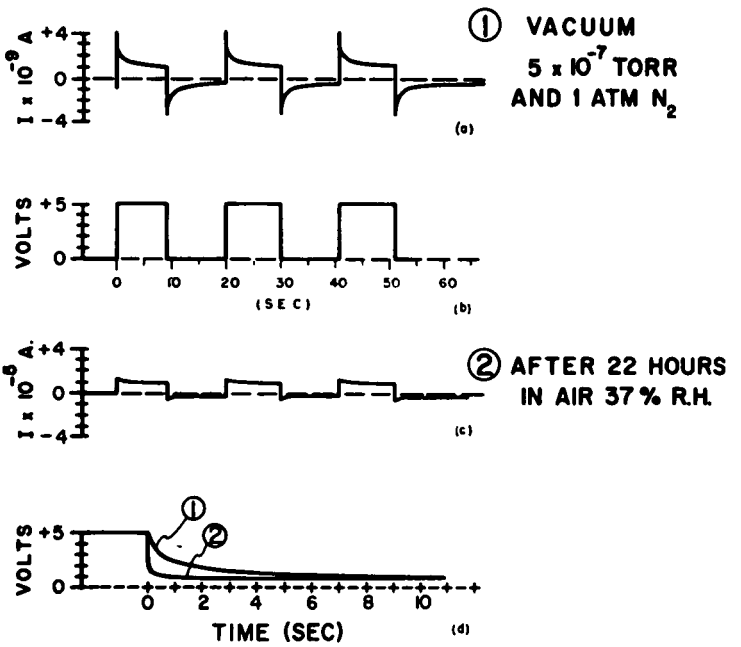

Fig 6 (*a*) Current responses when the sample was either in a vacuum of 5×10^{-7} torr or, after evacuation, in dry nitrogen at a pressure of 1 atm (*b*) Excitation voltages applied to the sample, the time scale shown applies also to (*a*) and (*c*) (*c*) Current responses when the sample was exposed for 22 hours, after evacuation, to air of 37% relative humidity The magnitude and shape of the current responses have changed with respect to those in (*a*) (*d*) Voltage decay curves when the excitation voltage is interrupted, curve 1 corresponds to the conditions specified in (*a*) and reflects the electrical properties of the rock matrix, whereas curve 2 corresponds to the conditions in (*c*) and shows the electrical alterations experienced by the rock matrix after exposure to atmospheric moisture

behavior is in agreement with a decrease in sample resistivity when moisture is present Furthermore, the modification of the relaxation times implies, through the Kramer-Kronig relations [*Landau and Lifshitz*, 1960], that the frequency responses are modified as well

Notice that the voltage decay for both curves reaches ~0 9 volt within 10 sec, this remaining voltage between the ends of the sample usually takes several hours to decay to half its value when the sample is in the vacuum, whereas at atmospheric conditions the voltage reaches ~0 2 volt within 10 min and remains around that value for more than 24 hours In fact, we have not observed it to go to zero even after 30 hours of measurements The currents associated with these voltages are usually found to be in the range 10^{-7}–10^{-10} amp

If one tries to observe the transient responses of the samples containing pyrite and galena reported previously, it will be seen that the voltage responses when one switches (Figure 1*b*) between positions 1 and 2 correspond to the shape of the excitation voltage (i e , a square pulse), no distortion being observed in the time scale of Figure 6*d* when either atmospheric or high-vacuum conditions prevail The corresponding currents through the sample are square pulses also, thus no Maxwell-Wagner effect is observed

On the basis of these observations, only a coarse classification of rocks can be made according to the effects produced on them by atmospheric moisture· (1) those whose resistivities experience changes of 2 orders of magnitude or more when alternate measurements are made at high vacuums (i e , ~10^{-7} torr) and at atmospheric conditions with more than 10% relative humidity and (2) those whose resistivities are not affected when they are determined at the two conditions stated above A more precise distinction between these two groups, although desirable, must wait for more experimental data

DISCUSSION

Once it is established that the resistivity of a considerable number of rocks is affected by the presence of atmospheric moisture, it is convenient to look into the possible mechanism responsible for the resistivity variation

Conduction through an aqueous electrolyte will be considered first, since it is a process of conduction that is known to predominate when rocks have aqueous electrolytic solutions in their pore systems [*Brace et al* , 1965] In the present case, though, we are interested in the formation of an aqueous electrolyte on the surface of the sample when air is admitted to the high-vacuum chamber, since one can assume that such an electrolyte is not present when the sample is evacuated at 10^{-7} torr

An aqueous electrolyte is formed when ions are dissolved in water. Thus the formation of an aqueous electrolyte on the sample surface implies the building up of a film of free water (i e , water not adsorbed to the surface) to constitute the aqueous medium in which ions from the surface can dissolve and move on the action of an external electric field But it is known [*Zisman*, 1965] that, if the partial pressure of a vapor is much below the saturation pressure, as is the case for water vapor when one admits air into the evacuated chamber, the adsorbed monolayer will have a low surface coverage Therefore in the first seconds of exposure to air of 37% relative humidity it is unlikely that a water monolayer will form on the sample surface, even less likely is the accumulation of enough water to form an aqueous film One would have to assume that times longer than a few seconds are involved in the film formation, but this assumption would imply a time lag in the resistance variation in contradiction with the experimental observations of Figure 5, which show an immediate (i e , within 1 sec) response to air admission

Furthermore, if a continuous electrolytic path were to be formed, at time $t = t_0$ after air admission, across the sample surface and connecting the metallic electrodes, the change in resistivity should be an abrupt one At this time conduction through the highly resistive bulk of the sample would be bypassed by at least one surface electrolytic path presenting a resistivity smaller than that of the rock matrix by several orders of magnitude As more electrolytic paths were formed, the overall resistivity would continue to vary in a gradual manner But the rate of resistance variation in the experiments is never an abrupt one (with the exception of the transient when one lifts the bell jar)

A further indirect indication that conduction through an aqueous electrolyte is not taking place is given by the results of *Fripiat et al* [1965] They studied the surface conductivity of montmorillonites and silicas containing first and second adsorbed water layers and concluded that the charge carriers involved in the surface conduction are not the ions in the monolayer but the protons originating from the dissociation of water molecules, which is enhanced by surface electric fields

From these considerations it is difficult to reconcile the experimental evidence with a model of aqueous electrolytic conduction at the surface, although other types of electrolytic conduction are not excluded [*Scanlon*, 1957, *Snow et al*, 1965] Rather, this evidence suggests a mechanism consisting of an alteration of the surface conductivity of the rock sample by fractions of a water monolayer adsorbing to its surface Such a mechanism would account for the immediate variation in resistivity upon air admission as well as for the long time (i e, around 24 hours) necessary to reach equilibrium after evacuation or air admission, these periods being necessary for adsorption or desorption of water in the innermost surfaces of the sample, which are connected to the exterior through the pore system The surface of the sample has to be considered not only as the external geometrical surface but also as the ensemble of all surfaces in which an air-matrix interface occurs

What kind of evidence is there for assuming that fractions of a water monolayer can affect the surface conductivity of some rocks? No study in the geophysical literature known to this author has shown direct evidence of such a mechanism But inorganic dielectrics and semiconductors have been shown to be strongly affected by various amounts of atmospheric moisture At present one has to resort to this kind of evidence to support the idea of such phenomena occurring in rocks, recalling the fact that most rocks in the upper crustal layers of the earth can be classified either as dielectrics or as semiconductors on the basis of the electrical properties of the minerals forming the rock

In the rest of this discussion we shall present a few of the many available examples of how water molecules affect some inorganic siliceous materials We have chosen to present these examples to stimulate the idea of similar phenomena occurring in the upper crustal layers, where silica accounts for around 58 wt % of the average chemical composition [*Ronov and Yaroshevsky*, 1969]

A large amount of work has been reported in the solid state physics literature about the surface properties of semiconductors [*Kingston*, 1956, *Many et al*, 1965], in which it has been recognized that adsorbed atoms or molecules may exchange charge with the semiconductor and thereby induce changes in its surface conductivity Adsorbed species can act as electron donors or acceptors creating additional allowed energy levels for the electrons inside the surface of the semiconductor and consequently induce changes in the number of available charge carriers, these changes take place usually in a region a few microns deep

Buck and McKim [1958], analyzing the effects of various atmospheres on the conductivity of n type silicon, have shown that it is possible to change its surface conduction from a strong n type condition to a strong p type condition passing through an intrinsic condition by a series of chemical treatments and exposures to oxygen and water vapor atmospheres, they conclude that, after any given chemical treatment, water vapor makes the surface more n type and oxygen makes it more p type

Nicollian et al [1971] report that, when water is diffused into a SiO_2 film at temperatures $\leq 200°C$ and electron currents are made to flow through it, a negative buildup occurs in the oxide, they attribute this behavior to the formation of water-related centers acting as electron traps Other types of semiconductors have also been shown to be influenced by the ambient relative humidity [*Kingston*, 1955]

The effects of moisture adsorption on the surface resistivity of insulators have long been observed, *Clark* [1962] points out that commercial inorganic insulators experience changes of 5 orders of magnitude in surface conductivity upon exposure to atmospheric moisture Furthermore, he states that the decrease in surface resistance is enhanced by a high degree of surface porosity, a fact of direct consequence to the rock specimens normally handled in laboratory measurements *Guyer* [1944] presents

data showing that the region of maximum variation for the surface resistance of fused quartz, lime glass, and borosilicate glass occurs between 30 and 80% relative humidity

CONCLUSIONS

The problems associated with determining the degree of dryness of a rock sample have been analyzed, and it has been concluded that heating or evacuating a sample produces only relative measures of its degree of dryness. It appears that, in order to obtain an absolute measure of the sample's water content, one will have to resort to methods such as nuclear magnetic resonance and possibly mass spectrometry. Correlations between the absolute amount of moisture in a sample and its electrical behavior have to be postponed until the former can be properly determined. At present, one can only study the relative variation of resistivity between the two different measuring conditions.

The variations of the electrical resistivity of a hematitic sandstone sample measured at vacuums of around 10^{-7} torr and at atmospheric conditions, as well as results obtained elsewhere on a wide variety of rocks at vacuums of around 10^{-3} torr, indicate that the electrical behavior of a large group of rocks is affected by atmospheric moisture, whereas our experiments on two samples of low resistivity indicate that there is another group not affected by it.

The possibility of aqueous electrolytic conduction on the surface of the hematitic sandstone sample is difficult to reconcile with the experimental evidence. An alternative process is suggested to account for the rock responses; it consists of modifying the surface conductivity of the sample by adsorption of quantities of H_2O possibly as small as fractions of a water monolayer. Examples of modification of surface conductivity by adsorbed water molecules in semiconductors and dielectrics have been presented. Because a large number of the rocks occurring in the upper crustal layers of the earth are either semiconductors or insulators, it seems plausible to expect them to exhibit similar effects of resistivity alteration by the presence of adsorbed water molecules.

The present study is in no way sufficient to prove that fractions of a water monolayer are in fact altering the electrical properties of a sample surface, but it seems to give a basis for putting forward the hypothesis that surface conduction in rocks, as induced by adsorption of water molecules, may be an important component of the ensemble of electrical conduction mechanisms in rocks.

Such a mechanism would be relevant to the study of the conductivity of the upper crustal layers in the earth and to the study of electrical conduction in the moon in the case of existence of subsurface water as well as to the effects of atmospheric contamination of lunar samples on earth. Finally, it may account, at least in part, for the differences observed in laboratory determinations of rock resistivities, which often amount to several orders of magnitude among the same type of rocks.

Acknowledgments. I wish to acknowledge H. F. Morrison, M. F. Merriam, A. F. Kip, and D. W. Strangway for criticisms and comments. Thanks are due to W. F. Brace and A. S. Orange for their critical review of the manuscript.

Acknowledgments are due to the Consejo Nacional de Ciencia y Tecnología, México, and to the National Aeronautics and Space Administration for financial support.

REFERENCES

Alvarez, R., Electrical conduction phenomena in rocks, Ph.D. thesis, 172 pp., Univ. of Calif., Berkeley, 1972.

Brace, W. F., Resistivity of saturated crustal rocks to 40 km based on laboratory measurements, *The Structure and Physical Properties of the Earth's Crust, Geophys. Monogr. Ser.*, vol. 14, edited by J. G. Heacock, p. 243, AGU, Washington, D.C., 1971.

Brace, W. F., and A. S. Orange, Further studies of the effect of pressure on electrical resistivity of rocks, *J. Geophys. Res.*, *73*, 5407, 1968.

Brace, W. F., A. S. Orange, and T. R. Madden, The effect of pressure on the electrical resistivity of water-saturated crystalline rocks, *J. Geophys. Res.*, *70*, 5669, 1965.

Buck, T. M., and F. S. McKim, Effects of certain chemical treatments and ambient atmospheres on surface properties of silicon, *J. Electrochem. Soc.*, *105*, 709, 1958.

Clark, F. M., *Insulating Materials for Design and Engineering Practice*, p. 976, John Wiley, New York, 1962.

Fripiat, J. J., A. Jelli, G. Poncelet, and J. André, Thermodynamic properties of adsorbed molecules and electrical conduction in montmorillonites and silicas, *J. Phys. Chem.*, *67*, 2185, 1965.

Guyer, E. M., Electric glass, *Proc. IRE*, *32*, 743, 1944.

Hill, H. J, and J. D. Milburn, Effect of clay and water salinity on electrochemical behavior of reservoir rocks, *Trans AIME, 207*, 65, 1956

Howell, B F, Jr, and P H Licastro, Dielectric behavior of rocks and minerals, *Amer Mineral, 46*, 269, 1961.

Keller, G. V., and P H Licastro, Dielectric constant and electrical resistivity of natural-state rocks, *U.S Geol Surv Bull., 1052-H*, 257, 1959

Kingston, R H., Water-vapor-induced *n*-type surface conductivity on *p*-type germanium, *Phys. Rev, 98*, 1766, 1955

Kingston, R H, Review of germanium surface phenomena, *J Appl Phys, 27*, 101, 1956

Landau, L D, and E. M Lifshitz, *Electrodynamics of Continuous Media*, p 259, Addison-Wesley, Reading, Mass, 1960

Mandel, P, Jr, J W Berg, Jr, and K L. Cook, Resistivity studies of metalliferous synthetic cores, *Geophysics, 22*, 398, 1957

Many, A, Y Goldstein, and N B Grover, *Semiconductor Surfaces*, p 346, North-Holland, Amsterdam, 1965

Nicollian, E H, C N Berglund, P F. Schmidt, and J. M Andrews, Electrochemical charging of thermal SiO_2 films by injected electron currents, *J. Appl Phys, 42*, 5654, 1971.

Parkhomenko, E I, *Electrical Properties of Rocks*, p 119, Plenum, New York, 1967

Ronov, A B, and A A. Yaroshevsky, Chemical composition of the earth's crust, in *The Earth's Crust and Upper Mantle, Geophys. Monogr. Ser*, vol. 13, edited by P. J Hart, p 37, AGU, Washington, D C., 1969.

Saint-Amant, M, and D. W Strangway, Dielectric properties of dry, geologic materials, *Geophysics, 35*, 624, 1970

Scanlon, W W, Surface studies on cleaved crystals of lead sulfide, in *Semiconductor Surface Physics*, edited by R H Kingston, p 238, University of Pennsylvania Press, Philadelphia, 1957

Scott, J H, R D Carroll, and D R Cunningham, Dielectric constant and electrical conductivity measurements of moist rock A new laboratory method, *J Geophys Res, 72*, 5101, 1967.

Snow, E H, A S Grove, B E Deal, and C T. Sah, Ion transport in insulating films, *J Appl Phys, 36*, 1664, 1965

Worz, O, Reproducibility of measurements of electric rock parameters on specimens, *Rep 65-32*, 11 pp, Air Force Cambridge Res Lab, Bedford, Mass, November 1964

Wu, T H, A nuclear magnetic resonance study of water in clay, *J. Geophys Res, 69*, 1083, 1964.

Wyllie, P J, A discussion of water in the crust, *The Structure and Physical Properties of the Earth's Crust, Geophys Monogr Ser*, vol 14, edited by J G Heacock, p 257, AGU, Washington, D C, 1971

Zisman, W A, Fundamental factors in detecting chemicals as adsorbed films, in *Surface Effects in Detection*, edited by J I Bregman and A Dravnieks, p 1, Spartan-Macmillan, Washington, D C, 1965

(Received June 7, 1972,
revised December 7, 1972)

Reprinted from
16 March 1973, Volume 179, pp 1122-1123

SCIENCE

Lunar Permafrost: Dielectric Identification

Romàn Alvarez

Lunar Permafrost: Dielectric Identification

Abstract. *A simulator of lunar permafrost at 100°K exhibits a dielectric relaxation centered at approximately 300 hertz. If permafrost exists in the moon between 100° and 213°K it should present a relaxation peak at approximately 300 hertz. For temperatures up to 263°K it may go up to 20 kilohertz.*

The controversy over the existence of water in the moon (*1*) will have an "in-depth" test when the electromagnetic soundings made during Apollo 17 have been analyzed (*2*). The results of those experiments will have to be interpreted in terms of models of the lunar regolith and its dielectric properties.

Permafrost is one of the two possible modes of existence of water in the moon, the other being liquid water. Models of the internal constitution of the moon in which the existence of H_2O is considered concur in locating the permafrost layer above the liquid water (*3*, *4*) The depth and extent of the permafrost layer is a matter of speculation. If we assume that such models are valid, electromagnetic signals would have to travel through permafrost before detecting liquid water.

Information on the dielectric properties of lunar samples is available at various frequency ranges and temperatures (*5*, *6*). However, little is known about the role of frozen moisture in the dielectric behavior of these samples at temperatures below 273°K. The interpretation of the lunar electromagnetic soundings, on the basis of the data presently available, may thus leave ambiguities regarding the presence of the permafrost layer. This report provides information on the typical response to electromagnetic excitations that may be expected from a permafrost layer in the moon.

Measurements of the dielectric permittivity (κ') and loss tangent (tan δ) of a lunar simulator (*7*) have been carried out in the frequency range of 30 to 10^5 hertz, at temperatures varying from 100° to 373°K and vacuums of around 7.0×10^{-8} torr, in an attempt to simulate conditions in the upper layers of the lunar regolith. A specially designed guarded-electrode system was used. Complete results of these experiments will be presented elsewhere (*8*). Here I shall restrict the discussion to the responses at 100°K.

In order to establish a basis of reference (*9*), I measured samples of the lunar simulator with packing densities of 1.80, 2 00, and 2.20 g/cm^3 containing initially atmospheric moisture (at 40 percent relative humidity). Before they were cooled to 100°K the samples were maintained at room temperature and 5.0×10^{-8} torr for periods of 2 to 3 hours, so that part of their initial moisture content was released. In Figs. 1 and 2 the values of κ' and tan δ for the samples at 100°K and 7.0×10^{-8} torr are plotted. Curves 1, 2, and 3 correspond to the densities cited above. Curves 4 (Figs. 1 and 2) were obtained for the sample of density 2.20 g/cm^3 after a cycle of heating (to 373°K) and cooling (to 100°K) took place in the high vacuum. The differences with respect to curves 3 are due to additional water losses occurring at the higher temperature. This result is in agreement with observations made of repeated heating and cooling cycles at other temperatures (*8*). Curves 1 through 4, for tan δ, present broad maxima between 100 and 300 hertz, while the corresponding κ' curves decrease slowly with increasing frequency

The sample that yielded curves 4 was used to prepare a new sample of density 1.90 g/cm^3, consisting of the lunar simulator (87.7 percent by weight) and distilled H_2O (12.3 percent). The sample had a doughy texture. At 100°K and 7.0×10^{-8} torr, the values obtained for

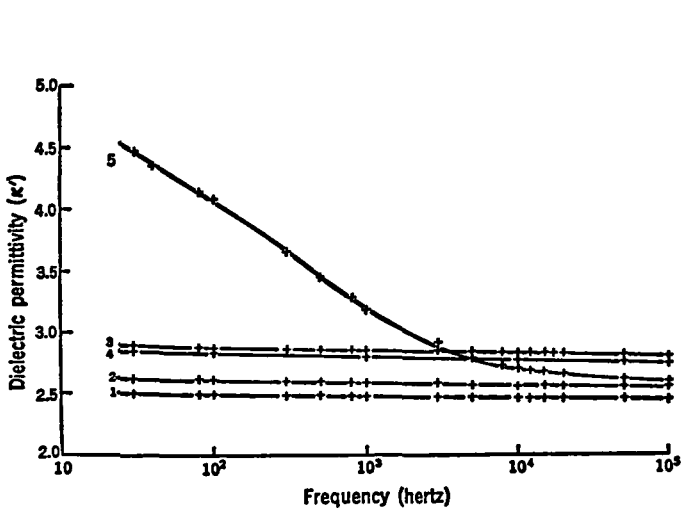

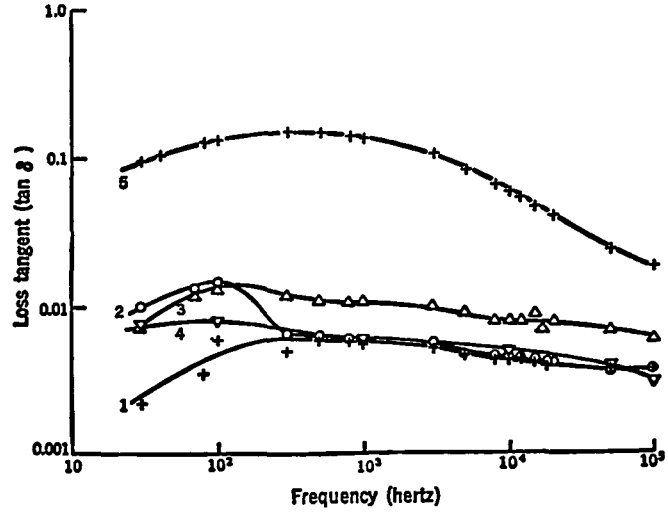

Fig. 1 (left). Dielectric permittivity (relative) of the lunar simulator at 100°K and 7.0×10^{-8} torr, plotted against frequency. Fig. 2 (right). Loss tangent of the lunar simulator at 100°K and 7.0×10^{-8} torr, plotted against frequency. Refer to the text for an explanation of the curve numbers.

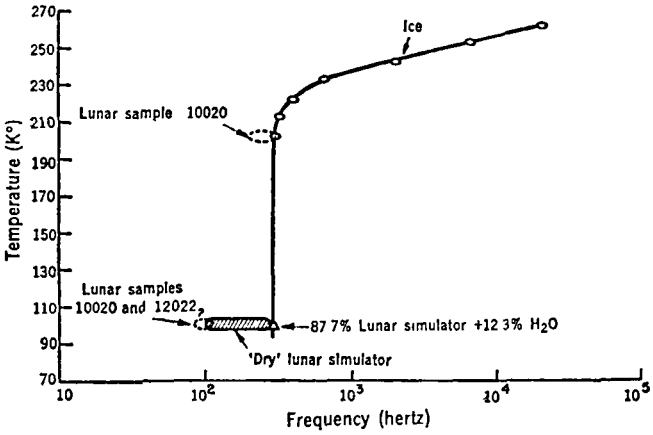

Fig 3 Temperature plotted against the frequency at which the peaks of dielectric relaxation occur for ice (*12*), lunar simulator plus water, "dry" lunar simulator, and two lunar samples (*5*)

κ' and tan δ are shown as curves 5 (Figs 1 and 2). If the same data are plotted as κ'' against κ' ($\kappa'' = \kappa' \tan \delta$), they correspond to a Cole-Cole distribution (*10*) given by

$$\kappa^* = \kappa_\infty' + \frac{\kappa_0' - \kappa_\infty'}{1 + (j\omega\tau)^{1-\alpha}} \qquad (1)$$

with $\kappa_0' = 4.90$, $\kappa_\infty' = 2\ 57$, $\tau = 6\ 5 \times 10^{-4}$ second, and $\alpha = 39$. The symbol κ^* denotes the complex (relative) dielectric permittivity, κ_0' and κ_∞' are the values of the real part of κ^* at zero and infinite frequency. The imaginary part of κ^* is κ'', $j = (-1)^{1/2}$, ω is 2π times the frequency, τ is the generalized relaxation time, and α is a parameter that can vary between 0 and 1.

These results show that with increasing amounts of moisture the dielectric behavior of the sample, in the frequency range of 30 to 10^5 hetrz and at 100°K, eventually becomes dominated by ice. The broad peaks observed in curves 1 through 4 (Fig. 2) are interpreted as relaxations occurring in the frozen moisture remaining in the sample. The corresponding κ' curves are in agreement with the existence of such relaxations. However, the small κ' increments with decreasing frequency preclude its consideration as positive evidence. The vapor pressure of ice at 120°K has been estimated as $1\ 4 \times 10^{-12}$ torr (*11*), therefore, the amount of water frozen at 100°K and 7.0×10^{-8} torr will remain in the sample as long as such conditions are maintained in the laboratory. Curves 3, 4, and 5 (Fig 2) qualitatively establish that the sample losses are proportional to their ice contents A quantitative evaluation of the amount of frozen moisture and its effect on κ' and κ'' is presently under way (*8*).

The existence of lunar permafrost is expected within the temperature range of 100° to 273°K (*4*) The results presented here represent the lower temperature limit It is known that the relaxation peak for ice moves toward lower frequencies when the temperature decreases (*12*) In Fig 3 I have plotted the ice temperature against the frequency at which the peak of the relaxation occurs The ellipses represent data for ice (*12*); the triangle corresponds to the peak in curve 5 (Fig 2) Extrapolation of the results for ice is in agreement with my results at 100°K.

Lunar samples 10020 and 12022 were contaminated by atmospheric moisture when the dielectric measurements were performed (*5*). Consequently, relaxation phenomena associated with the frozen contaminating water should be expected The peaks observed for tan δ in those measurements have been incorporated in Fig 3 The question mark by the lunar samples at 100°K indicates the possibility of the peak occurring at slightly lower frequencies

In conclusion the evidence presented indicates that if permafrost exists in the moon between 100° and 213°K it will have a dielectric relaxation peak at approximately 300 hertz If its temperature is between 213° and 263°K the relaxation peak will occur between 300 hertz and 20 khz. The frequency at which the relaxation maximum occurs may serve as a crude thermometer.

ROMÁN ALVAREZ

Engineering Geoscience,
University of California,
Berkeley 94720

References and Notes

1 T Gold, in *The Nature of the Lunar Surface*, W. N Hess, D H Menzel, J A O'Keefe, Eds (Johns Hopkins Press, Baltimore, 1966), p 107, H C Urey, *Nature* **216**, 1094 (1967)
2 E Driscoll, *Sci News* **102**, 268 (1972)
3 S H Ward, G R. Jiracek, W I Linlor, *IEEE Trans Geosci Electron* **7**, 19 (1969)
4 D H Chung, *Moon*, in press
5 ———, W B Westphal, G Simmons, *J Geophys Res* **75**, 6524 (1970), in *Proceedings of the Second Lunar Science Conference*, A A Levinson, Ed (M I T Press, Cambridge, Mass , 1971), p 2381
6 T. J Katsube and L S Collett, in *Proceedings of the Second Lunar Science Conference*, A A. Levinson, Ed (M I T Press, Cambridge, Mass , 1971), p 2367, T Gold, B T O'Leary, M Campbell, in *ibid*, p 2173, T Gold, M J Campbell, B T O'Leary, *Science* **167**, 707 (1970)
7 The lunar simulator of core S/N 2013 from Apollo 12 was a terrestrial basalt
8 R Alvarez, in preparation
9 ———, *J Geophys Res*, in press
10 K S Cole and R H Cole, *J Chem Phys* **9**, 341 (1941)
11 K Watson, B Murray, H Brown, *J Geophys Res* **66**, 1598 (1961).
12 C P. Smyth and C S Hitchcock, *J Amer Chem Soc* **54**, 4631 (1932)
13 I thank D W Strangway for providing the lunar simulator, H F Morrison and M F Merriam for discussion of the results, and B Jain for help in the laboratory Supported by NASA grant NGR 05-003-447

16 November 1972

LUNAR POWDER SIMULATOR UNDER LUNAR-LIKE CONDITIONS: DIELECTRIC PROPERTIES

Román Alvarez

Engineering Geoscience

University of California, Berkeley

Berkeley, California 94720

ABSTRACT

The dielectric response of a powdered basalt simulating lunar fines is studied in the temperature range found in the lunar surface while maintained at high-vacuum conditions. Two concurrent analyses are made: one regarding moisture contamination effects and the other related to the response of the lunar regolith. The atmospheric moisture remaining in the pore system of the sample in the high vacuum produces a low-frequency dispersion; this is attributed to the presence of isolated water adsorption centers in which the local conductivity values are raised with respect to the conductivity of the basalt. It is suggested that a change in the main electric conduction mechanism occurs between 300° and 370°K; close to 300°K conduction seems to be dominated by adsorbed moisture, while at 370°K the main conduction process appears to be controlled by thermally activated carriers. The dielectric response of the lunar regolith during a lunation is schematically described. It is found that during approximately seven tenths of a lunation the dielectric response of a 5 to 10 cm surface layer should be fairly constant; in the remaining three tenths it should undergo rapid changes. Changes in the dielectric properties of the surface layer should be controlled by temperature; in the subjacent layers such changes are thought to be controlled by the increasing density of the regolith.

INTRODUCTION

The temperature on the surface of the lunar regolith varies from approximately 100°K to 400°K during the lunar synodic period. The amplitude of the temperature wave is rapidly attentuated with depth (Robie and Hemingway, 1971; Hoyt et al, 1971) thus only the first few centimeters experience the full change in temperature. In the present study a terrestrial basalt simulating lunar powder has been subjected to temperature variations in the 100° to 373°K range while in a high vacuum. The changes in the dielectric properties of the lunar simulator have been determined and are thought to represent in a qualitative way the corresponding variations in the uppermost layer (i.e. 5 to 10 cm in depth) of the lunar regolith.

Although various measurements on the dielectric properties of actual lunar samples have been made (Chung et al, 1970, 1971, and 1972; Katsube and Collett, 1971; Strangway et al, 1972; Gold et al, 1970 and 1971) few have gone to temperatures below 273°K, none of these, however, under high-vacuum conditions. Similar studies on terrestrial samples (Strangway, 1969; Saint-Amant and Strangway 1970; Campbell and Ulrichs, 1969) also have not combined high vacuum and low temperatures.

In order to reach conditions similar to those in the lunar surface, a terrestrial powder has to lose a considerable amount of the atmospheric moisture usually adsorbed to its surfaces (Alvarez, 1973b); in so doing the sample experiences changes in its dielectric properties. An analysis of these changes yields an insight into the reverse process, namely that of dielectric variations arising from moisture contamination, undergone by lunar samples that have been in contact with atmospheric moisture (Strangway et al., 1972).

Low-temperature determinations are necessary to generate a complete theoretical description of the dielectric behavior of lunar samples, as well as to assist in the explanation of electrical phenomena occurring in the lunar night. For studies on terrestrial rocks low-temperature measurements offer the

advantage of freezing any water that may be present in the sample thus effectively reducing conduction effects associated with it.

EXPERIMENTAL TECHNIQUE

The experimental set-up consisted of a Davies and Wilder high-vacuum system model 616, a cryogenic thermometer with a range of 1°K to 300°K from American Magnetics, a thermistor calibrated in the 77-400°K temperature range, a General Radio capacitance measuring assembly model 1610-B and a guarded-electrode system; all are commercial instruments except the last one.

A detailed description of the guarded-electrode system will be given elsewhere, here we shall briefly outline its characteristics. A vacuum sealed stainless steel box (Figure 1) is used as a liquid nitrogen (LN) reservoir inside the high vacuum chamber. It is externally fed by means of adequate feedthroughs. A heavy copper strap is welded to the base of the LN reservoir; as long as there is LN in the reservoir the strap maintains the LN temperature.

At the top of the copper strap are located the guarded-electrode and the guard ring. The former is a copper disk held against the strap by copper screws. The latter is a copper ring electrically insulated from the copper strap by a teflon layer. The sample, in the case of solid rock specimens, or the sample holder in the case of powders, is placed above the guard and guarded electrodes. Heat is directly exchanged between the sample and the guarded-electrode, thereby cooling the sample in the high vacuum. The third (upper) electrode clamps the sample from above; adjustments in its position are made by means of a threaded guide.

Heat losses by radiation from the LN reservoir and sample are minimized by means of several layers of superinsulation (i.e. aluminized mylar sheets) that cover the electrode assembly in the evacuated chamber. In order to reach the higher temperatures (i.e. 373°K) pressurized air, or nitrogen, is made to flow through the reservoir after being heated to the appropriate temperature.

A set of measurements in the frequency range of 30 to 10^5 Hz, at one temperature, involved periods of 6 to 8 hours; of these, 3 to 4 hours were necessary to reach thermal quasi-equilibrium conditions, and the remaining time was dedicated to the actual dielectric measurements. It must be noted that with the present system it is not possible to reach complete thermal equilibrium, since heat exchange with the sample occurs only at one of its ends, namely the one in contact with the guarded electrode. Measurements were made at temperatures of 100°, 298°, and 373°K. The powdered sample was packed to densities of 1.8, 2.0, and 2.2 g/cm^3 in the working volume (area 17.9 cm^2 and thickness 0.5 cm) of the sample holder. This is made out of a good quality dielectric material (NEMA G-10) with suitable mechanical characteristics in the temperature range of interest.

The sample was packed in the sample holder at atmospheric conditions and set in place in the electrode assembly. Evacuation started slowly with the mechanical pump; in approximately 45 minutes the sample was exposed to the high vacuum. At this time the vacuum was usually between 6.0×10^{-7} and 3.0×10^{-6} torr depending on the packing density of the sample and the atmospheric humidity at which the sample was prepared. It was left to outgas in the high vacuum for approximately one hour more; in this time the pressure decreased to 3.0×10^{-8} - 3.0×10^{-7} torr. Liquid nitrogen was admitted to the LN reservoir and cooling of the sample started.

The temperature of the guarded-electrode reaches 82°K in 20 minutes, after the first filling of the LN reservoir, in a vacuum of 10^{-8} - 10^{-7} torr. The sample grains directly in contact with this electrode are expected to attain such a temperature in approximately the same time. We observed, however, that at places within the sample, not directly in contact with the electrode, heat propagation was extremely slow under high vacuum conditions. This is possibly due to a heat conduction mechanism in which radiation predominates (Cremers,

1972); whether this is the actual case cannot be ascertained from our experiments. For calibration purposes several temperature determinations were made inside the powder sample. It was found that temperature gradients of approximately 100°K/cm, in the direction of the symmetry axis of the sample holder, existed in the lunar simulator of density 1.80 g/cm^3 after 90 minutes of the first filling of the LN reservoir when the vacuum was in the 10^{-8} - 10^{-7} torr range.

Thus, the time necessary to reach thermal quasi-equilibrium conditions appeared to be unduly long. In order to reduce it, we increased the pressure in the vacuum chamber by means of dry nitrogen (i.e. 99.99% N_2), since it does not induce changes in the electrical response of "resistive" rock specimens (Alvarez, 1973b). It was observed that the thermal conduction of the sample improved markedly when the N_2 pressure was between 0.1 and 1.0 torr. While higher pressures only slightly improved thermal conduction in the sample they increased considerably the overall thermal losses of the system. With the sample at a pressure of 1.0 torr of N_2 the times necessary to reach thermal quasi-equilibrium were reduced to the 3 to 4 hour periods mentioned above. The thermal gradients, in the direction of the axis of the sample holder, were of approximately 20°K/cm when the dielectric responses were determined.

Having the sample in thermal quasi-equilibrium conditions the N_2 was removed by a re-evacuation, usually to a pressure in the 10^{-8} to 10^{-7} torr range, before the dielectric determinations were made. The high temperature (i.e. 373°K) was attained following the same sequence of evacuation, N_2 admission, and re-evacuation previously described, while heated air was being injected into the LN reservoir (Figure 1). After a cooling or heating process the sample was left in a N_2 atmosphere of around 1.0 torr for 8 to 12 hour periods in which room temperature was attained.

DIELECTRIC BEHAVIOR

A description of the material used as simulator of core S/N 2013 from Apollo 12 appears in Table I. The dielectric response in the vacuum as a function of frequency, temperature, and packing densities of 1.8, 2.0, and 2.2 g/cm^3 appear in Figures 2, 3, and 4 respectively. The experimental error limits have been estimated, for κ' , as $\pm$ .01 at all frequencies and temperatures; and for tan δ as: $\pm$ .001 (at 30 Hz) or better for values of tan δ lesser than .04; $\pm$ .005 (at 30 Hz) or better for values of tan δ between .04 and .09; and $\pm$ .01 (at 30 Hz) or better for values of tan δ greater than .09. Each curve corresponds to one of the temperatures 100°; 298° or 373°K; for a given density a sequence of determinations started at 100°K, continuing to 298° and 373°K, then repeating measurements at some of those temperatures. In order to distinguish the order in a sequence we use a subindex (A, B, or C) in the temperature value. This information is relevant to the correlation of moisture losses with dielectric responses. The subindex shall be dropped when making generical reference to a temperature.

The samples were frozen to $100°K_A$ as described in the previous section; from the rates of outgasing we inferred that a large portion of the original moisture content of a sample was lost in the high vacuum prior to freezing. At 100°K one expects the remaining moisture in the sample to be condensed in the form of ice. The dielectric responses of the samples at this temperature have been discussed elsewhere (Alvarez, 1973a). When the sample was allowed to thaw and reached $298°K_A$ some extra water losses occurred due to additional outgasing in the high vacuum. Heating the sample to $373°K_A$ increased the thermal energy of the water molecules remaining in the pore system of the sample, raising the pressure and forcing additional water to be lost. Therefore, when the sample cooled off to room temperature (i.e., $298°K_B$) the total moisture content in the pore system was less than at $298°K_A$.

A preliminary idea of how moisture is affecting the dielectric response of the sample is gained by comparing the dispersions at $298°K_A$ with those at $298°K_B$; the latter are markedly reduced (Figures 2, 3, and 4), such a reduction being attributed to the lesser amount of moisture. After the first cycle of heating, a second one (i.e. heating to $373°K_B$ and cooling to $298°K_C$, as in Figure 3) produced little further changes in the dielectric response of the sample, corresponding to comparatively smaller water losses during the second heating. Our observations agree with others (e.g. Howell and Licastro, 1961; Strangway et al, 1972) which have shown that small amounts of moisture affect mainly the response of the sample at the "lower frequencies" (the range of these lower frequencies depends on the amount of moisture in the sample and may go as high as 1 MHz). Notice the small but measurable effect that moisture release has on the sample at 100°K: Figure 4 shows measurements at $100°K_A$ and at $100°K_B$, the latter being obtained after a cycle of heating (to $373°K_A$) and cooling took place.

One must bear in mind in analyzing these results that the same amount of moisture in the pore system of the sample contributes differently to conduction and dielectric response at different temperatures. At 100°K the moisture is frozen whereas at room and higher temperatures it will become water or water vapor depending on the actual pressure in the inner pores of the sample. The dielectric and conduction properties of ice and water at the frequencies analyzed are totally different.

Interpretation of dielectric relaxations is facilitated by plotting the data in curves of κ'' against κ', where $\kappa'' = \kappa' \tan\delta$. In Figure 5 we have plotted such curves for densities of 1.8 and 2.0 g/cm^3 at temperatures of $298°K_A$ and $373°K_A$. The plots correspond to Cole-Davidson distributions (Davidson and Cole, 1951) given by

$$\kappa^* = \kappa'_\infty + \frac{\kappa'_0 - \kappa'_\infty}{(1 + j\omega\tau)^\beta} \qquad (1)$$

where κ^* is the complex (relative) dielectric permittivity, κ'_0 and κ'_∞ are the real parts of κ^* at zero and infinite frequency, ω is 2π times the frequency, τ is a relaxation time, β is a parameter that can assume values between zero and one, and $j = (-1)^{1/2}$; the imaginary part of κ^* is denoted κ''. In Table 2 are summarized the parameters of the Cole-Davidson distributions obtained for temperatures of 298°K_A, 373°K_A, and 373°K_B, and the three densities.

The data in Table 2 suggest that the relaxation time τ is controlled mainly by the temperature (in the temperature range of 298° to 373°K) although, as will be seen, moisture also has an effect on τ at 298°K; they show that increasing densities yield larger κ'_0 and κ'_∞ values, as expected for a given temperature, and suggest that increases in the parameter β occur for increasing temperatures, although the data for the latter observation do not seem to be conclusive. In addition, decreasing amounts of moisture produce decreasing values in κ'_0 at 298°K and 373°K; comparison of κ'_0 values at 298°K_A and 298°K_B (see Tables 2 and 3), and comparison of κ'_0 values at 373°K_A and 373°K_B for a density of 2.0 g/cm^3 (see Table 2, low-frequency relaxation) substantiate this observation. In spite of the change in κ'_0 between 373°K_A and 373°K_B the relaxation time τ and the parameter β do not experience significant variations, suggesting that moisture has little effect on them at 373°K. The 30 Hz frequency-points (Figure 5) for 373°K_A and densities 1.8 and 2.0 g/cm^3 have been interpreted as arising from a residual electrode impedance, based on the data plots at 298°K_A which clearly manifest this effect (Dansas et al, 1967).

The curves corresponding to the three densities at 298°K_B are plotted as κ'' against κ' in Figure 6. They could not be fitted to Cole-Davidson distributions;

instead two Cole-Cole distributions have been fitted to each set of data (Cole and Cole, 1941). The analytical expression for such a distribution is

$$\kappa^* = \kappa'_\infty + \frac{\kappa'_0 - \kappa'_\infty}{1 + (j\omega\tau)^{1-\alpha}} \qquad (2)$$

where the symbols correspond to those of equation (1), recalling the fact that the relaxation time has different meanings in a Cole-Cole and in a Cole-Davidson distribution and that α is a parameter that assumes values between zero and one. Equation (2) and the parameters shown in Table 3 fit the data within the error limits ($\Delta\kappa'$ and $\Delta\kappa''$) given in the same table. The relaxation times between the low and high-frequency relaxations differ by three orders of magnitude, strongly suggesting different causative mechanisms. The κ'_∞ values of the high-frequency relaxation at 298°K_B are essentially the same as those obtained for the Cole-Davidson distributions at 298°K_A, as expected from moisture effects.

DISCUSSION

The above observations establish a general pattern for the dielectric behavior of the lunar simulator and the effects introduced by varying amounts of moisture. The responses at 100°K show small dispersions, with maximums in tan δ at around 300 Hz, associated with the frozen moisture in the sample (Alvarez, 1973a); at this temperature and in the frequency range studied there is no evidence that the basalt powder itself presents relaxation phenomena. At 298°K_B (Figure 6) it is observed that two independent relaxations appear; the high-frequency relaxation is attributed to the dielectric properties of the powdered basalt. The low-frequency relaxation is attributed to interactions

between the moisture in the sample and the powdered basalt as follows: it has been proposed (Alvarez, 1973b) that adsorbed water molecules increase the surface conductivity of "resistive" rock specimens by creating additional allowed energy levels in the surface of the sample; in the present case we propose that the low amounts of moisture involved create a series of isolated adsorption centers in which the local conductivity value is raised, by the same mechanism, with respect to the surroundings.

This results in a model equivalent to that of conductive grains (e.g. spheres) imbeded in a resistive matrix which gives rise to a low-frequency relaxation of the Debye type through a Maxwell-Wagner effect (Koops, 1951; Alvarez, 1973c). The low frequency response in the present experiments actually corresponds to a Cole-Cole distribution of relaxation times instead of a single relaxation time (i.e. Debye relaxation); such an effect is attributed to a distribution of conductivities in the isolated centers and to the various shapes they must acquire. The plausibility of this explanation is brought about by the statistical nature of the adsorption and desorption processes, coupled to the variations in dielectric response induced by different shapes of conductive inclusions (Sillars, 1937).

When larger amounts of moisture, at the same temperature, are present in the pore system one would expect an increase in the density of isolated centers of higher conductivity. Accordingly, the magnitude of the Maxwell-Wagner effect would be increased producing larger κ'_o values as well as larger energy losses. This actually results when the distributions at $298°K_B$ and at $298°K_A$ are compared (i.e., Figures 5 and 6, and Tables 2 and 3); in the latter the amount of moisture is larger. As it increases in magnitude the low-frequency distribution affects higher frequencies creating a smoother transition between the low and the high-frequency relaxations. The response of the powder becomes overwhelmed by the

moisture effects and the two distributions coalesce into a single one approximately described by a Cole-Davidson distribution. The extrapolated κ'_∞ value remains essentially unchanged during the transition, in agreement with expected moisture effects.

The Cole-Davidson distributions at $373°K_A$ (Figure 5) present the peculiarity of having increased their relaxation times with respect to the distributions at $298°K_A$ (see Table 2). It is well known that when thermally activated mechanisms are present they produce increasing conductivities and decreasing relaxation times with increasing temperatures (e.g. Saint-Amant and Strangway, 1970). According to the increase in relaxation time at 373°K one would have to rule out the possibility of such a mechanism operating throughout the temperature range of 298°K to 373°K, and yet one would have to account for the higher conductivities at 373°K, as obtained from $\sigma = \kappa''\omega\varepsilon_o$ where σ represents the ohmic plus dielectric conductivities, ω is 2π times the frequency, $\kappa'' = \kappa' \tan\delta$ and $\varepsilon_o = 8.85 \times 10^{-12}$ f/m.

One could not attribute the increase in conductivity to water effects; at any rate one would expect a smaller density of isolated centers of higher conductivity at the higher temperature since water molecules should be excited to higher energies, reducing the population of adsorbed molecules. An indication that energy losses associated with moisture are not contributing significantly at 373°K is obtained comparing the κ' and $\tan\delta$ curves at $373°K_A$ and $373°K_B$ (Figure 3); they suggest that either little moisture remains in the sample or that its contribution to losses has diminished, in any event the energy losses would not be controlled by moisture at 373°K.

Thus it seems reasonable to assume that a change in the main conduction mechanism takes place between 298°K and 373°K. Up to some temperature value, above 298°K and below 373°K, the main conduction mechanism would be controlled by moisture and from there on a thermally activated mechanism would predominate as described elsewhere (e.g. Saint-Amant and Strangway, 1970; Strangway et al.,

1972; Chung et al., 1972). The last mechanism should cause the overall conductivity of the sample to be increased, contrasting with the water mechanism that would modify only isolated centers. The thermally activated mechanism should mask the contribution to energy losses arising from remaining adsorbed water molecules and should account for the increased relaxation time of the Cole-Davidson distribution at 373°K. Although the present data are not sufficient to prove these statements, the consistency of the results in three independent experiments at three different densities indeed supports them.

DIELECTRIC VARIATIONS IN THE REGOLITH

Some inferences can be made regarding the dielectric variations undergone by the lunar regolith as a function of temperature and density. These will be, of course, based on the present results and should be reviewed whenever similar studies on actual samples of the lunar regolith are available.

For the purpose of analyzing its dielectric variations the regolith can be divided into two layers: a surface layer of around 5-10 cm depth in which the dielectric response shall be controlled by surface temperature variations and a second layer, beneath the first one and extending down to the basement, in which the dielectric properties will be controlled by density.

The response of the surface layer can be outlined considering two temperature regions: one, between 100° and 300°K, in which κ' and $\tan\delta$ increase slowly with increasing temperature (i.e., corresponding to the present observations in which κ' increases up to 6% and $\tan\delta$ increases up to .07 from the values at 100°K); and the other, between 300° and 373°K, showing rapidly increasing values of κ' and $\tan\delta$ with increasing temperature (i.e., corresponding to increases in κ' of around 10% at 10^5 Hz and up to 65 % at 30 Hz and $\tan\delta$ increasing from .04 to .08, with respect to the values at 298°K). The limiting value of 300°K is only tentative, we believe that it may go up to 325°K.

In any event, equal temperature increments will produce different dielectric variations in the two temperature regions. When these observations are coupled

to the temperature variations in the lunar surface during a lunation (Robie and Hemingway, 1971), a clearly assymmetric response results for the dielectric properties of the surface layer: it will be fairly constant, and approximately represented by the response at 100°K, during roughly seven tenths of a lunation, while undergoing relatively strong variations in the remaining three tenths of the lunation.

The material below the surface layer (i.e. the second layer) has been found to vary rapidly in density with depth (Mitchell et al, 1972), while the surface temperature variations are strongly attenuated (Robie and Hemingway, 1971). Such a situation results in κ' being mostly dependent on density in the lower layer. The relative increments in κ' produced by temperature and density increments in the present experiments, also establish the preponderance of density over temperature as the controlling parameter: Figure 7 shows that only below 1 KHz an increment of approximately 300°K in temperature and an increment of .4 g/cm^3 in density (i.e., in the density range of 1.8 to 2.2 g/cm^3) produce similar variations in κ'; $\tan\delta$ seems to be rather independent of density in the density range analyzed.

We found that the data at room temperature (i.e., 298°K_B and 298°K_C) do not follow Rayleigh's mixing formula (Campbell and Ulrichs, 1969) in the frequency range 30 to 10^5 Hz. The difficulties involved in relating the density of the powdered material to its dielectric response, when temperature variations are involved at frequencies below 10^5, are obvious in Figure 7.

CONCLUSIONS

A powdered basalt simulating material of the lunar regolith was subjected to temperature variations similar to those found in the lunar surface during a lunation. In order to obtain the dielectric response under simulated lunar conditions all measurements were made in vacuums of 2.2×10^{-8} to 4.0×10^{-7} torr which, in addition, allowed for an evaluation of moisture effects in the powdered sample.

The dielectric responses at 298° and 373°K were identified as Cole-Cole or Cole-Davidson distributions, and their parameter values determined. Two Cole-Cole distributions were found for each set of data at $298°K_B$, one corresponding to a high-frequency relaxation (with τ in the 10^{-6} sec range) and another to a low-frequency relaxation (with τ in the 10^{-3} sec range). The former was attributed to the powdered basalt; it was proposed that the latter is caused by a Maxwell-Wagner effect which originates in isolated water adsorption centers; in such centers adsorbed water molecules would raise the conductivity with respect to the uncontaminated surroundings. The data at 298° and 373°K suggested a change in the main conduction mechanism taking place between these two temperatures: near 298°K conduction seems to be controlled by moisture, while near 373°K it appears to be controlled by thermally excited carriers.

The lunar regolith was divided into two layers: a surface layer 5 to 10 cm deep in which the dielectric response is thought to be controlled by temperature variations, and a subjacent layer in which the variations in κ' are thought to be controlled by density; in this layer the $\tan \delta$ values would probably be slowly varying functions of density. An assymmetry in the dielectric properties of the surface layer during a lunation was suggested: during approximately seven tenths of a lunation this layer would show a slowly varying behavior in its dielectric properties, undergoing rapid variations in the remaining three tenths of the lunation.

ACKNOWLEDGMENTS

The author acknowledges A. Dey, G. R. Olhoeft, and H. F. Morrison for comments on the manuscript, D. W. Strangway for providing the lunar simulator, and B. Jain for help in the laboratory. This work was made under NASA Grant NGR 05-003-447.

REFERENCES

Alvarez, R., Lunar permafrost: dielectric identification, Science, 179, in press, 1973a.

Alvarez, R., Effects of atmospheric moisture on rock resistivity, Jour. Geoph. Res., in press, 1973b.

Alvarez, R., Complex dielectric permittivity in rocks: a method for its measurement and analysis, Geoph., 38, in press, 1973c.

Campbell, M. J., and J. Ulrichs, Electrical properties of rocks and their significance for lunar radar observations, Jour. Geoph. Res., 74, 5867, 1969.

Chung, D. H., W. B. Westphal, and G. Simmons, Dielectric properties of Apollo 11 lunar samples and their comparison with earth materials, Jour. Geoph. Res., 75, 6524, 1970.

Chung, D. H., W. B. Westphal, and G. Simmons, Dielectric behavior of lunar samples: electromagnetic probing of the lunar interior, in Proc. Second Lunar Sci. Conf., edited by A. A. Levinson, p. 2381, MIT Press, Cambridge, Mass., 1971.

Chung, D. H., W. B. Westphal, and G. R. Olhoeft, Dielectric properties of Apollo 14 lunar samples, in Proc. Third Lunar Sci. Conf., edited by D. R. Criswell, p. 3161, MIT Press, Cambridge, Mass., 1972.

Cole, K. S., and R. H. Cole, Dispersion and absorption in dielectrics, J. Chem. Phys., 9, 341, 1941.

Cremers, C. J., Thermal conductivity of Apollo 14 fines, in Proc. Third Lunar Sci. Conf., edited by D. R. Criswell, p. 2611, MIT Press, Cambridge, Mass., 1972.

Dansas, P., P. Sixou, et R. Arnoult, Utilisation de l'effet Maxwell-Wagner pour l'étude de diélectriques présentent des pertes par relaxation dipolaire et une forte conductivité, in Proc. XIV Colloque Ampère, edited by R. Blinc, p. 647, North-Holland, Amsterdam, 1967.

Davidson, D. W., and R. H. Cole, Dielectric relaxation in glycerol, propylene glycol, and n-propanol, J. Chem. Phys., 19, 1484, 1951.

Gold, T., M. J. Campbell, and B. T. O'Leary, Optical and high-frequency electrical properties of the lunar sample, Science, 167, 707, 1970.

Gold, T., B.T. O'Leary, and M. Campbell, Some physical properties of Apollo 12 lunar samples, in Proc. Second Lunar Sci. Conf., edited by A. A. Levinson, p. 2173, MIT Press, Cambridge, Mass., 1971.

Howell, B. F., Jr., and P. H. Licastro, Dielectric behavior of rocks and minerals, Am. Mineralogist, 46, 269, 1961.

Hoyt, H. P., Jr., M. Miyajima, R. M. Walker, D. W. Zimmerman, J. Zimmerman, D. Britton, and J. L. Kardos, Radiation dose rates and thermal gradients in the lunar regolith: thermoluminescence and DTA of Apollo 12 samples, in Proc. Second Lunar Sci. Conf., edited by A. A. Levinson, p. 2245, MIT Press, Cambridge, Mass., 1971.

Katsube, T. J., and L. S. Collett, Electrical Properties of Apollo 11 and Apollo 12 lunar samples, in Proc. Second Lunar Sci. Conf., edited by A. A. Levinson, p. 2367, MIT Press, Cambridge, Mass., 1971.

Koops, C. G., On the dispersion of resistivity and dielectric constant of some semiconductors at audio frequencies, Phys. Rev., 83, 121, 1951.

Mitchell, J. K., W. N. Houston, R. F. Scott, N. C. Costes, W. D. Carrier, III, and L. G. Bromwell, Mechanical properties of lunar soil; density, porosity, cohesion, and angle of internal friction, in Proc. Third Lunar Sci. Conf., edited by D. R. Criswell, p. 3235, MIT Press, Cambridge, Mass., 1972.

Robie, R. A., and B. S. Hemingway, Specific heats of the lunar breccia (10021) and olivine dolerite (12018) between 90° and 350°K, in Proc. Second Lunar Sci. Conf., edited by A. A. Levinson, p. 2361, MIT Press, Cambridge, Mass., 1971.

Saint-Amant, M., and D. W. Strangway, Dielectric properties of dry, geologic materials, Geoph., 35, 624, 1970.

Sillars, R. W., The properties of a dielectric containing semiconducting particles of various shapes, Jour. Inst. Elec. Eng. (London), 80, 378, 1937.

Strangway, D. W., Moon: electrical properties of the uppermost layers, Science, 165, 1012, 1969.

Strangway, D. W., G. R. Olhoeft, W. B. Chapman, and J. Carnes, Electrical properties of lunar soil- dependence on frequency, temperature and moisture, Earth and Planetary Sci. Let., 16, 275, 1972.

TABLE I. Source and Sizes of Basalt Components of Lunar Simulator*

Source	Sieve	Sieve Opening (mm)	Percent Finer by Weight
Knippa	12	1.68	95
Knippa	50	0.297	79
Knippa	100	0.149	66
Berkeley	200	0.074	50

*Same grain distribution as Apollo 12 core tube S/N 2013, Sec. B.

TABLE 2. Parameters of the Cole-Davidson Distributions at 298°K_A, 373°K_A, and 373°K_B

Temperature	ρ (g/cm^3)	τ (sec)	β	κ'_o	κ'_∞	$\Delta\kappa'$ +	$\Delta\kappa''$ +
298°K_A	1.8	.004	.25	3.11	2.51	.03	.02
	2.0	.004	.28	3.88	2.60	.04	.05
	2.2	.004	.31	4.10	2.83	.07	.07
373°K_A	1.8	.010	.35	4.25	2.46	.02	.07
	2.0	.010	.28	4.57	2.55	.06	.04
	2.2	.010	.32	4.80	2.81	.03	.06
373°K_B	2.0	.009	.29	4.20	2.58	.04	.05

+ $\Delta\kappa'$ and $\Delta\kappa''$ represent the maximum discrepancy, at any frequency above 30 Hz, between an experimental and a theoretical value at the same frequency. These maximum discrepancies occur mainly in the frequency range of 100 to 1000 Hz.

TABLE 3.- Parameters of the two Cole-Cole Relaxation Mechanisms at 298°K[B]

	RELAXATION											
	LOW FREQUENCY*						HIGH FREQUENCY*					
ρ (g/cm³)	τ (sec×10⁻³)	α	κ_o'	κ_∞'	$\Delta\kappa'$ +	$\Delta\kappa''$ +	τ (sec×10⁻⁶)	α	κ_o'	κ_∞'	$\Delta\kappa'$ +	$\Delta\kappa''$ +
1.8	5.6	.45	2.91	2.48	.01	.01	10.8	.50	2.53	2.43	.01	.00
2.0	8.3	.51	3.38	2.68	.04	.02	4.1	.44	2.73	2.59	.00	.01
2.2	12.5	.49	3.63	2.90	.01	.01	8.8	.48	2.96	2.82	.01	.00

*Low frequency consists of the frequency range 30 to 1000 Hz, and high frequency consists of the frequency range 10 to 100 KHz.

+ $\Delta\kappa'$ and $\Delta\kappa''$ represent the maximum discrepancy between an experimental value in the low or high-frequency ranges and the one obtained from the theoretical distribution at the same frequency.

LIST OF FIGURE LEGENDS

Fig. 1. Schematic view of the guarded-electrode system. The whole assembly is maintained in the high vacuum; low and high temperatures are obtained when liquid nitrogen fills, or heated air flows through, the reservoir. The sample exchanges heat with the reservoir via the copper bar and the guarded electrode.

Fig. 2. (a) Dielectric permittivity against frequency and (b) loss tangent against frequency for the sample of packing density 1.8 g/cm^3. Temperatures followed the sequence $100°K_A$, $298°K_A$, $373°K_A$, and $298°K_B$. The pressures ranged from 2.2×10^{-8} torr at $100°K_A$ to 1.2×10^{-7} torr at $373°K_A$.

Fig. 3. (a) Dielectric permittivity against frequency and (b) loss tangent against frequency for the sample of packing density 2.0 g/cm^3. Temperatures followed the sequence $100°K_A$, $298°K_A$, $373°K_A$, $298°K_B$, $373°K_B$, and $298°K_C$. The pressures ranged from 3.0×10^{-8} torr at $100°K_A$ to 2.5×10^{-7} torr at $373°K_A$.

Fig. 4. (a) Dielectric permittivity against frequency and (b) loss tangent against frequency for the sample of packing density 2.2 g/cm^3. Temperatures followed the sequence $100°K_A$, $298°K_A$, $373°K_A$, $298°K_B$, and $100°K_B$. The pressures ranged from 2.5×10^{-8} torr at $100°K_B$ to 4.0×10^{-7} torr at $373°K_A$.

Fig. 5. κ'' against κ' plots for the distributions at temperatures of $298°K_A$ and $373°K_A$, and packing densities of 1.8 and 2.0 g/cm^3. The distributions are of the Cole-Davidson type and the sets of parameters describing them appear in Table 2. The numbers by the data points in the distribution of $373°K_A$ and of density 1.8 g/cm^3 represent frequencies in kilohertz; to avoid overcrowding only a few frequencies are indicated.

Fig. 6. κ'' against κ' plots for the distributions at a temperature of 298°K_B and densities of 1.8, 2.0, and 2.2 g/cm^3. Each one is described by two Cole-Cole distributions represented by dotted curves; the corresponding sets of parameters appear in Table 3. The numbers by the data points of the distribution of density 2.0 g/cm^3 represent frequencies in kilohertz.

Fig. 7. Dielectric permittivity against density, with temperature and frequency as parameters. Increments in density, from 1.8 to 2.2 g/cm^3, produce larger increments in K' than those produced by temperature variations from 100° to 373°K. Only for frequencies below 1 KHz the temperature effects become comparable to density effects in the ranges analyzed.

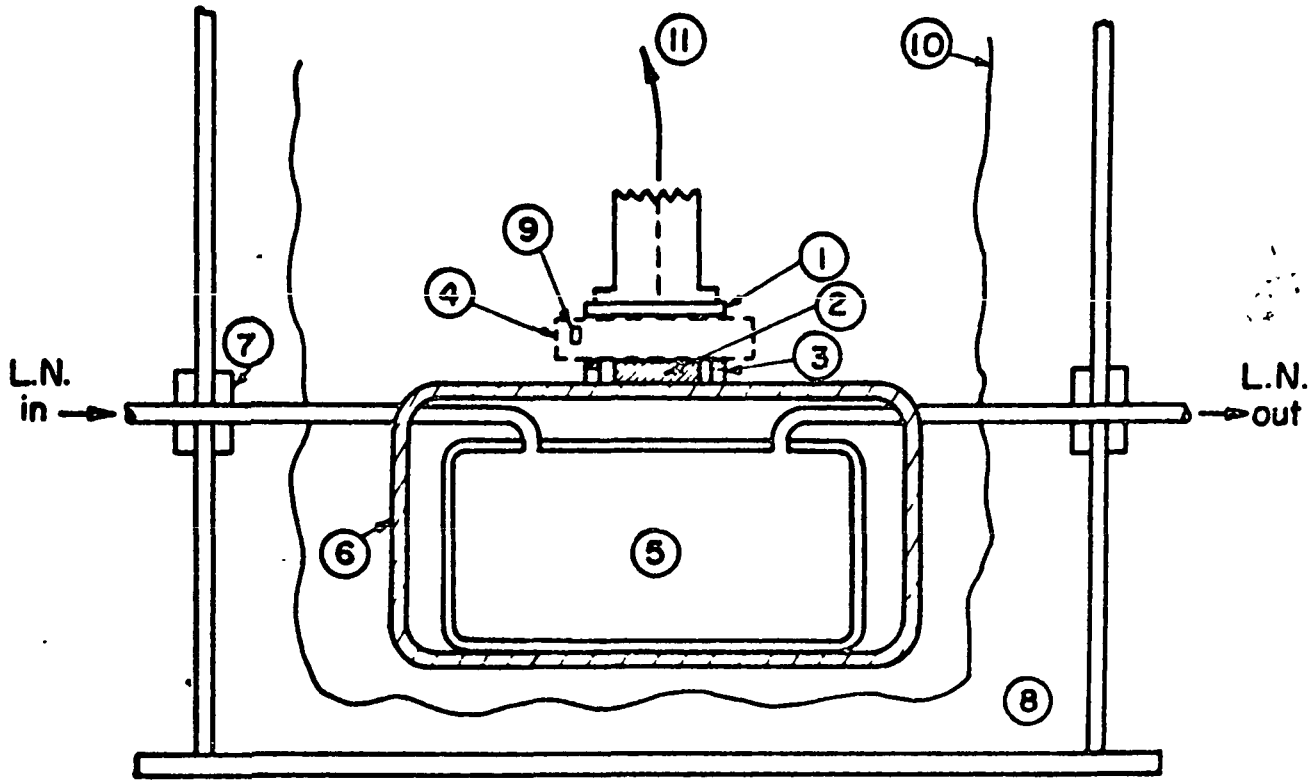

1. Upper electrode
2. Guarded electrode
3. Guard
4. Sample or sample holder
5. Liquid nitrogen reservoir
6. Copper bar
7. Liquid nitrogen feedthrough
8. Vacuum chamber
9. Cryogenic thermometer
10. Superinsulation layers
11. Electrically shielded cable

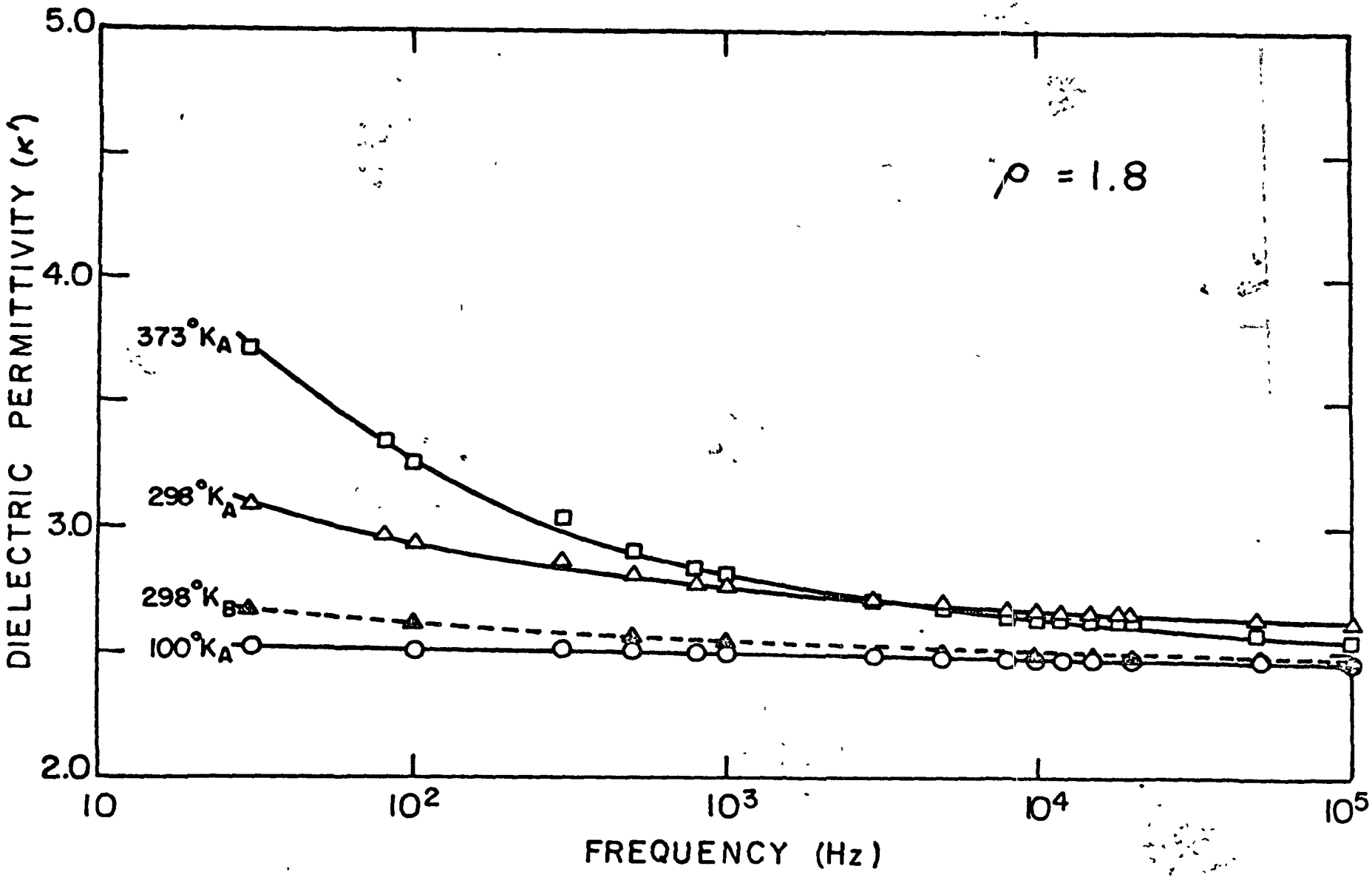

FIG. 2 (a) ALVAREZ

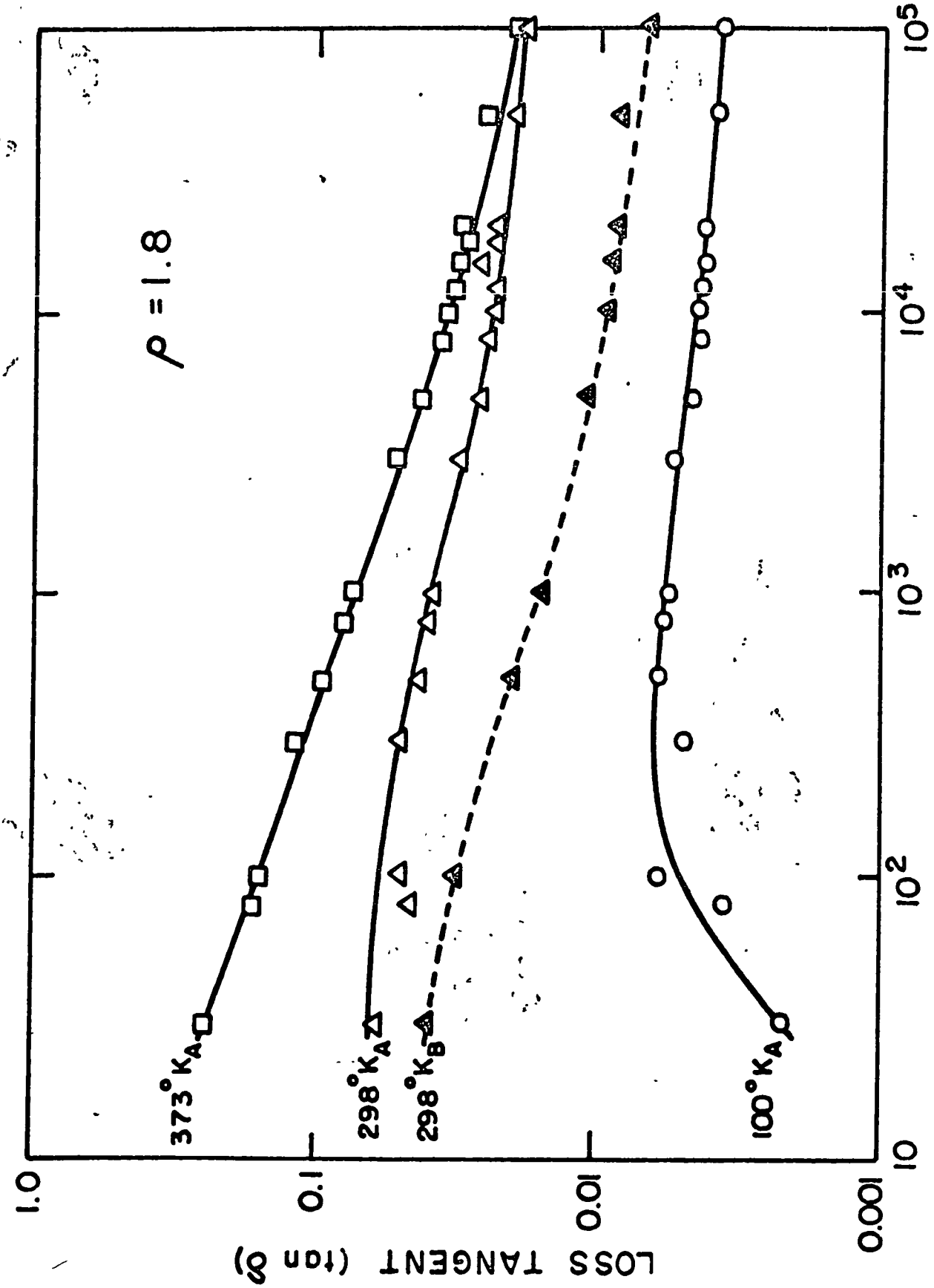

Fig. 2 (b) ALVAREZ

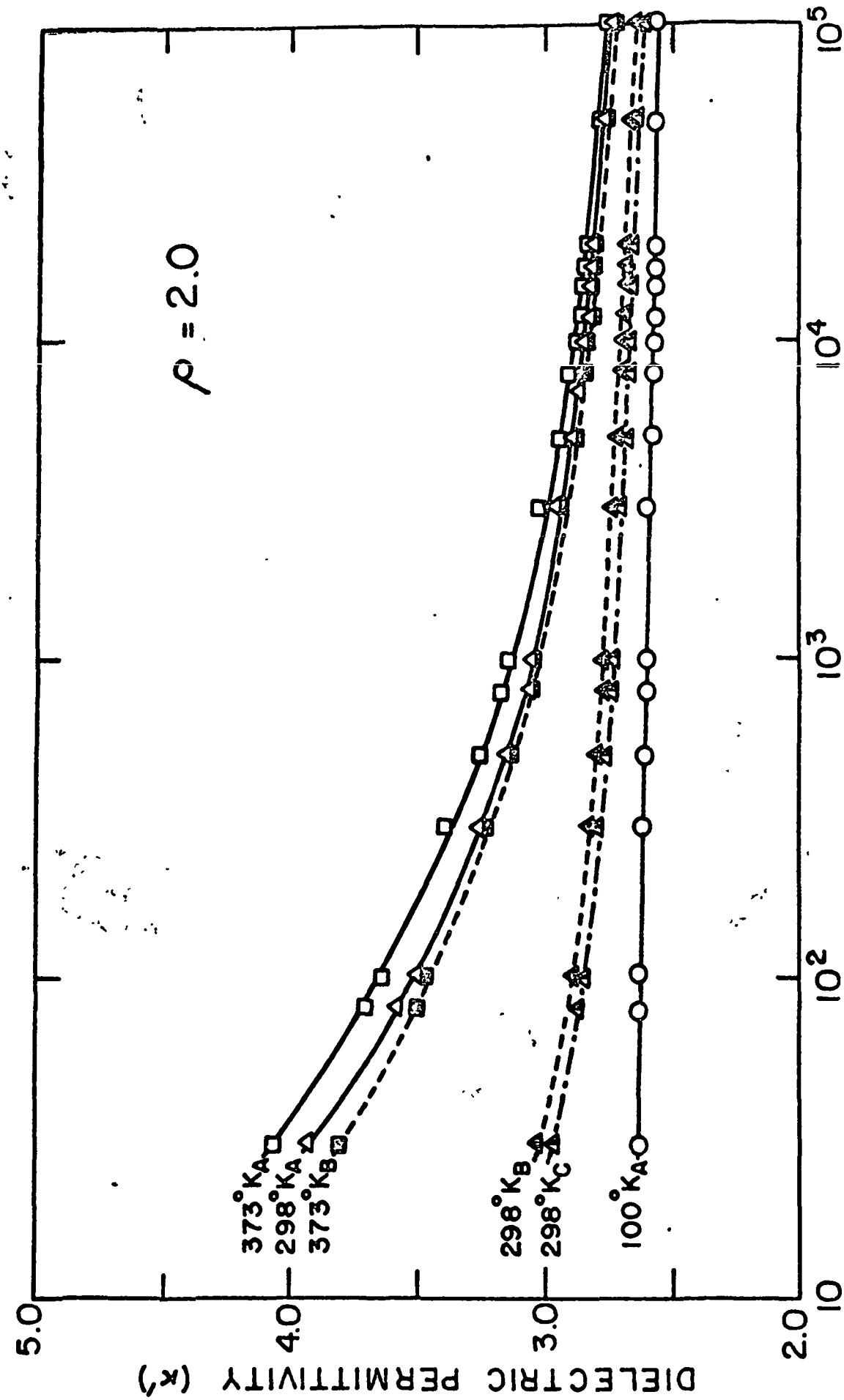

FIG. 3(a) ALVAREZ

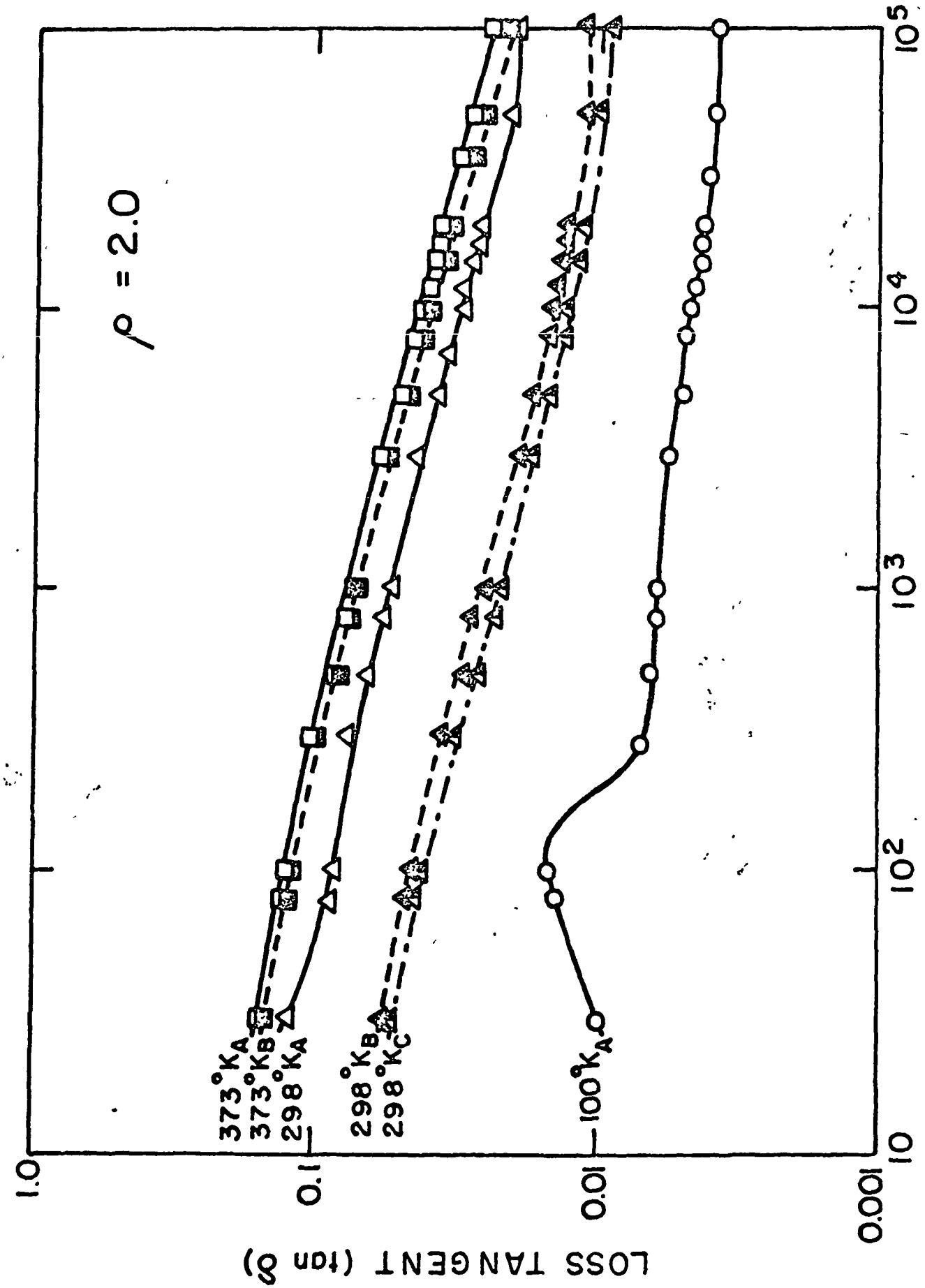

FIG 3(b) ALVAREZ

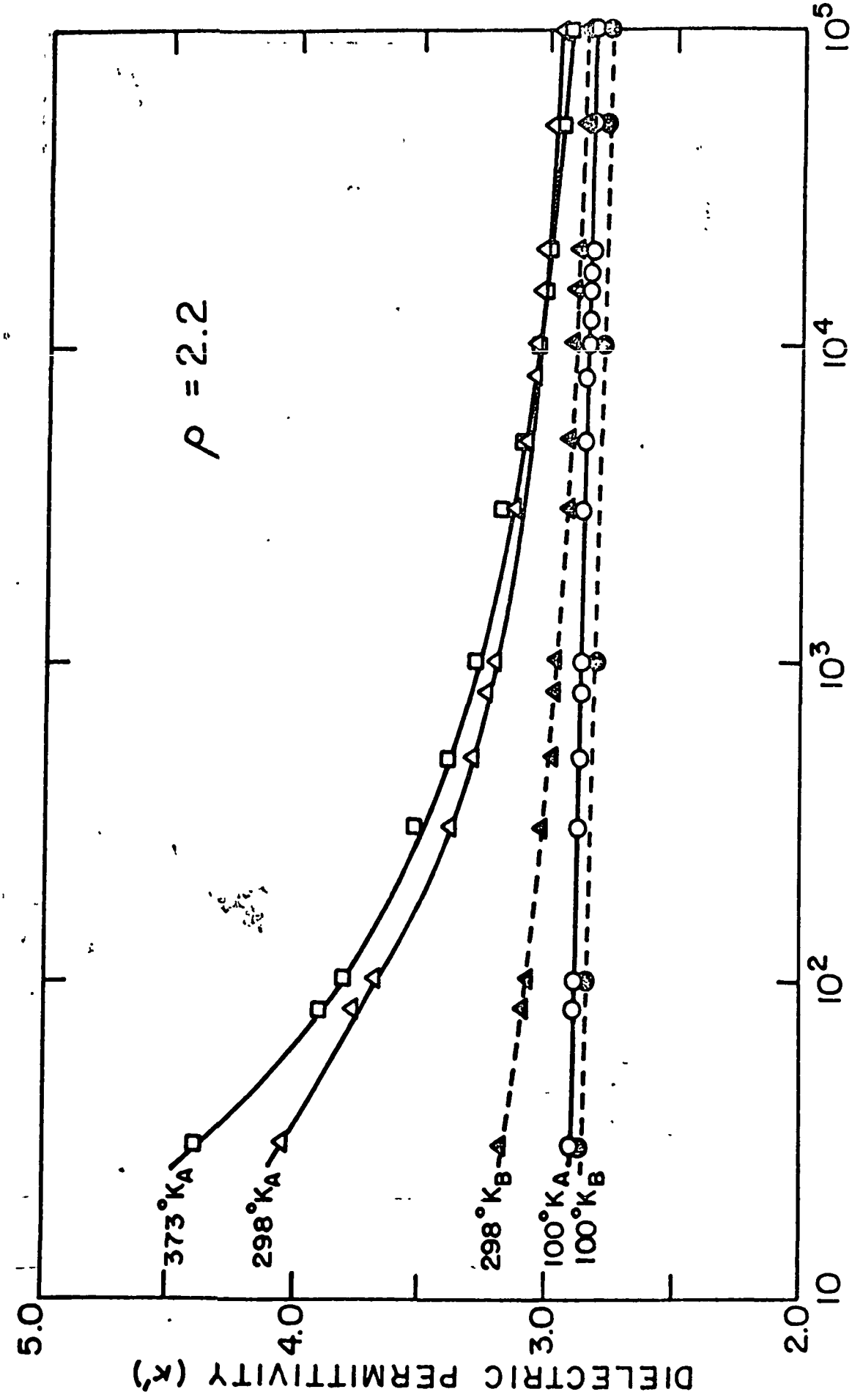

FIG. 4 (a) ALVAREZ

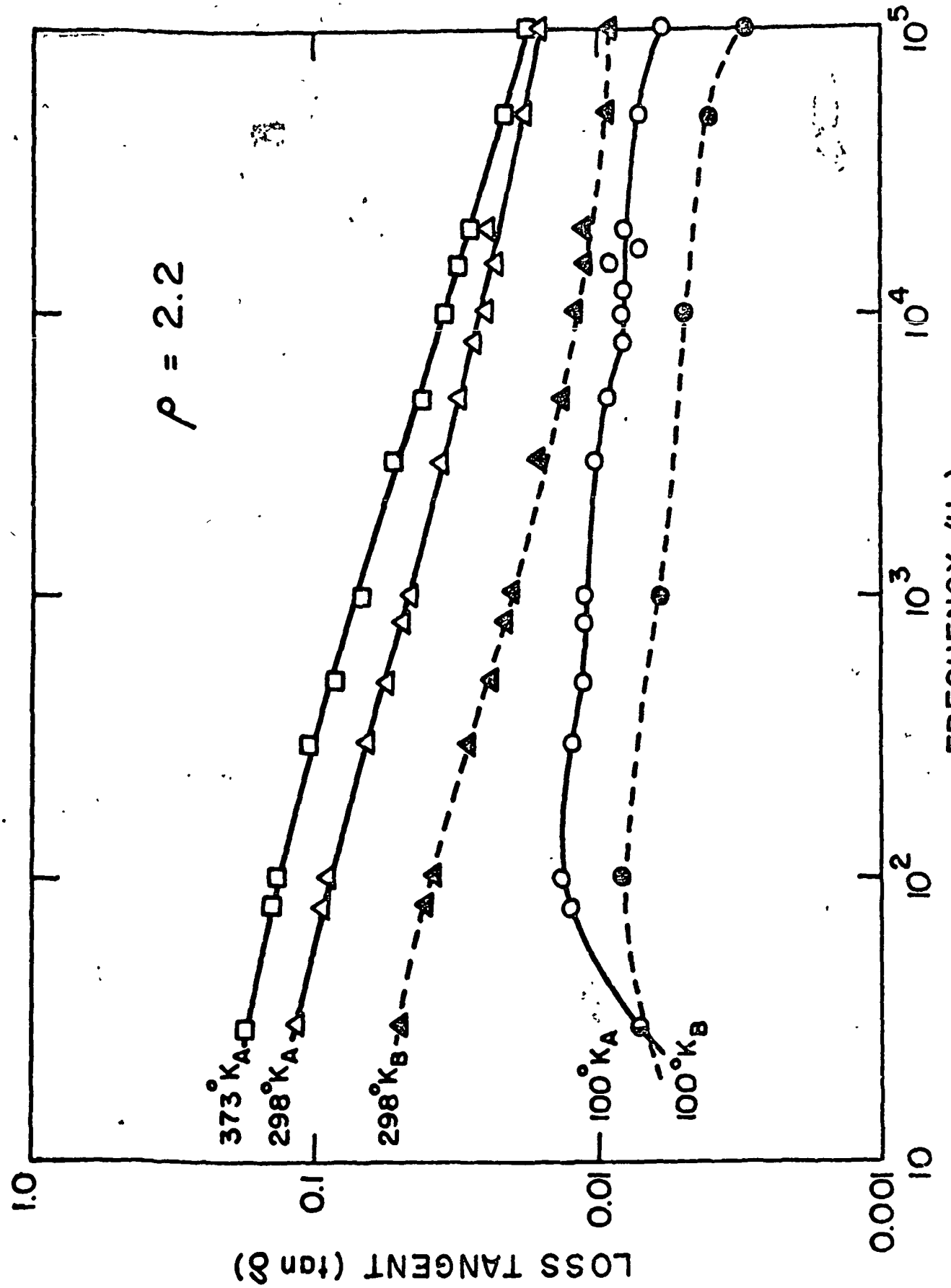

FIG 4(6) ALVAREZ

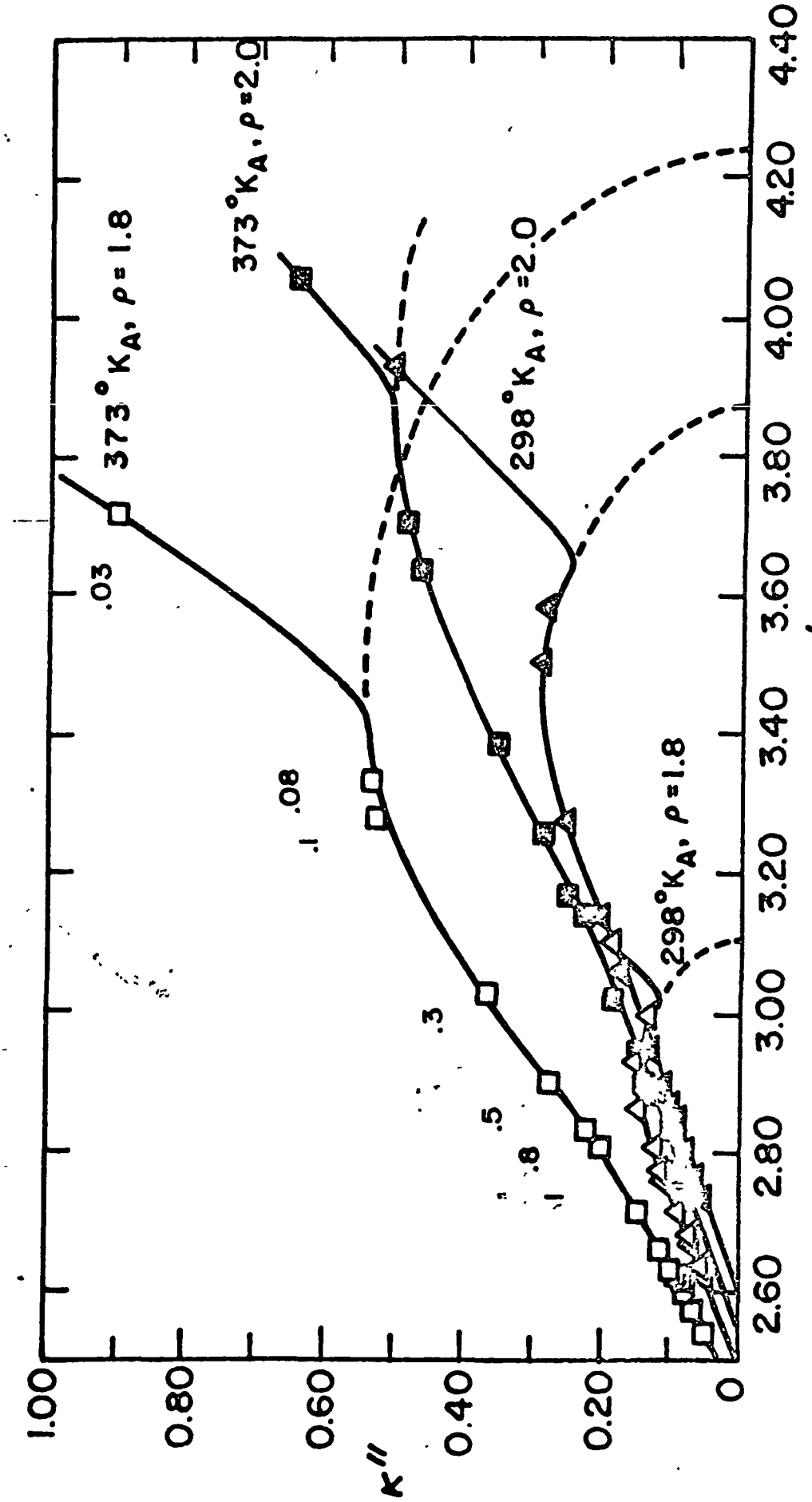

FIG. 5 ALVAREZ

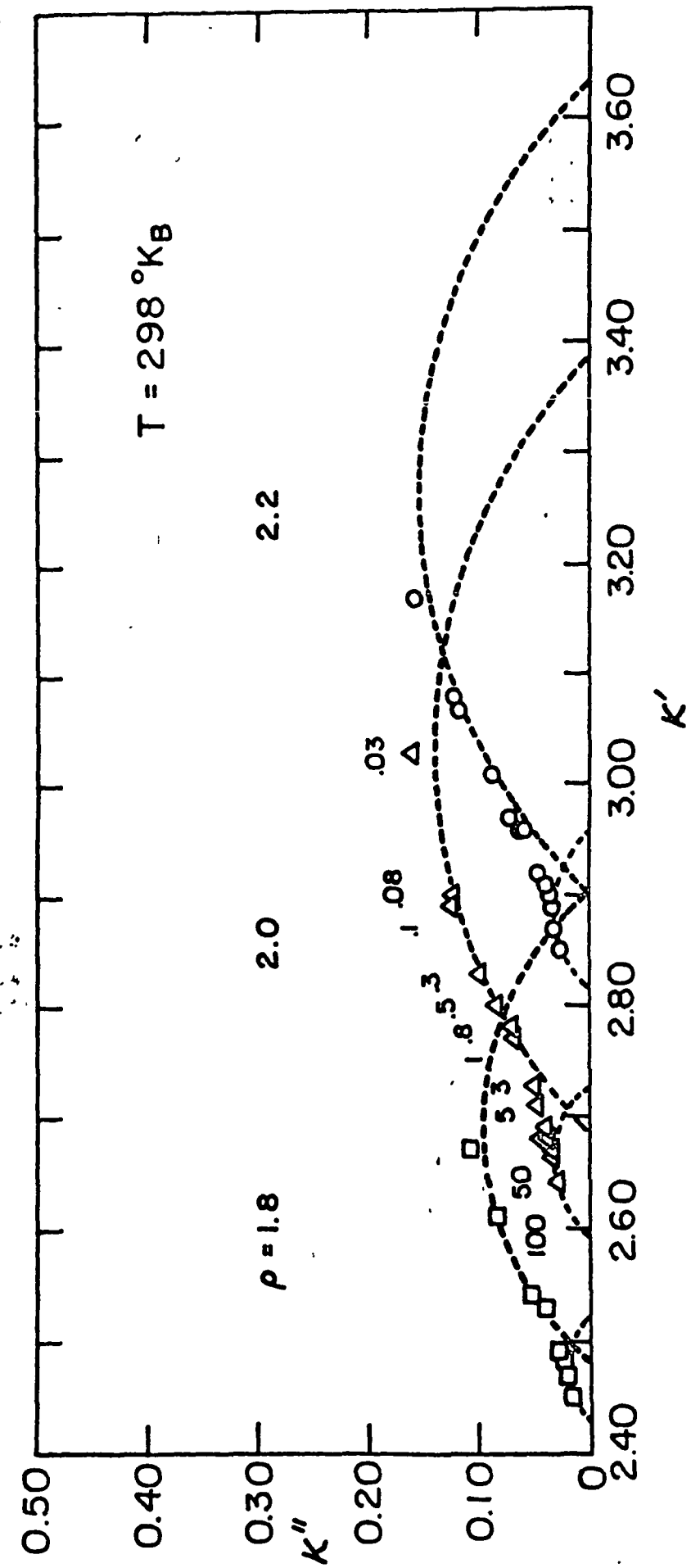

FIG 6 ALVAREZ

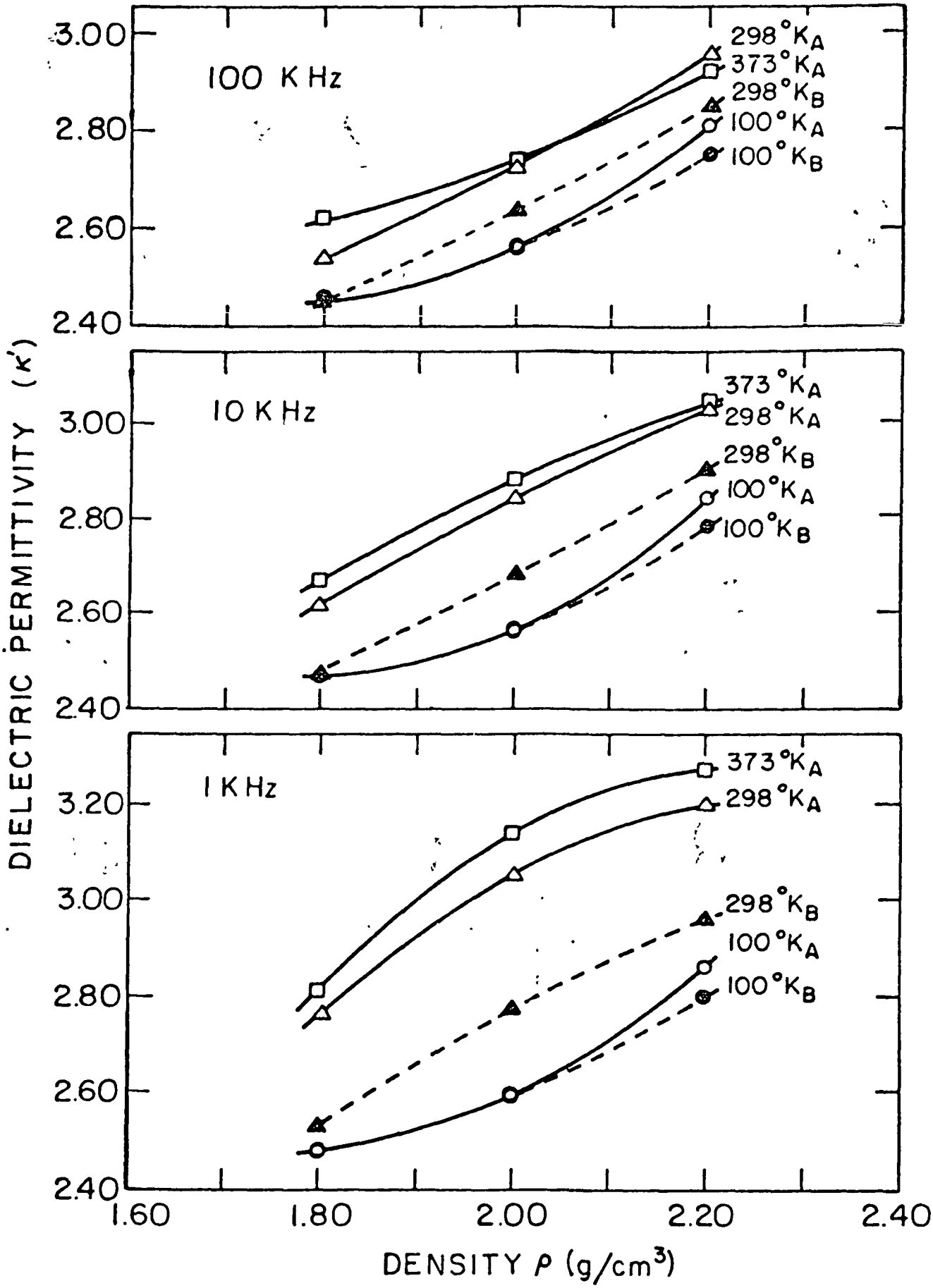

FIG 7 ALVAREZ

Complex Dielectric Permittivity in Rocks: A method for its measurement and analysis

Román Alvarez

Engineering Geoscience
University of California
Berkeley, Calif. 94720

ABSTRACT

The interfacial effects arising in electrical measurements of rocks, when a two-electrode system is used, are analyzed via the Maxwell-Wagner effect. The similarity in electrical behavior between rock samples and heterogeneous dielectrics with non-negligible ohmic conductivities leads to a general analysis of the Maxwell-Wagner effect, from which it is concluded that in order to have electrical steady state conditions in rock samples it is, in general, necessary to have volume charge accumulations at interfaces within the sample and at the electrode-sample interface. The expression for the charge accumulation at the interface as a function of frequency is obtained as well as expressions for the effective dielectric permittivity in a composite material; it is shown that the relaxation time associated with the charge accumulation and that of the effective dielectric permittivity are the same.

Given a sample consisting of two different materials it is shown that whenever both components have non-negligible ohmic conductivities, the imaginary component of the effective dielectric permittivity tends to infinity when the frequency tends to zero; such behavior is not observed when one of the two conductivities is negligible. This fact constitutes the basis of the method of

measurement for heterogeneous dielectrics with non-negligible ohmic conductivities proposed herein; it consists essentially of utilizing a dielectric with negligible ohmic and dielectric conductivities as one of the two components of the sample, which isolates the other one from the electrodes.

Theoretical examples of the behavior of such a composite material for various cases are analyzed and three experimental examples are presented. The method presents the advantage of permitting application of theory developed for dielectrics in general.

INTRODUCTION

Natural rocks are heterogeneous materials of considerable complexity from an electrical point of view. A given sample can be thought of as a multi-crystalline matrix with a system of pores among which a given degree of interconnection exist; these pores may contain some free water and, if ions are present in it, an electrolyte; in addition adsorbed water and gases are found at the matrix-air interfaces. Each component contributes to the electrical properties of the rock. The conductivity σ and the dielectric permittivity ε are the usually determined properties.[1]

σ = sigma
ε = epsilon

We shall deal with the problem of conduction effects at the electrode-sample interface when a rock sample is placed in a two-electrode system.[2] These effects are most clearly manifested in the dielectric permittivity measurements of rock samples at frequencies below 1 KHz, although this figure varies according to rock type and conditions of measurement. In any event, when the frequency tends to zero hertz, the values of dielectric permittivity increase according to an inverse power of frequency; the power value is usually found between 1 and 2, varying with author. The relative dielectric permittivity ($K = \varepsilon/\varepsilon_o$, where ε_o is the vacuum permittivity) reaches values of around 10^6 at frequencies of less than 100 Hz. At frequencies above 10^4 Hz the values of K are found to be "normal", where normal means the values to be expected from the contributions of dipolar, ionic and electronic polarizabilities in a given material. In the geophysical literature the values of $K \sim 10^6$ have often been called "abnormal", the abnormality stemming from the impossibility of explaining such values in terms of the mechanisms of polarization cited above.

[1] MKS units are used in this work.

[2] For a summary of other systems and their problems, see Fuller and Ward, 1970.

In homogeneous dielectric substances the value of K at zero frequency seldom goes above 10^2.

Rock measurements are not the only instances of K-values higher than 10^3 at frequencies of less than 1 KHz; they have also been observed in studying heterogeneous dielectrics and some types of semiconductors as well as in electrolytes.

Attempts have been made at evaluating or supressing the high K-values in rock samples at low frequencies. Some researchers have used mica sheets placed between the sample and electrodes (Tarkhov, 1948; Valeev and Parkhomenko, 1965) thereby achieving considerable reductions in the K-values. Others (Scott et al, 1967) have rejected this scheme in view of experimental problems and the lack of an adequate theoretical model to analyze the results.

The departures of K, from normal values become accentuated when measuring rocks with a considerable amount of moisture. Parkhomenko (1967) analyzes this problem and concludes that minor variations in water content may give rise to extreme variations in dielectric permittivity.

For "dry" rocks, and direct electrode-sample contact, the values of K have been found within reasonable limits for frequencies $\geqslant$ 100 Hz (Keller, 1966, p. 569; Parkhomenko, 1967, pp. 38-41). However, a tendency for K to increase has been observed at frequencies lower than 100 Hz even in rocks that have been oven and vacuum dried, (Keller and Licastro, 1959, p. 263). Furthermore, increases in K are systematically accompanied by higher losses (i.e. higher energy dissipations).

The above discussion is based primarily on measurements in rock samples. Summarizing those results one can establish that (i) the influence of the direct contacts between sample and metallic electrodes gives rise to high apparent values of dielectric permittivity K, (ii) such values can be reduced to normal values by avoiding the direct contact between sample and electrodes and (iii) a direct relation seems to exist between the ohmic conductivity of the sample and the high

values of K.

The similarity between the electrical behavior of rocks and that of heterogeneous dielectrics with non-negligible ohmic conductivities is illustrated by the works of Blechschmidt (1938), Koops (1951) and Krötzsch (1964), which also show values of $K \sim 10^3$ for frequencies below 1KHz accompanied by high energy losses. Dielectric liquids in contact with metallic electrodes yield similar results (Johnson and Cole, 1951; Dansas et al, 1967). Surprisingly the analyses made for these materials have not been fully applied to conduction phenomena in rocks.

As pointed out by Johnson and Cole (1951) the combined effects of dc (ohmic) conductivity and electrode polarization give rise to serious errors in the observed apparent dielectric permittivity and energy losses. However, suppressing electrode polarization does not suppress the effects arising from the heterogeneity of the sample, which will give rise to values of dielectric permittivity and energy losses higher than those obtained from homogeneous samples of equivalent compositions.

THE MAXWELL-WAGNER EFFECT

Discussions on the different causes of polarization in dielectrics most of the time include descriptions of dipolar, ionic and electronic mechanisms contributing to the total polarizability in given frequency ranges (Kittel, 1968; Hill et al 1969). A fourth type of contribution arises in heterogeneous materials due to accumulation of charges at the interfaces but its description is usually omitted possibly because, as Kittel (1968) points out

"This is of little fundamental interest, but it is of considerable practical interest because commercial insulating materials are usually heterogeneous."

Given the inherently heterogeneous character of rocks it should be recognized that, at least from a geophysical point of view, interfacial polarization may play an important role and deserves careful consideration in the context of electrical conduction in rocks.

The Maxwell-Wagner effect relates to the charge build-up at the interface between two media differing in conductivity and/or dielectric permittivity when a current flows across the interface. This phenomenon was first analyzed by Maxwell (1873), sec. 328; later on Wagner (1913) studied the effect of spherical particles of given conductivity and dielectric permittivity homogeneously distributed in a material of differing dielectric permittivity and zero conductivity. He found that the relaxation spectrum of such a material had a single relaxation time, presenting what is now known as a Debye relaxation in dielectrics (Debye, 1929).

Various treatments of this effect can be found in Hill et al (1969), p. 58 and p. 282, Von Hippel (1966), p. 228, Zheludev (1971), p. 474, and Arnoult et al (1965); they are equivalent inasmuch as they consider the two dielectrics having no dispersion and, thus, all the losses are due to the presence of the ohmic conductivities. It may be recognized that these conditions represent a particular case of a more general treatment, namely that of <u>dispersive</u> dielectrics with different ohmic conductivities.

We have approached the theoretical treatment of the Maxwell-Wagner effect in a way that differs from previous treatments. We consider it more general for it does not impose restrictive conditions in the dielectric permittivities of the media involved (i.e. we do not require K_1 and K_2 constants with frequency) neither is it confined to the case of sharply defined interfaces between the media.

Consider equations

$$\nabla \cdot \underset{\sim}{D} = \rho \qquad \underset{\sim}{J} = \sigma \underset{\sim}{E} \qquad \underset{\sim}{D} = \epsilon \underset{\sim}{E} \tag{1}$$

where the symbols correspond to the well known variables of electromagnetic theory; they are considered averaged over elements of volume containing several molecules

of a given material. $\underset{\sim}{D}$, $\underset{\sim}{J}$, and $\underset{\sim}{E}$ are frequency-domain variables. σ, ϵ, and ρ are frequency dependent. The dielectric permittivity ϵ and the ohmic conductivity σ will, in general, be functions of position.

With the continuity equation in the frequency domain

$$\nabla \cdot \underset{\sim}{J} = j\omega\rho \tag{2}$$

and relations (1) one can write

$$\nabla \cdot \underset{\sim}{D} = \nabla \cdot (\epsilon \underset{\sim}{E}) = \nabla\epsilon \cdot \underset{\sim}{E} + \epsilon \nabla \cdot \underset{\sim}{E} = \rho \tag{3}$$

$$\nabla \cdot \underset{\sim}{J} = \nabla \cdot (\sigma \underset{\sim}{E}) = \nabla\sigma \cdot \underset{\sim}{E} + \sigma \nabla \cdot \underset{\sim}{E} = j\omega\rho \tag{4}$$

$$\therefore \quad (\epsilon - j\frac{\sigma}{\omega}) \nabla \cdot \underset{\sim}{E} + \underset{\sim}{E} \cdot \nabla(\epsilon - j\frac{\sigma}{\omega}) = 0$$

Defining

$$\epsilon^* = \epsilon - j\frac{\sigma}{\omega} \tag{5}$$

the last expression becomes

$$\epsilon^* \nabla \cdot \underset{\sim}{E} + \underset{\sim}{E} \cdot \nabla\epsilon^* = 0$$

and from Gauss' theorem the condition

$$\epsilon^* E_n = \text{const} \tag{6}$$

is satisfied across an interface, $\mathcal{E}_n$ being the normal component of $\underset{\sim}{\mathcal{E}}$ to the interface.

The treatment of the classical Maxwell-Wagner effect requires ϵ and σ constants with frequency. Let these conditions hold in the following discussion. Further ahead we shall come back to the case of dispersive dielectrics. From equations (2), (3), and (4)

$$j\omega\rho(\omega) = -\frac{\sigma}{\epsilon}\rho(\omega) + \frac{\sigma^2}{\epsilon}\left[\nabla(\epsilon/\sigma)\cdot\underset{\sim}{\mathcal{E}}(\omega)\right] \qquad (7)$$

and the steady state condition $\nabla\cdot\underset{\sim}{J} = 0$ (this implies either $\rho = 0$ for $\omega \neq 0$ or $\omega = 0$. The case $\rho = 0$ is trivial; therefore we shall consider $\omega = 0$) one obtains

$$\rho(0) = \sigma\left[\nabla(\epsilon/\sigma)\cdot\underset{\sim}{\mathcal{E}}(0)\right] \qquad (8)$$

where $\rho(0)$ and $\underset{\sim}{\mathcal{E}}(0)$ indicate the values of $\rho(\omega)$ and $\underset{\sim}{\mathcal{E}}(\omega)$ at $\omega = 0$.

It can be seen that if ϵ and/or σ vary as a function of position in a given volume, the value of $\nabla(\epsilon/\sigma)$ will be non-zero; consequently charge accumulations will occur as defined by ρ in equation (8). If ϵ and σ are uniform throughout such a volume, then $\rho = 0$. The term $\nabla(\epsilon/\sigma)$ is the one that gives rise to the Maxwell-Wagner effect.

Therefore if a material is homogeneous it has no volume charge concentrations in the steady state, whereas if the material is inhomogeneous steady state conditions cannot be realized without the presence of a volume charge density as defined by equation (8). Furthermore the volume charge $\rho(x, y, z)$ is a function of the electric field $\underset{\sim}{\mathcal{E}}(x, y, z)$ at that position.

Equation (8) stresses the fact that in order to have a Maxwell-Wagner effect it is sufficient to have either ϵ or σ varying in a region, a fact often obscured in the classical presentations by the assumption that the two media differ in both ϵ and σ. Notice, however, that no Maxwell-Wagner effect will appear if the ratio ϵ/σ has the same value in both media, even if the individual values of ϵ

and σ are different for each medium.

Another aspect of the Maxwell-Wagner effect is brought about by the vector relation between the gradient of the ϵ/σ properties and the electric field: only the normal component of the electric field to the interface will contribute to space-charge build-up. The interface we refer to is a surface, say z = const. in a cartesian coordinate system, that has the same ϵ and σ values at any point on that surface; a volume in which ϵ and/or σ vary would be made out of a succession of such surfaces.

Time-domain excitation

Equation (7) can be written in time domain by means of a Fourier transformation:

$$\frac{\partial \rho(t)}{\partial t} = \frac{-\sigma}{\epsilon}\rho(t) + \frac{\sigma^2}{\epsilon}\left[\nabla(\epsilon/\sigma)\cdot \underline{E}(t)\right] \qquad (9)$$

where the dependence of ρ on time has been explicitly indicated. σ and ϵ are constants in time and $\underline{E}(t)$ is the time dependent electric field.
By requiring now that $\nabla\cdot\underline{J} = 0$, a time independent relation is obtained

$$\rho_o = \sigma\,\nabla(\epsilon/\sigma)\cdot \underline{E}_o \qquad (10)$$

Equation (10) holds for dc steady state flow of current in a material in which $\nabla(\epsilon/\sigma) \neq 0$. In particular, if a dc excitation is applied to a sample consisting of two slabs of area A and thicknesses d_1 and d_2 with electrical properties ϵ_1, σ_1 and ϵ_2, σ_2 respectively, a charge concentration will build up at the interface between media 1 and 2. When steady state conditions are reached the charge concentration is given by equation (10).

The charge build up can also be seen through Zheludev's (1971) derivation for the current density and electric fields in such a material:

From the continuity of conduction plus displacement currents at the interface

$$\sigma_1 \underline{E}_1(t) + \epsilon_1 \frac{\partial \underline{E}_1(t)}{\partial t} = \sigma_2 \underline{E}_2(t) + \epsilon_2 \frac{\partial \underline{E}_2(t)}{\partial t} \qquad (11)$$

and the condition

$$E_1(t)d_1 + E_2(t)d_2 = V \tag{12}$$

where V is the externally applied dc voltage, he obtains

$$E_1(t) = \frac{(\epsilon_2\sigma_1 - \epsilon_1\sigma_2)d_2V}{(\epsilon_1 d_1 + \epsilon_2 d_1)(\sigma_1 d_2 + \sigma_2 d_1)} e^{-t/\tau} + \frac{\sigma_2 V}{\sigma_1 d_2 + \sigma_2 d_1} \tag{13}$$

and

$$J(t) = \frac{(\epsilon_2\sigma_1 - \epsilon_1\sigma_2)^2 d_1 d_2 V}{(\epsilon_1 d_2 + \epsilon_2 d_1)^2(\sigma_1 d_2 + \sigma_2 d_1)} e^{-t/\tau} + \frac{\sigma_1\sigma_2 V}{\sigma_1 d_2 + \sigma_2 d_1} \tag{14}$$

with

$$\tau = \frac{\epsilon_1 d_2 + \epsilon_2 d_1}{\sigma_1 d_2 + \sigma_2 d_1}$$

where J is given by either side of equation (11). Notice that

$$J = J_o = \frac{\sigma_1\sigma_2 V}{\sigma_1 d_2 + \sigma_2 d_1} \quad \text{in the steady state.}$$

The response of the current to a voltage V applied between times $t = 0$ and $t = t_1$; is shown in Figure 1. At $t = 0$ the current J acquires its maximum value. The first term on equation (14) tends to zero as t increases while the second remains constant. The first term is known as the absorption current and it flows as long as the accumulation of free charge continues at the interface. The second term corresponds to a residual current (i.e. the current J_o flowing in the steady state). When the external voltage is supressed at $t = t_1$ the charge stored at the interface is retrieved in the form of a current described by the first term in equation (14), but of opposite polarity.

This type of response we have systematically observed in resistive rock samples (i.e. granite, limestone, etc.) when metallic electrodes are in contact with the sample (Alvarez, 1971). Low resistivity samples (i.e. pyrite, galena, etc.) in contact with metallic electrodes do not show such a behavior. Similar examples can be found in Parkhomènko (1971).

The previous development corresponds to a "sharp" interface between media 1 and 2 (i.e. the electrical properties change abruptly at the interface). In this case the volume charge distribution (ρ) becomes a surface charge distribution (Σ) since only at the interfacial plane $\nabla(\epsilon/\sigma) \neq 0$.

However, an equivalence can be established between the charge stored at a sharp interface and the charge stored in a volume (Alvarez, 1972, p. 21). Consider two media of ϵ_1 , σ_1 and ϵ_2, σ_2 separated by a volume $\mathcal{V}$, of area A normal to the applied field, in which ϵ and σ are arbitrary functions of position. Then, under steady state conditions, the amount of charge Q stored in the volume $\mathcal{V}$ is the same as the charge stored at a sharp interface of equal area A between the two media, provided the current density Jo is the same in both cases. The surface charge density Σ is given by

$$\Sigma = \frac{Q}{A} = J_o \left(\frac{\epsilon_2}{\sigma_2} - \frac{\epsilon_1}{\sigma_1} \right) \tag{15}$$

With equations (12) and (14) (steady state) substituted in equation (15) the surface charge density is obtained in terms of the fields E_1 and E_2 (steady state values) in materials 1 and 2, as

$$\Sigma = \frac{E_1 d_1 + E_2 d_2}{\sigma_1 d_2 + \sigma_2 d_1} \left(\epsilon_2 \sigma_1 - \epsilon_1 \sigma_2 \right) \tag{16}$$

Frequency-domain excitation

We turn now to the analysis of the response of a material presenting spatial variations in ϵ and/or σ when the applied voltage is of the form

$$V = V_o e^{j\omega t}$$

We are interested, as a first step, in determining the behavior of the charge concentration as a function of frequency at the interface between two materials in which ϵ and σ are frequency independent.

From equation (7)

$$\rho(\omega) = \frac{\sigma \nabla(\epsilon/\sigma) \cdot \underset{\sim}{E}}{1 + j\omega \epsilon/\sigma} = \frac{\rho(0)}{1 + j\omega\tau} \tag{17}$$

where $\rho(o)$ is the charge concentration at $\omega = 0$ given by equation (8). This is the maximum value ρ can attain at the interface for a given $\underline{\mathcal{E}}$ and a given contrast between the ϵ/σ values in both media. For $\omega > 0$ $\rho < \rho_0$; furthermore if $\omega \to \infty$ $\rho \to 0$.

There is a phase lag between the applied field and the charge concentration given by

$$\phi = - \tan^{-1} \frac{\omega \epsilon}{\sigma}$$

corresponding to a loss tangent

$$\tan \delta = \frac{\sigma}{\omega \epsilon}$$

From these considerations it can be seen that the charge concentration behaves in the same fashion, except for some constants, as does a dielectric presenting a Debye relaxation, i. e. such a dielectric has zero ohmic conductivity and is represented by

$$\epsilon^* = a + \frac{b}{1 + j\omega\tau} \qquad (18)$$

where ϵ^* is the complex dielectric permittivity and a and b are constants. This comparison hints immediately at the origin of the Debye-like behavior of a substance presenting the Maxwell-Wagner effect.

Equation (17) cannot be directly applied to the case of a sharp interface to yield the surface charge density $\sum$ as a function of frequency. The difficulty arises from the values to be assigned to ϵ and σ at the interface (Alvarez, 1972, p. 27). A possible way to obtain $\sum$ for the two-layer material we have been discussing is as follows:

From equations (11) and (12) in the frequency domain

$$\mathcal{E}_1(\omega) = \frac{(\sigma_2 + j\omega\epsilon_2)\, V}{(\sigma_1 d_2 + \sigma_2 d_1) + j\omega(\epsilon_2 d_1 + \epsilon_1 d_2)} \qquad (19)$$

The surface charge density at the sharp interface is given by

$$\sum = \epsilon_2 \mathcal{E}_2 - \epsilon_1 \mathcal{E}_1 = \frac{\epsilon_2 V}{d_2} - \left(\frac{d_1}{d_2}\epsilon_2 + \epsilon_1\right)\mathcal{E}_1 \; ; \qquad (20)$$

substituting equation (19) in equation (20)

$$\sum^*(\omega) = \frac{\sum(0)}{1 + j\omega\tau} \qquad (21)$$

where

$$\sum(0) = \frac{V_0}{\sigma_1 d_2 + \sigma_2 d_1}\left(\epsilon_2\sigma_1 - \epsilon_1\sigma_2\right) \quad \text{and} \quad \tau = \frac{\epsilon_2 d_1 + \epsilon_1 d_2}{\sigma_2 d_1 + \sigma_1 d_2}$$

The symbol $\sum^*$ shall be used in analogy with the complex dielectric permittivity ϵ^* to denote the complex character of the function. The real and imaginary parts of $\sum^*$ will be denoted $\sum'$ and $\sum''$ respectively. $\sum^*$ plots as a circle in the complex plane.

Complex dielectric permittivity: definitions. - The expression

$$\epsilon^* = \epsilon' - j\epsilon''$$

usually represents the complex dielectric permittivity of a homogeneous material. The real part (ϵ') corresponds to the dielectric "constant" and the imaginary part (ϵ'') to the energy losses in the material.

Energy losses arise from two different mechanisms: (1) rotation of dipoles or bound charges and (2) motion of free charge carriers. Thus, ϵ'' contains two parts

$$\epsilon'' = \epsilon''_{DIEL} + \frac{\sigma_{OHMIC}}{\omega}$$

It is common practice to associate the dielectric losses ϵ''_{DIEL} to a "dielectric conductivity"

$$\sigma_{DIEL} = \omega\,\epsilon''_{DIEL} \qquad \therefore \qquad \epsilon'' = \frac{\sigma_{DIEL} + \sigma_{OHMIC}}{\omega}$$

But, unfortunately, lumping σ_{DIEL} and σ_{OHMIC} in one single conductivity has led to the widespread but erroneous practice of applying it in relations as

$$\sigma = \omega\epsilon'' \qquad \text{or} \qquad \sigma = \omega\epsilon' \tan\delta$$

where σ , then, is implicitly considered to be σ_{OHMIC} or σ_{DIEL} only. The experimentally determined parameters are usually ϵ' and $tan\delta$.

Under some circumstances the error will be small, that is when $\sigma_{OHMIC} \gg \sigma_{DIEL}$ (or viceversa when it is assumed that there is only σ_{DIEL} in the sample). But, for resistive rock samples σ_{OHMIC} may be comparable in some frequency range to σ_{DIEL} and the error will be considerable for that case.

Warnings about such a way of proceeding have been previously made (Campbell and Ulrichs, 1969), but for some reason they have not received adequate attention. Furthermore, there are standard procedures for evaluation of both contributions when simultaneously present in one sample (Brockman and White, 1971).

The method to be introduced allows for the determination of both σ_{DIEL} and σ_{OHMIC} . The following convention will be adopted:

$$\epsilon^* = \epsilon - j \frac{\sigma_{OHMIC}}{\omega}$$

where

$$\epsilon = \epsilon' - j \epsilon''_{DIEL}$$

There is no need to maintain the subindexes DIEL and OHMIC; it will be understood that ϵ'' will refer only to ϵ''_{DIEL} and σ to σ_{OHMIC} . Thus

$$\epsilon^* = \epsilon' - j\epsilon'' - j \frac{\sigma}{\omega} = \epsilon - j \frac{\sigma}{\omega} \qquad (22)$$

Finally, whenever the material is not known to be homogeneous for certain, misleading values of dielectric permittivity may be found experimentally (Hill et al, 1969) and the ratio C/C_o should be considered as a relative effective (or apparent) dielectric permittivity K_{eff}, where C is the experimentally determined value of the capacity of the sample and C_o is its geometrical capacitance. Furthermore

$$\epsilon_{eff} = K_{eff}\, \epsilon_o$$

where ϵ_o is the free space permittivity and ϵ_{eff} is the effective (or apparent) dielectric permittivity of the sample; ϵ_{eff} may be complex and in such a case it

will be written as ϵ^*_{eff}. Since we know that the samples we are dealing with are not homogeneous ϵ^*_{eff} will be used throughout the following developments.

General expressions for ϵ^*_{eff} - Equations (1) through (6) were established for ϵ and σ frequency dependent. In the subsequent developments we analyzed various cases in which ϵ and σ were restricted to be frequency independent. We shall now consider ϵ to be frequency dependent while maintaining σ frequency independent. These conditions correspond to dispersive dielectrics having constant ohmic conductivities. The case in which the ohmic conductivities are frequency dependent shall not be treated here, although the same formalism can be applied in such a case.

Consider the two-layer material described previously. From equation (6)

$$\epsilon_1^* \mathcal{E}_1 = \epsilon^*_{eff} \mathcal{E}_{eff} \qquad \text{with} \quad \mathcal{E}_{eff} = \frac{\mathcal{V}}{d}$$

where $\mathcal{V}$ is the voltage across the sample and d is its total thickness. The interface is considered normal to the field; thus subindex n for the normal component of the fields has been dropped.

Substituting equation (19) in the above expression one obtains

$$\epsilon^*_{eff} = \frac{(\epsilon_1 - j\frac{\sigma_1}{\omega})(\sigma_2 + j\omega\epsilon_2)\, d}{(\sigma_1 d_2 + \sigma_2 d_1) + j\omega(\epsilon_1 d_2 + \epsilon_2 d_1)} \tag{23}$$

which can be finally written as

$$\epsilon^*_{eff} = \frac{(d_1+d_2)\,\epsilon_1^*\,\epsilon_2^*}{\epsilon_1^* d_2 + \epsilon_2^* d_1} \tag{24}$$

or as

$$\epsilon^*_{eff} = \frac{\epsilon_1 - j\frac{\sigma_1}{\omega}}{\epsilon_1 d_2 + \epsilon_2 d_1}(d_1+d_2)\left[\epsilon_2 - \frac{d_2}{\mathcal{V}}\sum^*(\omega)\right] \tag{25}$$

Equations (24) and (25) are the general expressions for the effective dielectric permittivity of a composite material made out of two homogeneous slabs of area A and thicknesses d_1 and d_2, and characterized electrically by ϵ_1^* and ϵ_2^*. Equation (25) gives the explicit dependence of ϵ^*_{eff} on the charge concentration at the

interface. Furthermore, the relaxation time obtained for $\sum^*$ and the relaxation time associated with the ϵ^*_{eff} of a composite material with non-dispersive dielectrics (Von Hippel, 1966; Zheludev, 1971), are the same.

The experimentally determined quantities are the components of ϵ^*_{eff}, namely ϵ'_{eff} and ϵ''_{eff}. The two limiting cases $\omega \to 0$ and $\omega \to \infty$, for the components of ϵ^*_{eff}, are of interest:

From equation (25)

$$\epsilon'_{eff} \underset{\omega \to 0}{\longrightarrow} \frac{(d_1+d_2)\epsilon'_1\sigma_2}{\sigma_1 d_2 + \sigma_2 d_1} \quad \text{and} \quad \epsilon''_{eff} \underset{\omega \to 0}{\longrightarrow} -\infty \tag{26}$$

$$\epsilon''_{eff} \underset{\omega \to \infty}{\longrightarrow} \frac{(d_1+d_2)\epsilon'_1\epsilon'_2}{\epsilon'_1 d_2 + \epsilon'_2 d_1} \quad \text{and} \quad \epsilon''_{eff} \underset{\omega \to \infty}{\longrightarrow} 0 \tag{27}$$

where we have written ϵ'_1 and ϵ'_2 instead of ϵ_1 and ϵ_2 because ϵ''_1 and ϵ''_2 will be zero when $\omega \to 0$ and when $\omega \to \infty$.

From the limiting case $\omega \to 0$ it is seen that the absolute value of $\epsilon''_{eff} \to -\infty$; we shall label this a "divergent behavior"; thus, there will be cases in which it will become very difficult to determine experimentally, with any accuracy, the two components of ϵ^*_{eff} in this limit since one of them will be much larger than the other. It is worth noticing that the divergence occurs only for one component and only in one limiting case; in fact, the problems arise from the two ohmic conductivities σ_1 and σ_2 being non-negligible., If one of them (i.e. σ_1 in equation (25) is negligible, such divergence is eliminated and the two components of ϵ^*_{eff} become finite in the two limiting cases expressed by relations (26) and (27).

METHOD FOR DETERMINATION OF ϵ AND σ IN ROCK SPECIMENS

The scheme for measuring electrical rock properties we shall introduce consists of placing a "good" (or lossless) dielectric material (i.e. one in which σ_{OHMIC} and σ_{DIEL} are negligible) between the electrodes and the sample to be analyzed. The former is, of course, considered as homogeneous, whereas the latter is known or assumed to be heterogeneous. The composite sample, in

any event, will be heterogeneous. We want to apply the results obtained for two homogeneous materials to a system composed of one homogeneous material and one heterogeneous material. This way of proceeding is justified inasmuch as the heterogeneous material can be represented by an effective dielectric permittivity which may itself be constituted by two or more different electrical components.

Therefore we shall be dealing with two Maxwell-Wagner effects of different origin; one, deliberately established and controlled by the interfaces between the good dielectric and the sample and, the other, occurring within the sample and controlled by its constituents and their particular distribution (i.e. geometry). The first one we can alter by varying the thickness of the good dielectric as will be shown later, the second we cannot modify without changing the properties of the sample.

Once $\mathcal{E}^*_{eff}$ has been obtained experimentally as a function of frequency it will be possible to model it theoretically; this can be done by assuming a specific functional form for $\mathcal{E}^*_{eff}$ and fitting the model parameters to the data. The final properties of the sample will be given as a set of parameters, one being ohmic conductivity and the others related to the dielectric properties. We shall elaborate more about the modelling once we have examined various other problems related to the method.

The discussion about $\mathcal{E}^*_{eff}$ was centered around a specimen composed of two homogeneous materials. It can be easily shown that the results obtained are not altered if these materials are subdivided into slabs and stacked in series, while maintaining the condition that the total lengths d_1 and d_2 of the components remain unchanged. From the arguments leading to equation (15) it follows that if the first and last elements in the stacked sample are of the same material, say 1, the net charge stored in the sample is zero, whereas if they correspond to different materials the net charge, added up from all interfaces within the material, will be equal to the charge stored at the single interface.

As a consequence of these considerations the arrangements in Figures 2(a) and (b) are equivalent as far as total impedance is concerned; the only difference between them is that in Figure 2(a) the net charge stored is zero whereas in Figure 2(b) it is different from zero.

Consider material 4 as made out of an arrangement of two homogeneous materials, 1 and 2, in contact (Figure 2c), while assuming that material 3 is a good dielectric. The $\mathcal{E}^*_{eff}$ of material 4 will be given by equations (24) or (25), and according to the limiting case given by equation (26) its imaginary component will diverge when $\omega \to 0$. The question arises regarding possible divergencies in the response of the composite material formed by $\mathcal{E}^*_3$ and $\mathcal{E}^*_4$ since the last one presents the divergent behavior mentioned above.

The total effective permittivity of the composite material in Figure 2(c) can be written as

$$\mathcal{E}^*_T = \frac{(d_3 + d_4)\,\mathcal{E}'_3 \mathcal{E}^*_4}{\mathcal{E}'_3 d_4 + \mathcal{E}^*_4 d_3}$$

where $\mathcal{E}^*_3 = \mathcal{E}'_3$ and $\mathcal{E}^*_4$ is the effective permittivity of $\mathcal{E}^*_1$ and $\mathcal{E}^*_2$ as given by equation (24).

The limiting cases $\omega \to 0$ and $\omega \to \infty$ show that no divergencies appear in the components of $\mathcal{E}'_T$ and $\mathcal{E}''_T$. If material 4 was constituted of three or more components, an iteration of the process used to obtain $\mathcal{E}^*_T$ shows that these results still hold. As long as the two end materials are good dielectrics the divergencies will be avoided. On the contrary, if material 3 is a metal (i.e. an electrode) a similar analysis (Alvarez, 1972, p. 29) shows that the divergent behavior reappears when $\omega \to 0$.

The two domains of absorption

In what follows material 1 will be the good dielectric and material 2 will represent the sample to be analyzed. In the usual treatments of the Maxwell-Wagner effect it is implicitly or explicitly assumed that the dielectrics involved are non-dispersive (i.e. $\mathcal{E}''_1 = \mathcal{E}''_2 = 0$); this makes the conductivities

σ_1 and σ_2 responsible for the Debye-type behavior, except for the divergence at low frequencies. If material 1 is a good dielectric the Debye-type behavior of the composite material is complete even at low frequencies (i.e. $\varepsilon^*_{eff} \to 0$ when $\omega \to 0$). This case has been treated by Arnoult et al (1965). It is easily realized that the treatment of the Maxwell-Wagner effect under the restriction $\varepsilon_1'' = \varepsilon_2'' = 0$ strongly limits its applicability. If this restriction is relaxed, only for one material, one can then analyze dispersive dielectrics having non-negligible ohmic conductivities such as rock samples and a series of heterogeneous semiconductors: ceramics, ferrites and the like.

The only attempt, known to this author, to treat the Maxwell-Wagner effect considering a dispersive dielectric is that of Dansas et al (1967). They proposed that if two materials of thicknesses d_1 and d_2 are placed together forming a sample, one of them being a good dielectric (i.e. $\varepsilon_1^* = \varepsilon_1'$) and the other presenting a Debve relaxation and ohmic conductivity σ_2 ; i.e.

$$\varepsilon_2^* = \varepsilon'_{\infty 2} + \frac{\varepsilon'_{o2} - \varepsilon'_{\infty 2}}{1 + j\omega\tau_2} - j\,\frac{\sigma_2}{\omega}$$

then, the effective dielectric permittivity of the composite sample can be expressed as

$$\varepsilon^*_{eff} = \varepsilon'_{\infty\beta} + \frac{\varepsilon'_{o\beta} - \varepsilon'_{\infty\beta}}{1 + j\omega\tau_\beta} + \frac{\varepsilon'_{o\alpha} - \varepsilon'_{\infty\alpha}}{1 + j\omega\tau_\alpha}$$

where subindexes α and β refer to two different domains of absorption (Figure 3).

The α-domain corresponds to a low-frequency energy loss due to the motion of free charge carriers (i.e. due to the Maxwell-Wagner effect) and the β-domain corresponds to dielectric losses arising from the dispersion of material 2.

They claim that the two domains plot as semicircles as shown in Figure 3. However, we have shown that this is an erroneous result (Alvarez, 1972, p. 46) since the point at which the α- and β-domains meet is not a zero; at most it is a minimum. Consequently the two domains of absorption cannot be represented by semicircles.

Instead of their expression for ε^*_{eff} we obtained its components as

$$\varepsilon'_{eff} = (1+Q)\varepsilon'_1 \left[1 - \frac{Q\varepsilon'_1 \left(\varepsilon'_{\infty 2} + Q\varepsilon'_1 + \frac{\varepsilon'_{o2} - \varepsilon'_{\infty 2}}{1+\omega^2 \tau_2^2} \right)}{\left[\varepsilon'_{\infty 2} + Q\varepsilon'_1 + \frac{\varepsilon'_{o2} - \varepsilon'_{\infty 2}}{1+\omega^2 \tau_2^2} \right]^2 + \left[\frac{\varepsilon'_{o2} - \varepsilon'_{\infty 2}}{1+\omega^2 \tau_2^2} \omega \tau_2 + \frac{\sigma_2}{\omega} \right]^2} \right] \qquad (28)$$

and

$$\varepsilon''_{eff} = -(1+Q)\varepsilon'_1 \frac{Q\varepsilon'_1 \left(\frac{\varepsilon'_{o2} - \varepsilon'_{\infty 2}}{1+\omega^2 \tau_2^2} \omega \tau_2 + \frac{\sigma_2}{\omega} \right)}{\left[\varepsilon'_{\infty 2} + Q\varepsilon'_1 + \frac{\varepsilon'_{o2} - \varepsilon'_{\infty 2}}{1+\omega^2 \tau_2^2} \right]^2 + \left[\frac{\varepsilon'_{o2} - \varepsilon'_{\infty 2}}{1+\omega^2 \tau_2^2} \omega \tau_2 + \frac{\sigma_2}{\omega} \right]^2} \qquad (29)$$

by substituting the given values of ε^*_1 and ε^*_2 in equation (24), and with $Q = \frac{d_2}{d_1}$.

Figures 4, 5 and 6 show plots in the complex plane of these functions when specific values are assigned to the parameters involved. The existence of the two absorption domains is readily discernible. The data points do not plot in semicircles (dashed lines).

Substances with a distribution of relaxation times

In the previous discussion we have dealt with a substance presenting a Debye relaxation and a given ohmic conductivity; this is the case treated by Dansas et al (1967). This, of course, is a particular model and one should not be surprised of finding substances that do not behave in the way prescribed by the corresponding ε^*_{eff} (i.e. equations (28) and (29)). But nothing in our previous treatment prevents us from generalizing the considerations made for the Debye substance to other types of relaxations.

This generalization is of importance since it will permit us to treat substances that present a distribution of relaxation times, rather than a single one as in a Debye substance. Multi-crystalline materials, such as rocks, are likely to present this behavior. As illustrations of applicability of the method we have chosen the functions known as the Cole-Cole arc (Cole and Cole, 1941) and the Cole-Davidson arc (Davidson and Cole, 1951) which represent cases of substances exhibiting a continuous distribution of Debye relaxation times.

The Cole-Cole arc is represented by

$$\varepsilon^* = \varepsilon'_\infty + \frac{\varepsilon'_o - \varepsilon'_\infty}{1 + (j\omega\tau)^{1-h}} \qquad 0 \le h < 1$$

and its plot corresponds to a semicircle whose center lies below the K' axis, the parameter h is a measure of how much the behavior differs from the corresponding Debye relaxation process (i.e. when h = 0). The Cole-Cole arc corresponds to a symmetrical distribution of relaxation times.

Assuming that material 2 behaves in this manner and has ohmic conductivity σ_2, and that material 1 is a good dielectric we want to find the corresponding ε^*_{eff} (i.e. equation 24).

Since $$\varepsilon_1^* = \varepsilon'_1$$

and $$\varepsilon_2^* = \varepsilon'_{\infty 2} + \frac{\varepsilon'_{o2} - \varepsilon'_{\infty 2}}{1 + (j\omega\tau_2)^{1-h}} - j\frac{\sigma_2}{\omega} ,$$

and defining $$R = 1 + \cos\left[\frac{\pi}{2}(1-h)\right](\omega\tau_2)^{1-h} \qquad \pi = pi$$

and $$I = \sin\left[\frac{\pi}{2}(1-h)\right](\omega\tau_2)^{1-h} ,$$

then

$$\varepsilon'_{eff} = (1+Q)\varepsilon'_1\left[1 - \frac{Q\varepsilon'_1\left[\varepsilon'_{\infty 2} + Q\varepsilon'_1 + \frac{(\varepsilon'_{o2} - \varepsilon'_{\infty 2})R}{R^2 + I^2}\right]}{\left[\varepsilon'_{\infty 2} + Q\varepsilon'_1 + \frac{(\varepsilon'_{o2} - \varepsilon'_{\infty 2})R}{R^2 + I^2}\right]^2 + \left[\frac{(\varepsilon'_{o2} - \varepsilon'_{\infty 2})I}{R^2 + I^2} + \frac{\sigma_2}{\omega}\right]^2}\right] \qquad (30)$$

and

$$\varepsilon''_{eff} = -(1+Q)\varepsilon'_1 \frac{Q\varepsilon'_1\left[\frac{\varepsilon'_{o2} - \varepsilon'_{\infty 2}}{R^2 + I^2} I + \frac{\sigma_2}{\omega}\right]}{\left[\varepsilon'_{\infty 2} + Q\varepsilon'_1 + \frac{(\varepsilon'_{o2} - \varepsilon'_{\infty 2})R}{R^2 + I^2}\right]^2 + \left[\frac{(\varepsilon'_{o2} - \varepsilon'_{\infty 2})I}{R^2 + I^2} + \frac{\sigma_2}{\omega}\right]^2} \qquad (31)$$

are the components of ε^*_{eff} when the dispersive sample presents a Cole-Cole distribution of relaxation times.

The Cole-Davidson arc is represented by

$$\varepsilon^* = \varepsilon'_\infty + \frac{\varepsilon'_o - \varepsilon'_\infty}{(1+j\omega\tau)^\alpha} \qquad 0<\alpha\leq 1$$

when plotted in the complex plane this function is a skewed arc, α being a measure of skewness. This distribution of relaxation times is not symmetrical, rather it consists of contributions that diminish in importance as the frequency increases producing values of ε'' smaller than the corresponding Debye relaxation (i.e. $\alpha = 1$) towards the high-frequency end. Just as in the previous case we can obtain ε^*_{eff} for the composite substance in Figure 7 when ε^*_2 is described by a Cole-Davidson arc; in this case

$$\varepsilon^*_1 = \varepsilon'_1 \qquad \text{and} \qquad \varepsilon^*_2 = \varepsilon'_{\infty 2} + \frac{\varepsilon'_{o2} - \varepsilon'_{\infty 2}}{(1+j\omega\tau_2)^\alpha} - j\frac{\sigma_2}{\omega}$$

then

$$\varepsilon'_{eff} = (1+Q)\varepsilon'_1\left[1 - \frac{Q\varepsilon'_1\left[\varepsilon'_{\infty 2} + Q\varepsilon'_1 + (\varepsilon'_{o2}-\varepsilon'_{\infty 2})(\cos\phi)^\alpha \cos\alpha\phi\right]}{\left[\varepsilon'_{\infty 2} + Q\varepsilon'_1 + (\varepsilon'_{o2}-\varepsilon'_{\infty 2})(\cos\phi)^\alpha\cos\alpha\phi\right]^2 + \left[(\varepsilon'_{o2}-\varepsilon'_{\infty 2})(\cos\phi)^\alpha \sin\alpha\phi + \frac{\sigma_2}{\omega}\right]^2}\right] \qquad (32)$$

and

$$\varepsilon''_{eff} = -(1+Q)\varepsilon'_1 \frac{Q\varepsilon'_1\left[(\varepsilon'_{o2}-\varepsilon'_{\infty 2})(\cos\phi)^\alpha \sin\alpha\phi + \frac{\sigma_2}{\omega}\right]}{\left[\varepsilon'_{\infty 2} + Q\varepsilon'_1 + (\varepsilon'_{o2}-\varepsilon'_{\infty 2})(\cos\phi)^\alpha\cos\alpha\phi\right]^2 + \left[(\varepsilon'_{o2}-\varepsilon'_{\infty 2})(\cos\phi)^\alpha \sin\alpha\phi + \frac{\sigma_2}{\omega}\right]^2}, \qquad (33)$$

with $\phi = \tan^{-1}\omega\tau_2$,

are the components of ε^*_{eff} when the dispersive sample presents a Cole-Davidson distribution of relaxation times.

In equations (30), (31), (32), and (33) we have shown that the generalization of this method of measurement and analysis may be carried out straightforwardly to substances presenting a distribution of relaxation times.

The parameter Q

A discussion on the role of the parameter Q, the ratio of thicknesses d_2/d_1, is necessary since it controls the magnitude of ε'_{eff} and ε''_{eff}.

When analyzing the limiting cases of the general equation for ε^*_{eff} we obtained equation (26) as

$$\varepsilon'_{eff} \xrightarrow[\omega \to 0]{} \frac{(d_1+d_2)\,\varepsilon'_1 \sigma_2}{\sigma_1 d_2 + \sigma_2 d_1}$$

If material 1 is a good dielectric $\sigma_1 = 0$ and the above equation can be written as

$$\varepsilon'_{eff} = (1+Q)\varepsilon'_1 \qquad when \quad \omega = 0.$$

Thus, the maximum value of ε'_{eff} depends on Q and the (constant) value of the dielectric permittivity of material 1. Once the latter is chosen, and therefore its ε'_1 is fixed, it will be sufficient to vary its thickness throughout a series of experiments to obtain larger or smaller values of the static ε'_{eff}, while maintaining fixed the sample thickness. Obviously not only ε'_{eff} at zero frequency is affected by such a change in Q, but all other values $(for\ \omega \neq 0)$ of ε'_{eff} and ε''_{eff} will change proportionally. The net result of having large Q-values (i.e. $Q \sim 20$ or higher) will be the enhancement of the α-domain while small values of Q (i.e. $Q < 10$) will permit a clearer definition of the β-domain. Large Q-values imply larger values of both ε'_{eff} and ε''_{eff} than the corresponding ones for low Q-values.

Thus the overall effect of Q on the values of ε'_{eff} and ε''_{eff} is that: (1) when Q has large values one obtains magnified values of the components of ε^*_{eff} while an enhancement of the α-domain occurs, and (2) when Q has small values the components of ε^*_{eff} present diminished values while enhancement of the β-domain occurs. The meanings attached to magnified and diminished are, of course, relative; a more precise signification evolves when dealing with a particular set of parameters.

Varying the parameter Q implies varying the magnitude of the applied electric field in material 2 (i.e. the sample). This is the physical phenomenon responsible for the modification of the $\mathcal{E}^*_{eff}$ values when Q varies (Alvarez, 1972, pp. 52-56).

For example, when decreasing Q (increasing d_1 and decreasing d_2) a smaller electric field is established in material 2, which will make decrease the losses in it (ohmic and dielectric) as well as in the composite sample. The response of material 1 is not affected since it is a lossless dielectric.

The experimental ability to modify the response of a given sample without altering its geometry or electrical properties, as well as the possibility of enhancing a given domain of absorption represent a definite advantage to the study of rock samples since they allow us to make a more detailed study of the regions of interest, in particular the low-frequency region which is the one that traditionally has presented more experimental problems.

Effects of parameters variation on K^*_{eff} plots

A few examples shall illustrate the variations of K^*_{eff} due to variations of the parameters involved. Relative dielectric permittivities ($K^* = \mathcal{E}^*/\mathcal{E}_o$) will be used since they are more commonly found in reporting experimental results.

Six or seven parameters will characterize each example: K'_1 will be the (constant) value of the relative permittivity of material 1; K'_{oz} and $K'_{\infty z}$ will be the extreme values of the K' of material 2; τ_2 the dielectric relaxation time of material 2 and σ_2 its ohmic conductivity; Q is the thickness ratio d_2/d_1. A Debye substance is completely characterized through equations (28) and (29) and the parameters listed above. If a Cole-Cole arc or a Cole-Davidson arc are modeled, an additional parameter is necessary: h for the former and α for the latter. The corresponding equations are (30), (31), (32) and (33).

Table I establishes the relation between the figure number and the corresponding parameter values. In Figures 4 through 13 the frequencies are given in kilohertz and the axes are simply labeled K' and K'' instead of K'_{eff} and K''_{eff}.

Figures 4, 5 and 6 constitute an example of how the parameter Q affects the plots of K^*_{eff} in the complex plane when material 2 is assumed to behave as a Debye substance. Q takes up values 4, 12, and 48, while the rest of the parameters are kept fixed at values: $K'_1 = 6.0$, $K'_{\infty 2} = 4.0$, $K'_{o2} = 250$, $\tau_2 = 7.95 \times 10^{-7}$ sec, and $\sigma_2 = 1.0 \times 10^{-6}$ $(\Omega\text{-m})^{-1}$. The value $K'_{o2} = 250$ may seem too high if one thinks in terms of a homogeneous substance but when substance 2 is considered heterogeneous the Maxwell-Wagner effect will give rise to that kind of values for the static dielectric permittivity. The value of $\tau_2 = 7.95 \times 10^{-7}$ sec corresponds to a critical frequency of 200 kilohertz.

The presence of the α- and β- domains is clearly discernible in Figures 4, 5 and 6. The frequency range 30 Hz-100 MHz was chosen for the theoretical examples because it corresponds to an easily accessible range with commercial bridges. Notice how the α-domain becomes enhanced in going from low to high values of Q. The dashed lines correspond to the semicircles proposed by Dansas et al (1967); obviously the K^*_{eff} plots are not semicircles. The point at which the α- and β-domains meet presents a non-zero, although small, K''_{eff} value.

Figures 7 and 8 show the effect of variation in the conductivity σ_2 of a sample presenting a Cole-Cole distribution of relaxation times (equations 30 and 31). A tendency is observed to fuse the two domains of absorption into only one when the ohmic conductivity increases; this trend is observed in other types of substances (i.e. Debye, Cole-Davidson, etc.) whenever σ_2 increases. A shifting of the points towards higher K'_{eff} values also takes place.

Figures 9 and 10 show the effect of variation of the parameter α in a Cole-Davidson distribution (equations 32 and 33). The closer is α to unity the closer will be the behavior of the Cole-Davidson distribution to a Debye relaxation. The α-domain remains practically unchanged upon α variations while the β-domain is drastically modified.

A comparison can be made between Debye and Cole-Davidson relaxations with the aid of Figures 5, 9 and 10; all parameters, except α, are the same in these figures. A more complete evaluation of the effects of parameters variation has been made elsewhere (Alvarez, 1972, pp. 56-64).

EXPERIMENTAL DISCUSSION

We want to show now an experimental instance in which the two domains of absorption appear clearly differentiated. Three sets of measurements will be reported, all of them made on a sample of hematitic sandstone at room conditions. Each set corresponds to a different Q-value so that the predicted variation in the response of the sample can be checked experimentally.

The only aim we have in mind in presenting these examples is to exhibit the applicability to rock samples of the method discussed herein. Future work designed specifically to obtain handbook-type values of various rock specimens will have to include a complete mineralogical description of the samples as well as full information on the particular experimental conditions under which the measurements were made. Such studies lie beyond the scope of the present work and will not be found in the examples to be presented.

Two impedance bridges were used in the experimental measurements; a General Radio Capacitance Measuring Assembly Type 1610-B was used to analyze the 30 Hz-100 KHz range and a Boonton Q-Meter Type 160-A was used to analyze the 100 KHz - 20 MHz range of frequencies. The former has an accuracy of $\pm$ 0.1 % $\pm$ 0.6 pf for capacitance measurements and a dissipation factor (D) accuracy of $\pm$ 0.00005, while the latter has $\pm$ 2% and $\pm$ 10% nominal accuracy for capacitance and Q-measurements respectively. Further descriptions of these instruments can be found in the manufacturer's literature (General Radio, 1965, and Boonton Radio).

The General Radio Assembly includes a type 716-P4 guard circuit which permits three-terminal measurements to be made. All our measurements in the range of frequencies covered by this bridge were made in the three-terminal sub-

stitution method of measurement; therefore all contributions arising from parasitic capacitances were cancelled out and the measurements in the 30 Hz - 100 KHz range are considered free, within the error limits stated, of such contributions. The sample was located, in all measurements, in an electrically shielded enclosure to avoid noise pick-up.

The Boonton Q-Meter does not have capabilities for three-terminal measurements and consequently there is the possibility of contributions from parasitic capacitances, especially at the higher frequencies.

Considering all sources of error, instrumental and geometrical, we have estimated the overall accuracy in our measurements as $\pm$ 5% in the 30 Hz - 100 KHz range for K'_{eff} and K''_{eff}; $\pm$ 10% for K'_{eff} and $\pm$ 15% for K''_{eff} in the 100 KHz - 10 MHz range, and $\pm$ 15% and $\pm$ 20% for K'_{eff} and K''_{eff} respectively in the 10 - 20 MHz range.

As the good dielectric we used mica sheets of various thicknesses. The metallic electrodes were made of Indium-Mercury (In-Hg) amalgam which has proved to be an excellent substance for making intimate contacts with rock samples in general although in the present cases it was placed in one surface of the mica sheets.

The thicknesses of the mica sheets and sample were independently determined with a micrometer of 1/100 mm/div accuracy. Several measurements were made at various places for each dimension and then these were averaged to obtain a representative value.

The values for the dielectric constant of mica (K'_1) were experimentally determined, over the range of frequencies studied, prior to mounting them in the composite sample. At the low frequency end (i.e $f < 300$ Hz) the losses in the mica usually increased by about an order of magnitude; typically $K'' = 0.18$ at 30 Hz which in all cases was the lowest frequency employed. Three different values were obtained for the three cases analyzed: $K'_1 = 4.11$, $K'_1 = 6.70$ and $K'_1 = 6.90$. It should be mentioned that the mica samples used came from at least two different types of mica; one of them presenting black streaks while the other was clearer and of a uniform color.

Table 2 displays the geometrical parameters involved; the rock sample was the same in all three cases; d_1 is the mica thickness, d_2 the sample thickness, Q is the ratio d_2/d_1 and A is the area of the electrodes. They are related to the figure number in which the experimental results are found as crosses joined by a thick line; the numbers by the crosses represent the frequencies, in kilohertz, at which the value was obtained (Figures 11, 12 and 13).

As Q increases, both K'_{eff} and K''_{eff} increase while the general shape of the experimental curve is maintained. The point at which the α-and β-domains meet is around f = 0.8 KHz. Both domains are only partially sketched by the experimental points, due to experimental limitations at both ends of the frequency range, but there is no doubt about their presence.

A very interesting feature appears in Figures 12 and 13; this is a strong and narrow absorption which was missed in the first experimental measurements with Q = 4.82 when we went from 700 KHz to 2 MHz; notice that it is only inferred in Figure 11, but in the next two experiments (i.e. Q = 9.54 and Q = 24.1) the peak appeared quite clearly. In fact we had to repeat the experiments corresponding to these two last values of Q, measuring again around 1 MHz, in order to make sure that it was not a resonance due to some particular geometrical configuration of sample holder and leads, as was pointed out to us as a possibility by Westphal (1971). We hold the view that the peak is a true absorption peak associated with the hematitic sandstone sample studied, not a false absorption due to instrumentation, for the following reasons: (i) the peak appears only for hematitic sandstone and not for other samples we have studied, although not reported in this work, and (ii) the peak is reproducible not only when repositioning the sample in the sample holder but when the overall thickness of the composite sample is varied. Since any explanation of the presence of this absorption peak would have to be made in terms of a particular group of molecules present in the sample we shall offer no such explanation at this point.

In Figures 11, 12 and 13 we have included, in addition to the experimental data, the theoretical points corresponding the the same frequencies used in the experiments as obtained from equations (28) and (29). We assumed that the experimental response was due to a sample in which there was a distribution of relaxation times dominated, in the low frequency region (i.e. $f < 500$ KHz), by a Debye process. This was suggested by the shape of the experimental curves. Since the high absorption peak occurs at frequencies around 1 MHz, and since there are only a few experimental points above it, we considered it unnecessary for the purpose of these examples to try to fit another theoretical function to the experimental data.

The theoretical points are shown as empty circles joined by a thin line and the numbers correspond to the frequencies. The theoretical parameters K_1' and Q are the same as in the experimental cases; they were kept fixed while $K_{\omega 2}'$, K_{02}', τ_2, and σ_2 were varied, using the functions given by equations (28) and (29), to fit the experimental points. The fit has not been optimized since our purpose is only to show the mechanism by which the parameters corresponding to the rock sample can be extracted from the experimental data. Once the set of parameters $K_{\omega 2}' = 80$, $K_{02}' = 400$, $\tau_2 = 4.0 \times 10^{-6}$ sec, and $\sigma_2 = 4.52 \times 10^{-7}$ $(\Omega \cdot m)^{-1}$ was fixed for $Q = 9.54$ and the theoretical points in Figure 12 obtained, the values of Q and K_1' were changed to those shown in Figures 11 and 13, so that the corresponding theoretical curves could be obtained. Thus in Figures 11, 12 and 13, it is shown how well a single set of theoretical parameters correspond simultaneously to the three sets of experimental data. Notice that the theoretical minimum at $K_{0\beta}' = K_{\omega\alpha}'$ correspond closely to the experimental minima, although the former tends to concentrate several frequencies around such point while the latter shows a smoother spreading of them.

The parameters K_{02}' and $K_{\omega 2}'$ had to be assigned large values in order for the theoretical points to fall at the positions shown; smaller values (i.e. $K_{02}' = 200$ and $K_{\omega 2}' = 40$) gave theoretical point positions not related at all to the experimental ones. The value of 400 for K_{02}' is attributed to the Maxwell-Wagner

effect taking place within the rock sample and should be contrasted to the values of $K' \sim 10^3$ at 1 KHz obtained when we made direct contacts between electrodes and sample. The value $K'_{\omega_2} = 80$ suggests the presence of a water effect in the sample, but this constitutes only a speculation at the present stage of analysis.

Although there are discrepancies that indicate that the assumed Debye behavior at the low frequency end is at best an approximation to the real behavior of the sample in such a region (as the one just discussed for the distribution of points around $K'_{0\beta} = K'_{\omega\alpha}$), such discrepancies tend to be the same in the three cases studied.

We want to emphasize once more that the conductivity σ_2 obtained with this method refers only to the ohmic conductivity of the sample. The contribution to the losses arising from the dielectric properties, that is, the dielectric conductivity, can be obtained for every frequency from the parameters K'_{02}, $K'_{\omega 2}$ and τ_2 and the adequate functions describing its behavior (i.e. Debye, Cole-Cole, etc.).

We have presented, in this experimental discussion, evidence of the applicability of the method proposed in this work to the measurement of rock samples. Also we have tried to suggest some possible ways of analyzing the response of the rock, but obviously much more research is needed in this respect to fully exploit the possibilities furnished by the method.

CONCLUSIONS

The similarity in electrical behavior between rock samples and heterogeneous dielectrics with non-negligible ohmic conductivities has led us to a general analysis of the Maxwell-Wagner effect; from this it has been concluded that in order to have electrical steady state conditions in that type of materials it is

necessary to have volume charge accumulations at the interfaces within the sample. The expression for the charge density ($\sum^*$) accumulated at an interface as a function of frequency has been obtained and shown to plot as a semicircle in the complex plane. Expressions for the effective dielectric permittivity ($\mathcal{E}^*_{eff}$) of a composite material have been presented showing that the relaxation time associated to it was the same as the one for the charge density $\sum^*$ when the sample components were considered to be non-dispersive dielectrics of different ohmic conductivities.

The analysis of the divergence of the imaginary component of $\mathcal{E}^*_{eff}$ has made it clear that such divergence arises whenever the two components of a composite sample have non-negligible ohmic conductivities, whereas if this parameter is negligible for one of them the divergence at low frequencies is avoided. This has made it possible to develop the method of measurement for heterogeneous dielectrics having non-negligible ohmic conductivities by requiring that one of the two components in a composite material be a good dielectric.

The ideas advanced by Dansas et al (1967) about the behavior of the function $\mathcal{E}^*_{eff}$ were discussed. We indicated that their conclusion about the two domains of absorption plotting as semicircles in the complex plane does not hold; instead the correct expressions have been obtained. Furthermore the method has been generalized to include dielectric substances presenting a distribution of relaxation times instead of the single one involved in the Debye behavior. A few examples on three materials presenting different behavior (Debye, Cole-Cole and Cole-Davidson) have been analyzed to illustrate the type of responses to be expected from this method. Three experimental examples have shown the feasibility of studying electrical rock properties by means of this method.

As can be appreciated, the method presents the advantage of permitting application of the pertinent theory already existent for dielectrics; we have only touched upon this matter when extending the discussion to substances having

a distribution of relaxation times. There are many other interesting possibilities such as that of evaluating the effects of a distribution of ohmic conductivities in the material.

The need for further work in the area of interpretation of results as obtained with this method has been stressed; meanwhile the possibility of obtaining new data on rock samples is opened, as may be the case with many sulfides (i.e. FeS_2, PbS, Cu_2S, etc.) whose dielectric properties are almost unknown and poorly described. The main reason for such a lack of data is their relatively high conductivities which heretofore have prevented their measurement in the frequency region of interest in exploration geophysics.

ACKNOWLEDGEMENTS

The author wishes to acknowledge H.F. Morrison, M.F. Merriam, A.F. Kip and D.W. Strangway for criticisms and comments.

Acknowledgements are due to the Consejo Nacional de Ciencia y Tecnología, México, and to the National Aeronautics and Space Administration for financial support.

REFERENCES

Alvarez, R., 1971, Effects of atmospheric moisture in rock resistivity: (Abstract) AGU Transactions, v. 52, p. 918. Paper presented at the 1971 Fall Annual Meeting, San Francisco.

Alvarez, R., 1972, Electrical conduction phenomena in rocks: Ph.D. thesis, University of California, Berkeley, 172 p.

Arnoult, R., Sixou, P., et Dansas, P., 1965, Spectres hertziens d'absorption de diélectriques hétérogènes en couches. Polarisation interfaciale: Rev. Gén. Electr., v. 74, p. 944.

Blechschmidt, E., 1938, Dielecktrische Eigenschaften von Manganferriten: Phys. Zeitschr., v. 39, p. 212.

Boonton Radio Co., Manual of Radio Frequency Measurements for Q-meter type 160-A: Boonton, N.J.

Brockman, F. G. and White, R.P., 1971 Nickel-Zinc ferrites: III, Dielectric properties of stoichiometric Nickel-Zinc ferrites: Jour. Am. Ceramic Soc., v. 54, p. 183.

Campbell, M.J. and Ulrichs, J., 1969, Electrical properties of rocks and their significance for lunar radar observations: Jour. Geoph. Res., v. 74, p. 5867.

Cole, K.S. and Cole, R.H., 1941, Dispersion and absorption in dielectrics: J. Chem. Phys., v. 9, p. 341.

Dansas, P., Sixou, P. et Arnoult, R., 1967, Utilisation de l'effet Maxwell-Wagner pour l'étude de diélectriques présentant des pertes par relaxation dipolaire et une forte conductivité: Proc. XIV Colloque Ampère, Amsterdam, North Holland.

Davidson, D.W. and Cole, R.H., 1951, Dielectric relaxation in glycerol, propylene glycol, and n-propanol: J. Chem. Phys, v. 19, p. 1484.

Debye, P., 1929, Polar moelcules: New York, Chemical Catalog Co.

Fuller, B.D. and Ward, S.H., 1970, Linear system description of the electrical parameters of rocks: IEEE, Transactions on Geosc. Electr., v. GE-8, p. 7.

General Radio Co., 1965, Manuals 716-C and 716-P4: West Concord, Mass.

Hill, N.E., Baughan, W.E., Price, E.H. and Davies, M., 1969, Dielectric properties and molecular behaviour: London, Van Nostrand.

Johnson, J.F. and Cole, R.H., 1951, Dielectric polarization of liquid and solid formic acid: J. Am. Chem. Soc., v. 73, p. 4536.

Keller, G.V., and Licastro, P.H., 1959, Dielectric constant and electrical resistivity of natural-state rocks: Geol. Survey Bull 1052-H.

_____, 1966, Electrical properties of rocks and minerals: in Handbook of Physical Constants, Clark, S.P. ed., New York, Geol. Soc. Am.

Kittel, C., 1968, Introduction to solid state physics: 3rd ed., New York, John Wiley.

Koops, C.G., 1951, On the dispersion of resistivity and dielectric constant of some semiconductors at audio frequencies: Phys. Rev., v. 83, p. 121.

Krötzsch, M., 1964, Über die Niederfrequenzdispersion der dielektrizitätskonstanten und der elektrischen Leitfähigkeit polykristalliner Ferrite: Phys. Status Solidi, v. 6, p. 479.

Maxwell, J.C., 1873, Electricity and magnetism: v. I, Oxford, University Press.

Parkhomenko, E.I., 1967, Electrical properties of rocks: New York, Plenum Press.

_____, 1971, Electrification phenomena in rocks: New York, Plenum Press.

Scott, J.H., Carroll, R.D. and Cunningham, D.R., 1967, Dielectric constant and electrical conductivity measurements of moist rock: a new laboratory method: Jour. Geoph. Res., v. 72, p. 5101.

Tarkhov, A.G., 1948, On the resistivity (ρ) and dielectric constant (ε) of rocks in alternating electric fields: Geofizika VSEGEI, v. 12, p. 3.

Valeev, K.A. and Parkhomenko, E.I., 1965, Electrical properties of rocks in constant and alternating electric fields: Izv., Phys. Solid Earth, (English Trans.), p. 803.

Von Hippel, A. R., 1966, Dielectrics and waves: Cambridge, MIT Press.

Wagner, K.W., 1913, Erklärung der dielectrischen Nachwirkungen auf Grund Maxwellscher Vorstelungen: Arch. Elektrotech, v. 2, p. 371.

Westphal, W.B., (1971), Personal communication. Laboratory for Insulation Research, MIT.

Zheludev, I.S., 1971, Physics of crystalline dielectrics: v. 2, New York, Plenum.

Fig.	K_1'	$K_{\omega 2}'$	Q	K_{02}'	τ_2 (sec)	σ_2 $(\Omega\text{-m})^{-1}$	h	α
				DEBYE				
4	6.0	4.0	4	250	7.95×10^{-7}	1.0×10^{-6}	–	–
5	"	"	12	"	"	"	–	–
6	"	"	48	"	"	"	–	–
				COLE-COLE				
7	"	"	12	40	7.95×10^{-9}	"	0.75	–
8	"	"	"	"	"	1.0×10^{-2}	0.75	–
				COLE-DAVIDSON				
9	"	"	"	250	7.95×10^{-7}	1.0×10^{-6}	–	0.25
10	"	"	"	"	"	"	–	0.75

TABLE 1. Parameters used in the computation of examples in which the dispersive dielectric is characterized by Debye, Cole-Cole and Cole-Davidson relaxations.

Fig.	d_1 (mm)	d_2 (mm)	A (cm^2)	Q
11	0.85	4.10	3.84	4.82
12	0.43	4.10	3.84	9.54
13	0.17	4.10	3.84	24.10

TABLE 2: Dimensions of sample electrodes and micas used in the experimental examples.

TABLE OF FIGURES

frequency, a point acquires larger K'_{eff} values when the conductivity increases.

Fig. 9. K^*_{eff} variations arising from changes in the parameter α. Compare to Figure 10. Material 2 is described by a Cole-Davidson relaxation. Compare to Figure 5 described by a Debye relaxation.

Fig. 10. K^*_{eff} variations arising from changes in the parameter α. Compare to Figure 9. The α-domain remains unaffected while the β-domain undergoes a considerable modification. Material 2 is described by a Cole-Davidson relaxation. Compare to Figure 5 described by a Debye relaxation.

Fig. 11. Experimental values of K^*_{eff} for a hematitic sandstone sample, of 3.84 cm^2 area and 4.10 mm thickness, are indicated by crosses joined by the thick line. The points shown as empty circles correspond to a Debye substance characterized by the theoretical parameters indicated; these are the same for the three experimental cases and therefore show how well a single set of theoretical parameters correspond simultaneously to the three sets of experimental data (see Figures 12 and 13). It was assumed that the experimental plot was dominated by a Debye relaxation in the frequency region ≤ 500 KHz.

Fig. 12. Experimental values of K^*_{eff} for the same sample as in the previous figure. The value of Q is 9.54. There is an increase in K'_{eff} and K''_{eff} values with respect to the plot of Q = 4.82. A strong absorption peak is delineated by five experimental values around 1.4 MHz; in the case Q = 4.82 this absorption was not detected due to the lack of measurements between 700 KHz and 2MHz. Its presence has only been inferred in that case.

Fig. 13. Experimental values of K^*_{eff} for the same sample as in Figures 11 and 12. The value of Q is 24.10. K'_{eff} and K''_{ef} have further increased from the previous figures. The strong absorption peak is delineated by four points around 900 KHz. The experimental curve is smoother than the previous ones; this effect is thought to be due to a different atmospheric moisture content at the time of measurement.

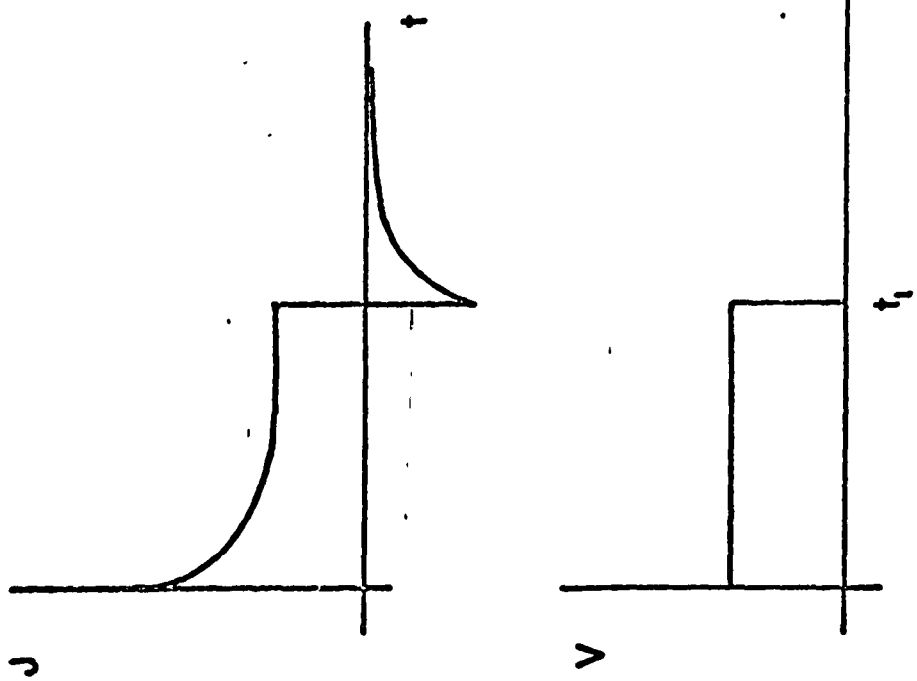

Fig. 1

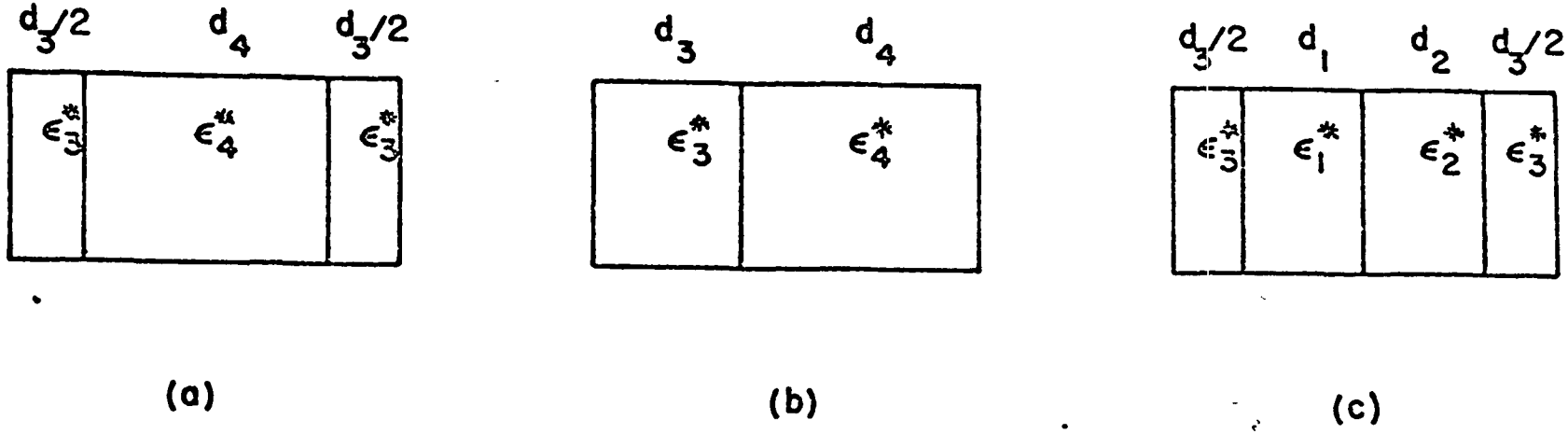

Fig. 2

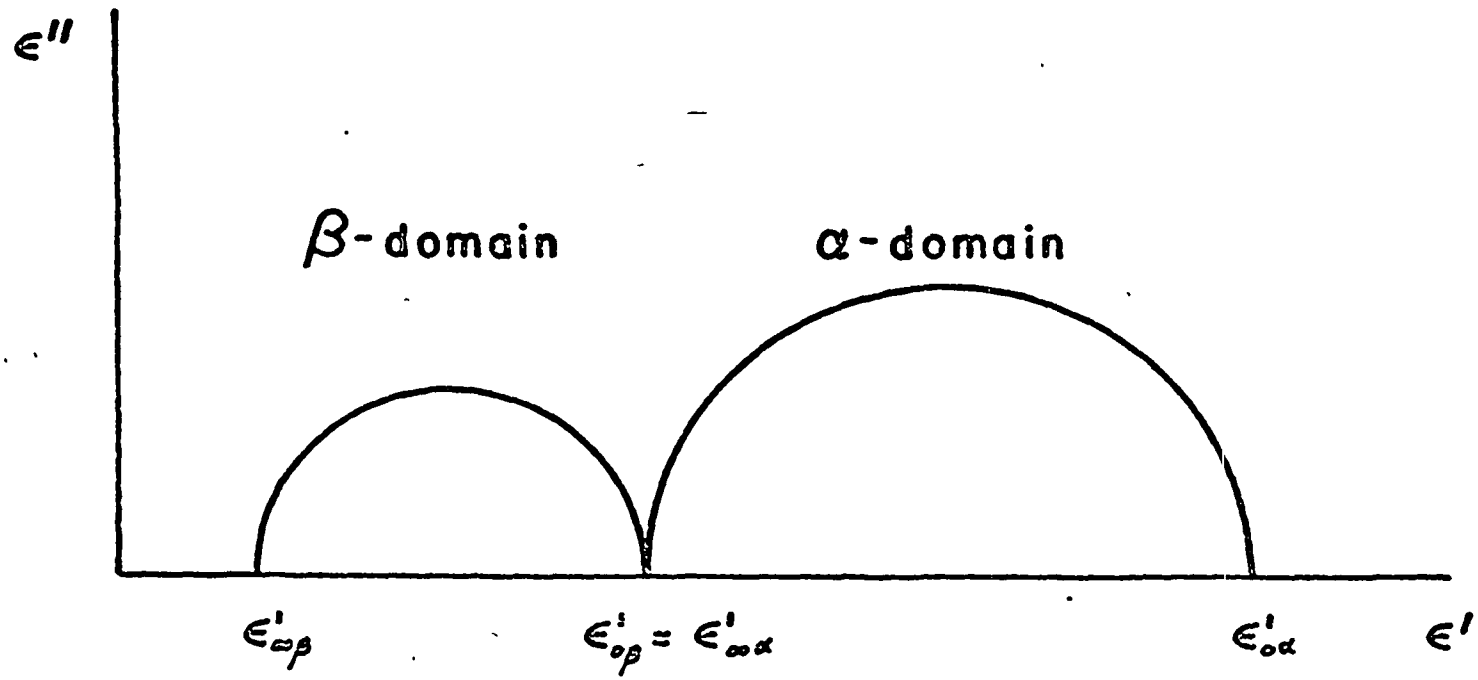

Fig. 3

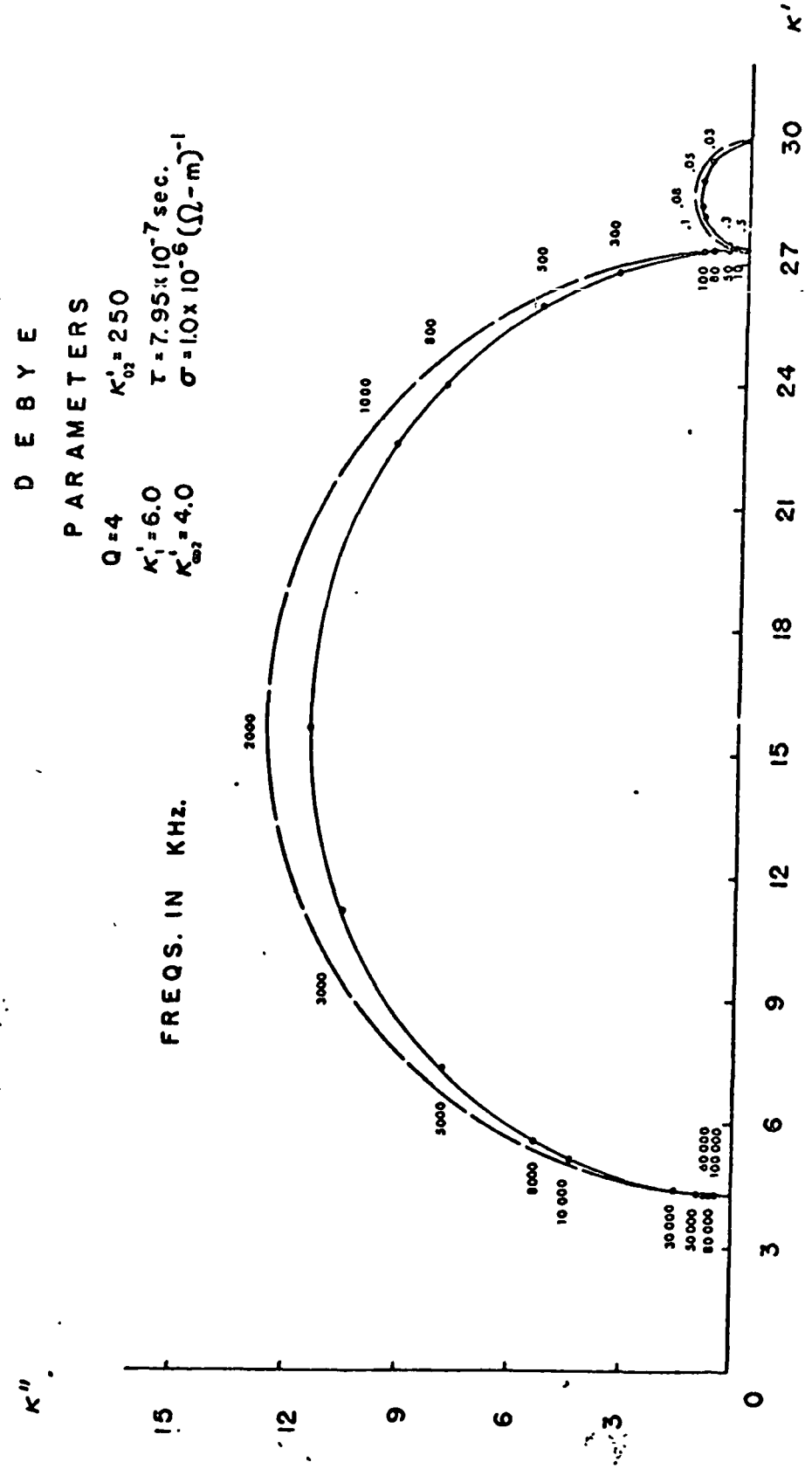
DEBYE
PARAMETERS
Q=4
κ'_{02}=250
κ'_1=6.0
$\kappa'_{\infty 2}$=4.0
τ=7.95x10^{-7}sec.
σ=1.0x10^{-6}(Ω-m)$^{-1}$
FREQS. IN KHz.
κ''
κ'
0
3
6
9
12
15
18
21
24
27
30
2000
1000
800
500
300
100
80
10
.1
.08
.05
.03
.3
3000
5000
8000
10 000
30 000
50 000
80 000
100 000
40 000

Fig. 4

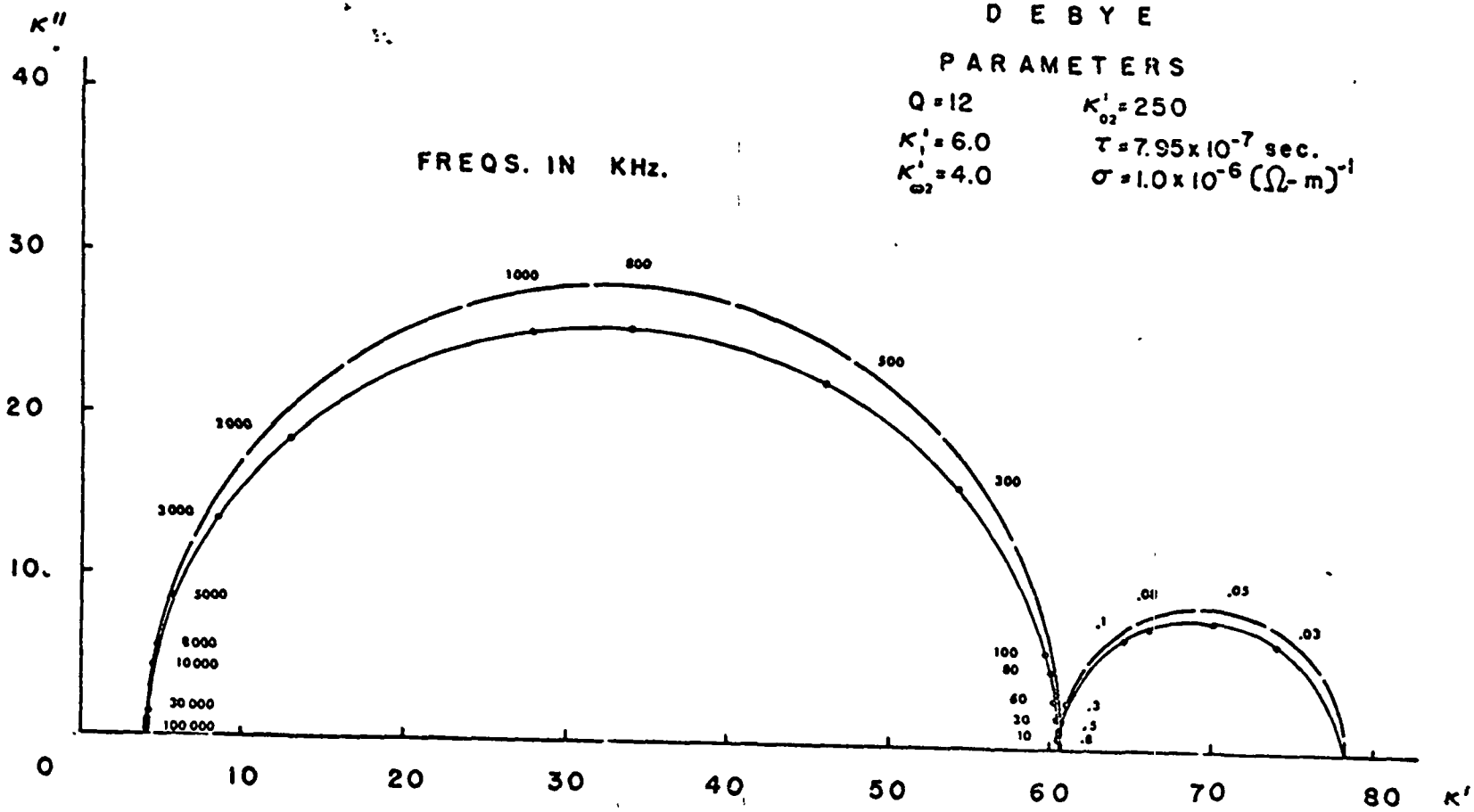
D E B Y E
PARAMETERS
Q = 12
K'_{02} = 250
K'_1 = 6.0
τ = 7.95 x 10^{-7} sec.
$K'_{\omega 2}$ = 4.0
σ = 1.0 x 10^{-6} (Ω-m)$^{-1}$
FREQS. IN KHz.
K''
K'
40
30
20
10.
0
10
20
30
40
50
60
70
80
1000
800
500
2000
300
3000
5000
8000
10000
30 000
100 000
100
80
60
30
10
.011
.05
.1
.03
.3
.5
.8

Fig. 5

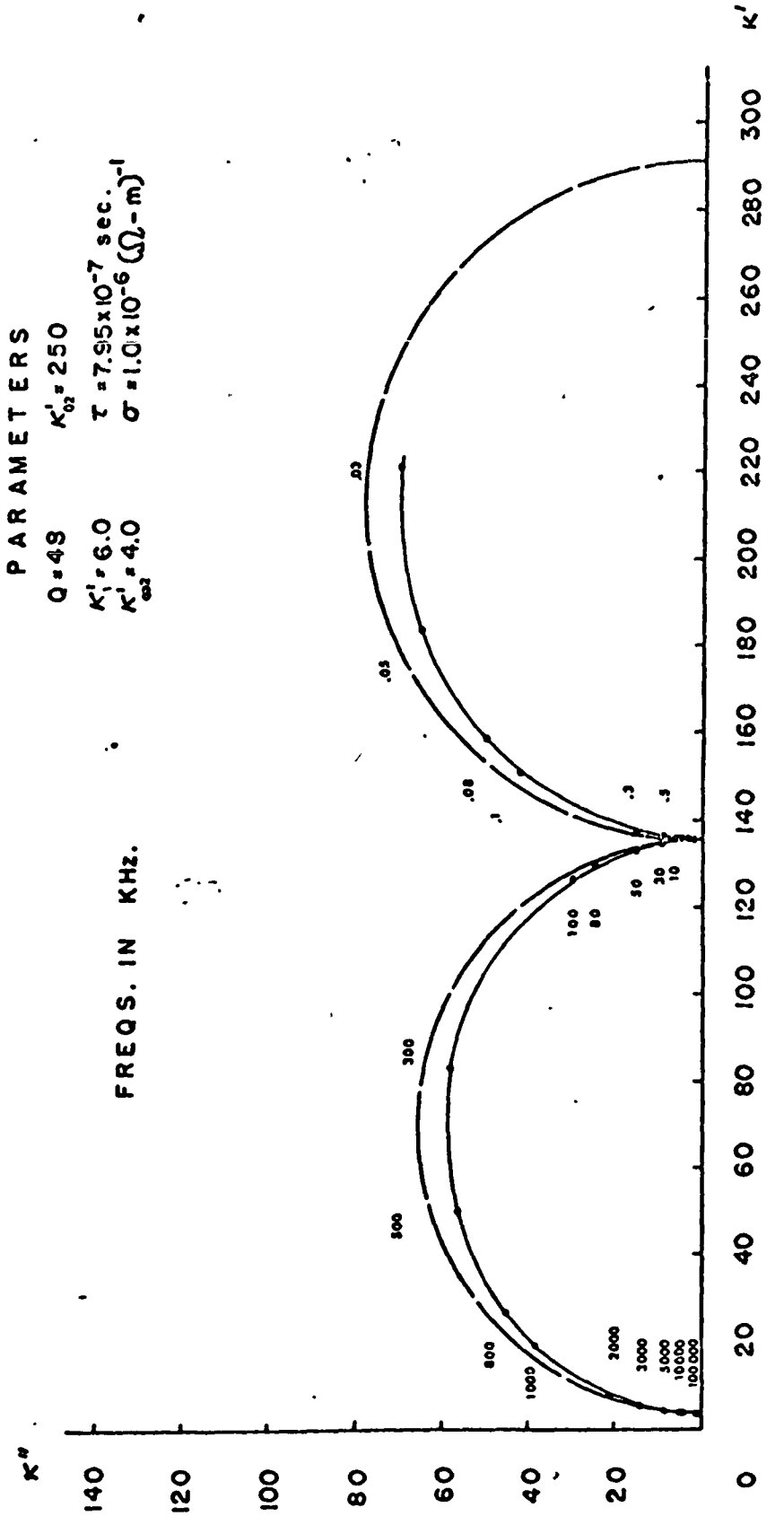
DEBYE
PARAMETERS
Q=43
$K'_{\infty 2}$=250
K'_1=6.0
$K'_{\infty 1}$=4.0
τ=7.95x10⁻⁷ sec.
σ=1.0x10⁻⁶ (Ω-m)⁻¹
FREQS. IN KHz.
K''
K'
0
20
40
60
80
100
120
140
160
180
200
220
240
260
280
300
.02
.05
.08
.1
.3
.5
1
2
3
5
10
20
50
80
100
300
500
800
1000
2000
3000
5000
10000
100000

FIG 6

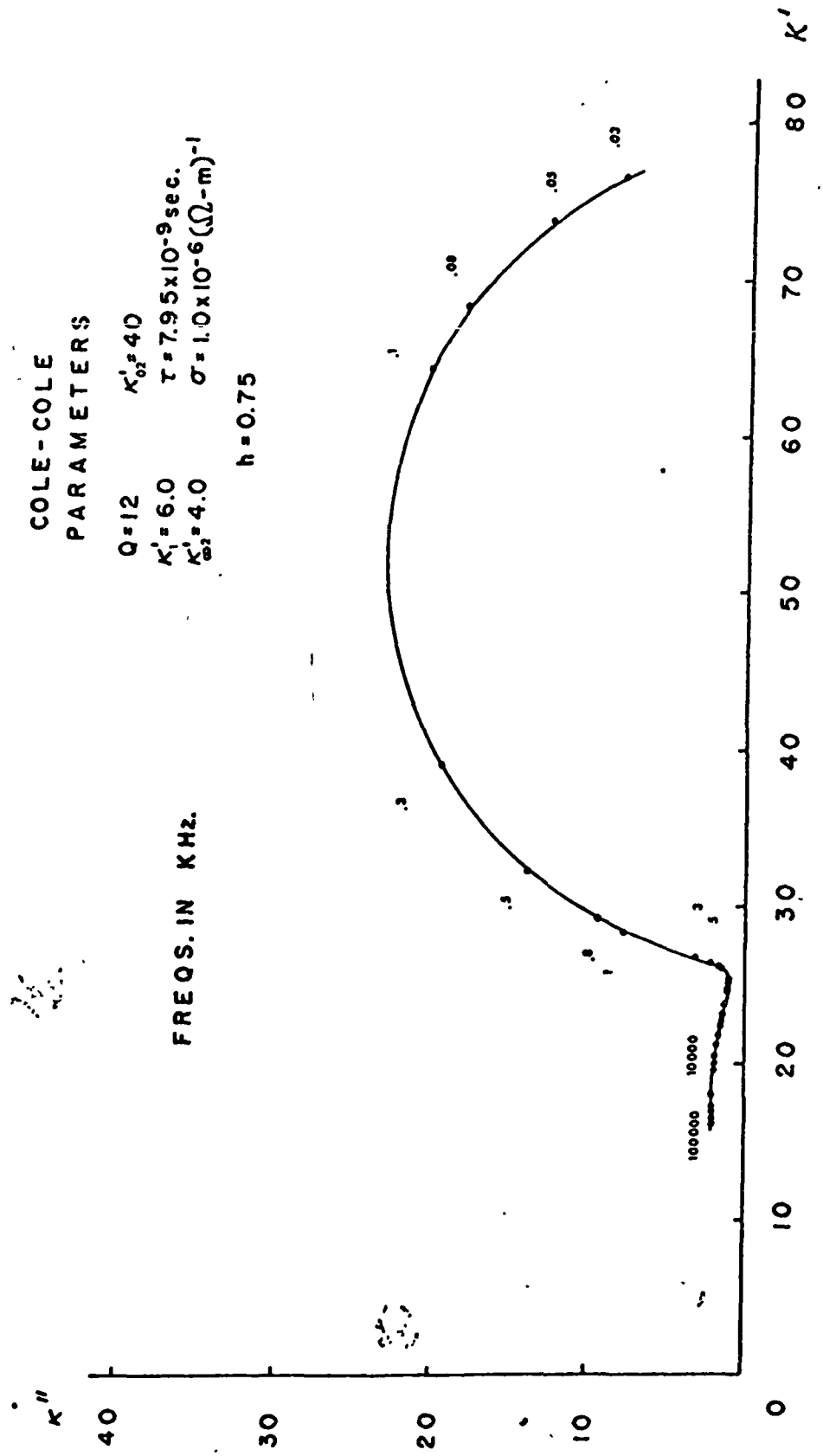
COLE-COLE
PARAMETERS
Q=12
K_1'=6.0
$K_{\infty 2}'$=4.0
$K_{\infty 2}'$=40
τ=7.95x10^{-9}sec.
σ=1.0x10^{-6}(Ω-m)$^{-1}$
h=0.75
FREQS. IN KHz.
.1
.3
1
3
10000
100000
K''
K'
0
10
20
30
40
50
60
70
80

Fig. 7

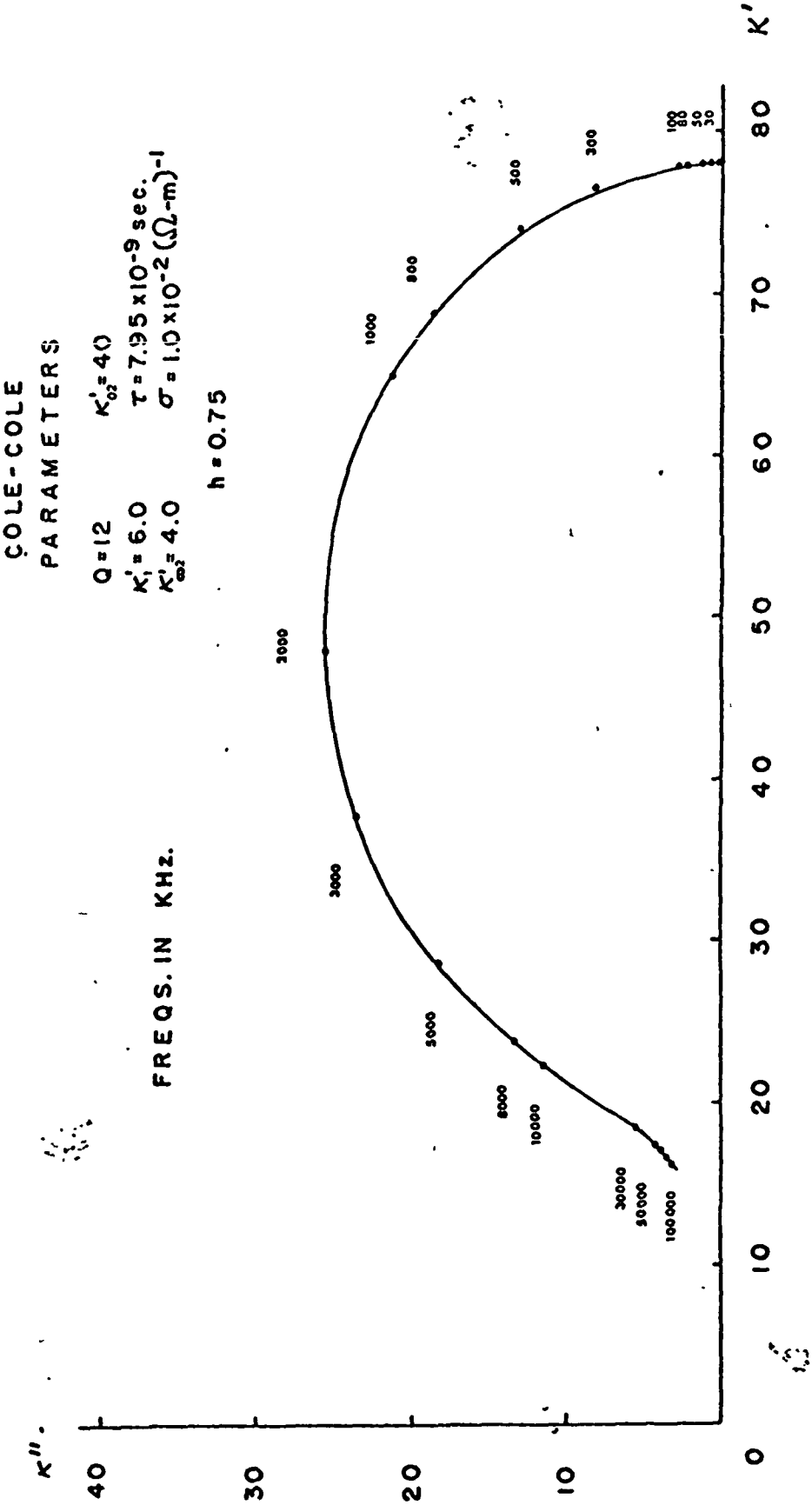
COLE-COLE
PARAMETERS
Q=12
K'_1 = 6.0
$K'_{\omega 2}$ = 4.0
$K'_{\sigma 2}$ = 40
τ = 7.95 x10^{-9} sec.
σ = 1.0 x10^{-2} (Ω-m)$^{-1}$
h = 0.75
FREQS. IN KHz.
100000
50000
30000
10000
8000
5000
3000
2000
1000
800
500
300
100
80
50
30
K''
K'
0
10
20
30
40
50
60
70
80

FIG. 8

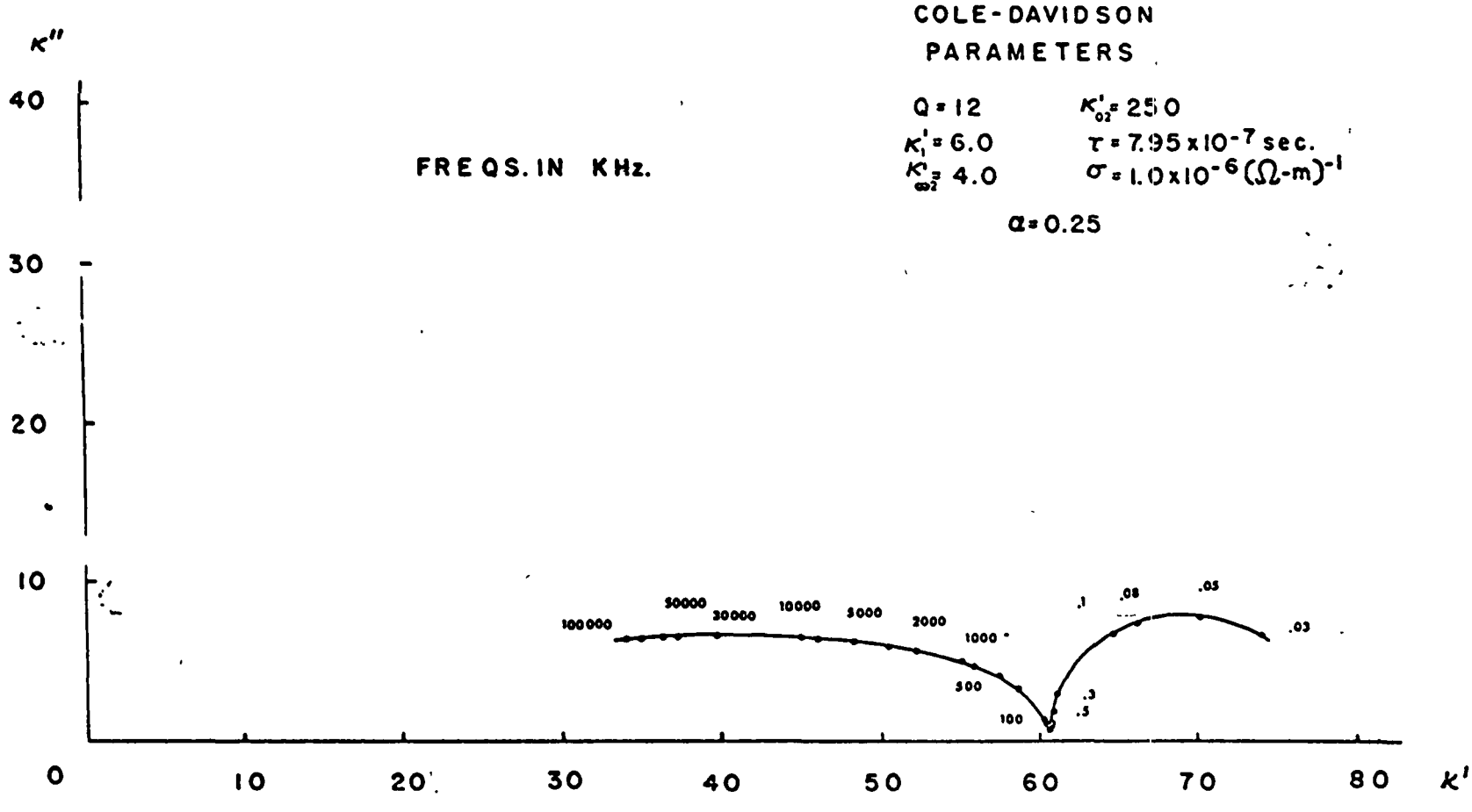
COLE-DAVIDSON
PARAMETERS
Q = 12
$\kappa_1' = 6.0$
$\kappa_{\omega 2}' = 4.0$
$\kappa_{02}' = 25.0$
$\tau = 7.95 \times 10^{-7}$ sec.
$\sigma = 1.0 \times 10^{-6} (\Omega\text{-m})^{-1}$
$\alpha = 0.25$
FREQS. IN KHz.
κ''
κ'
40
30
20
10
0
10
20
30
40
50
60
70
80
100000
50000
30000
10000
5000
2000
1000
500
100
.1
.08
.05
.03
.3
.5

Fig. 9

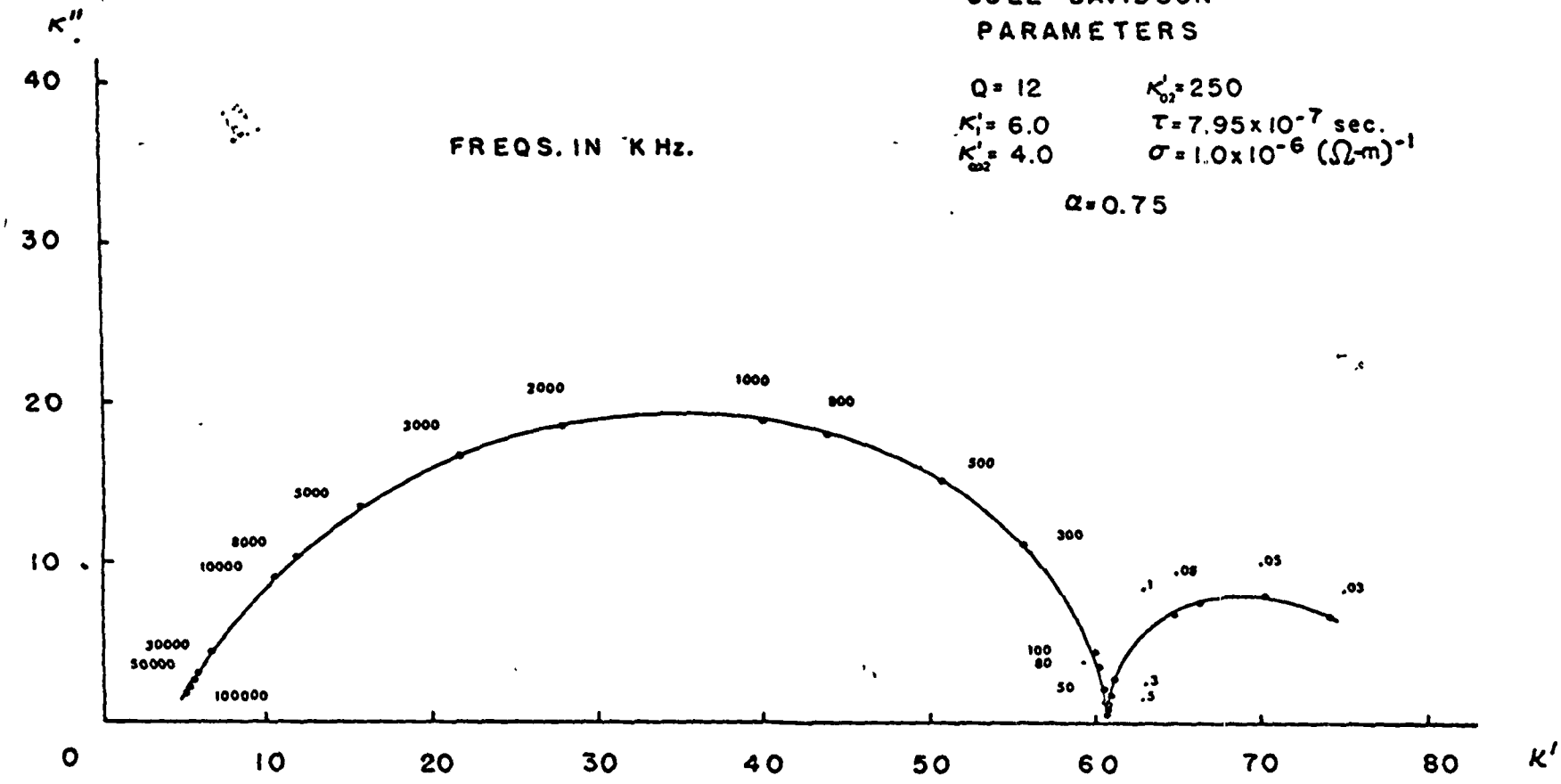
COLE-DAVIDSON
PARAMETERS
Q = 12
K'_1 = 6.0
$K'_{\infty 2}$ = 4.0
K'_{02} = 250
$\tau = 7.95 \times 10^{-7}$ sec.
$\sigma = 1.0 \times 10^{-6}$ $(\Omega\text{-m})^{-1}$
$\alpha = 0.75$
FREQS. IN K Hz.
K''
K'
0
10
20
30
40
50
60
70
80
100000
50000
30000
10000
8000
5000
3000
2000
1000
800
500
300
100
80
50
.1
.08
.05
.03
.3
.5

Fig. 10

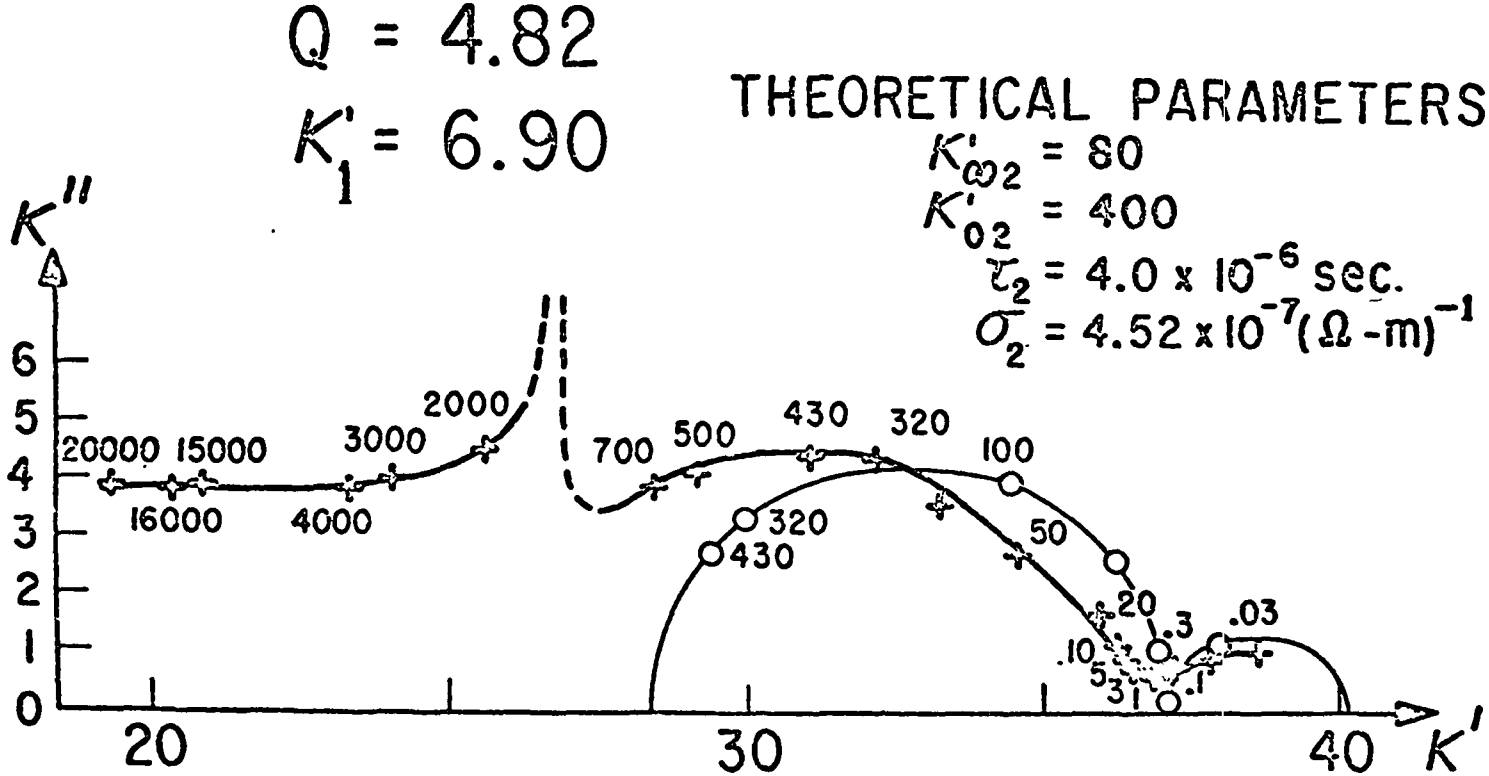
Q = 4.82
K'1 = 6.90
THEORETICAL PARAMETERS
K'ω2 = 80
K'02 = 400
τ2 = 4.0 x 10^-6 sec.
σ2 = 4.52 x 10^-7 (Ω-m)^-1
K''
K'
20000
15000
16000
4000
3000
2000
700
500
430
320
100
50
20
.3
.03
.10
5
3
1
.1
320
430
0
1
2
3
4
5
6
20
30
40

Fig. 11

$Q = 9.54$

$K_1' = 6.70$

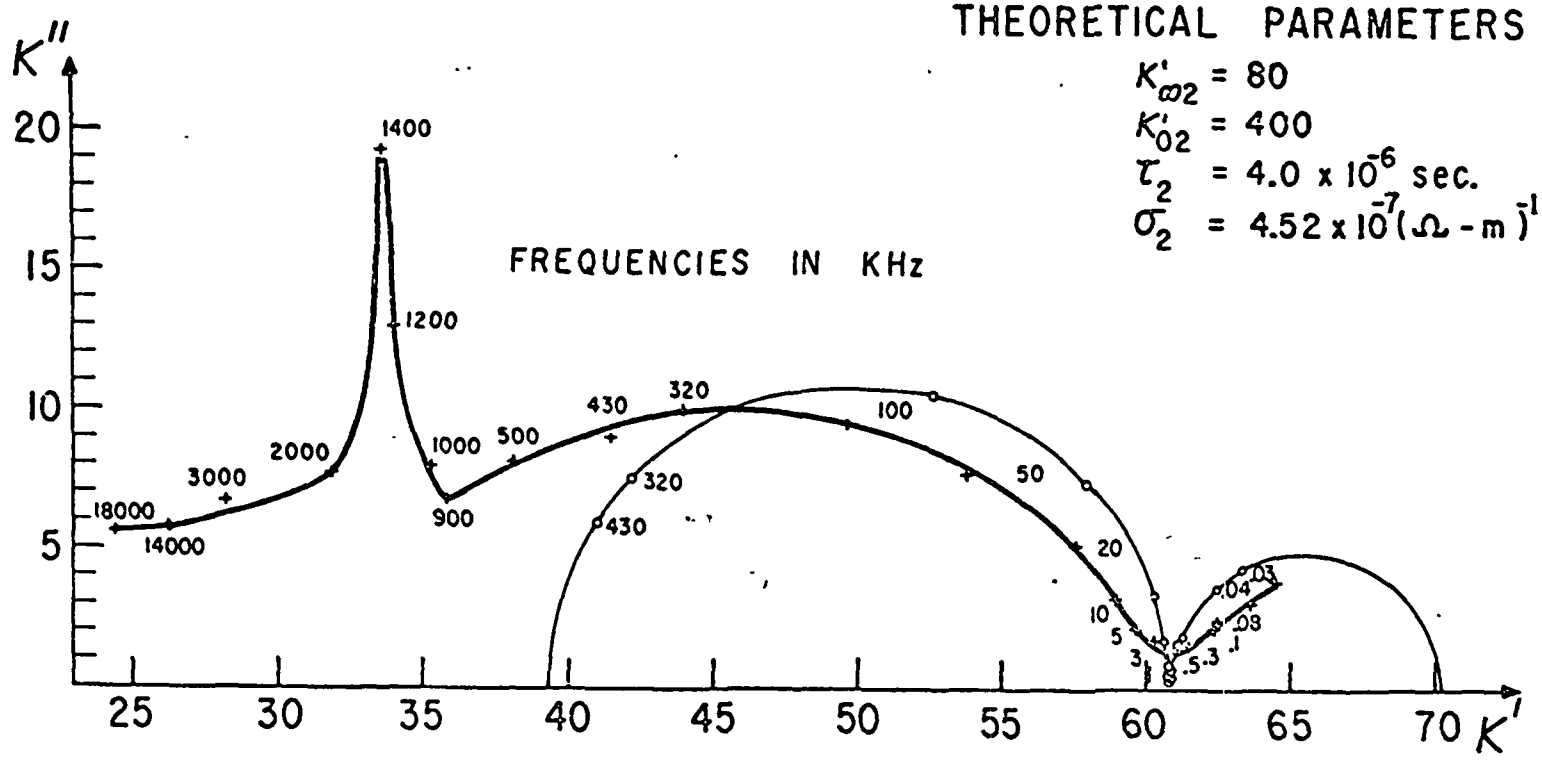

Fig. 12

$Q = 24.1$

$K_1' = 4.11$

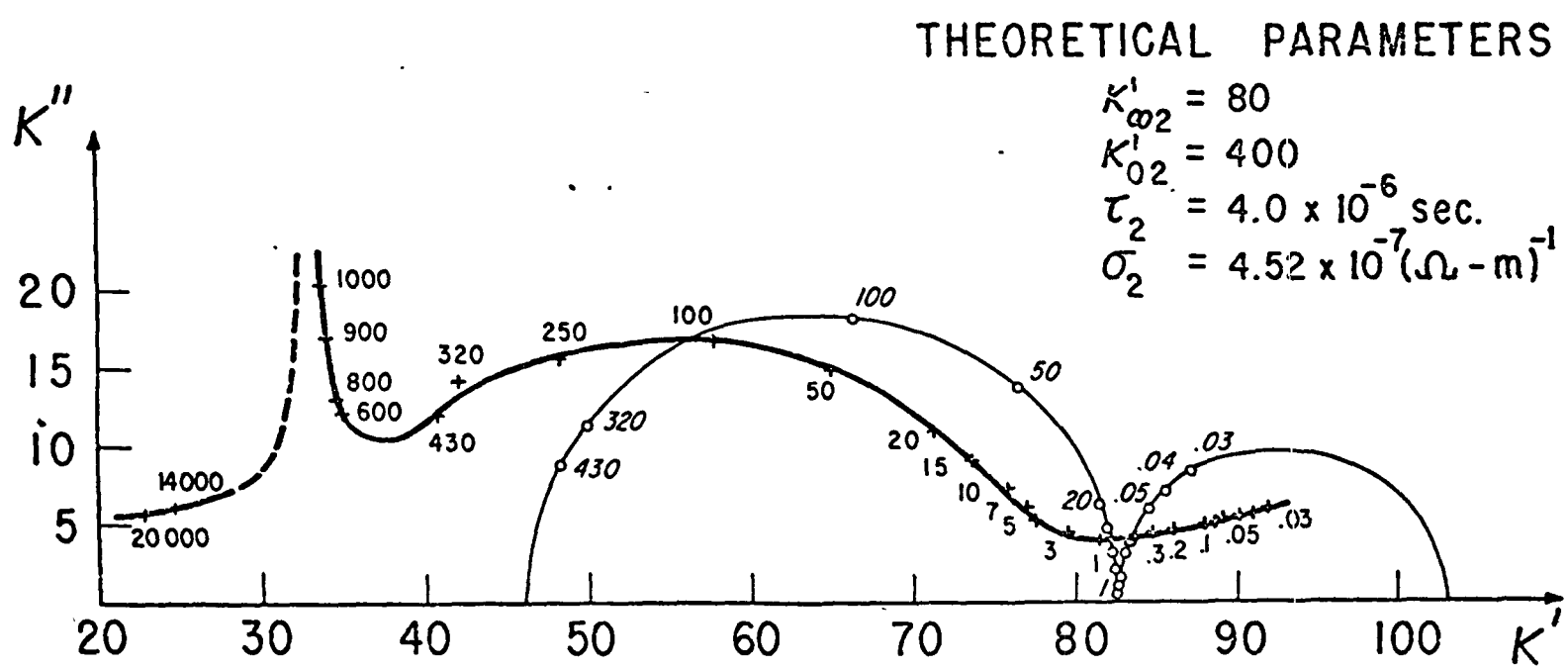

FIG. 13

Electrical Non-linear Behavior in Rocks

Román Alvarez

Engineering Geoscience

University of California

Berkeley, California

94720

ABSTRACT

Previous studies on rocks saturated with electrolytes have shown that there is an upper limit for current density, up to which linear behavior is observed.

Evidence of the opposite behavior in some dry resistive rocks in contact with metallic electrodes is presented, showing the existence of a non-linear region followed by a linear one when the voltage, or current density, is increased.

This effect is attributed to interfacial phenomena occurring at electrode-sample interfaces. It has been shown elsewhere that metal-insulator or metal-semiconductor interfaces may give rise to linear or non-linear behavior depending on the type of electric contact established: ohmic, blocking, or neutral.

Five resistive and two conductive samples were analyzed. Of the resistive group, limestone, granite and hematitic sandstone showed a non-linear region, whereas argillaceous sandstone and muscovite schist did not, suggesting that different type of contacts are established by the same metallic electrode (indium-mercury amalgam) in the various samples. Galena and pyrite, samples of the conductive group, behaved linearly, as expected.

The existence of small polarization voltages was observed in the resistive group of samples; they were attributed to space charge concentrations at the electrode sample boundary. Experimental determination of the potential distribution on a sample surface reveals high non-uniformity of the electric field in that region as well as the presence of space charges immediately adjacent to the electrodes.

The polarization voltages observed give rise to a displacement of the current vs voltage characteristics from the origin. It is shown that if the I-V characteristics do not go through the origin, the corresponding resistivity vs current density plot will appear to be non-linear even when the I-V characteristic is linear. A warning is made regarding the use of resistivity vs current density plots to decide on non-linear behavior.

Finally, it is suggested that interfacial phenomena and non-linear effects may be common features in two- and four-electrode systems.

Electrical Non-linear Behavior in Rocks

INTRODUCTION

In the study of electrical properties of rocks the assumption of linear behavior is often made. In addition, it is admitted that rocks exhibit linearity up to a given current density value; above it non-linear effects appear. The existence of an upper limit in current density has been established in studies such as those of Madden and Marshall (1959) and Anderson and Keller (1964).

Information on the subject of non-linearity is scant and often incidental to other studies of electrical conduction in rocks. McEuen et al (1959) observed, for synthetic metalliferous ore, an impedance that was dependent on current density. Scott and West (1969) observed a decrease of resistivity with increasing current density in samples containing disseminated sulfides. Zonge (personal communication) has observed non-linear effects while studying IP responses, and Katsube and Collett (1972) have recently reported on electrical non-linearity using ac excitation. Possibly the only systematic approach to the problem has been that of Shaub (1965 and 1969; Shaub and Ivanov, 1971).

While studies in electrochemistry (Shaw and Remick, 1950) may serve as a guideline to understand non-linear effects in rocks in which porous electrolytic conduction predominates, care should be exercised not to extrapolate results to samples in which such conditions may not be applicable.

When sufficiently intense electric fields are applied to a material, it will eventually undergo an irreversible change in electrical properties; before arriving at such a limit electrical non-linear phenomena will appear.

A system described electrically by the relation

$$\underset{\sim}{J} = \sigma \underset{\sim}{E} , \tag{1}$$

in which $\sigma \neq \sigma(E)$, exhibits a linear (or ohmic) behavior. $\underset{\sim}{J}$ is the current density, $\underset{\sim}{E}$ the electric field and σ the conductivity.[1]

If the conductivity σ, in equation (1), is a function of the electric field, that is, if $\sigma = \sigma(E)$, the relation between the current density and the electric field can be generally written as a polynomial

$$J = \sigma' E + \sigma'' E^2 + \sigma''' E^3 + \ldots . \tag{2}$$

in which the coefficients σ', σ'', ...are constants. Relation (2) describes a non-linear behavior.

If the total electric field $\underset{\sim}{E}$ is the sum of two independent electric fields $\underset{\sim}{E}_1$ and $\underset{\sim}{E}_2$, it is readily verified that superposition holds for relation (1)

$$\underset{\sim}{J} = \sigma \left(\underset{\sim}{E}_1 + \underset{\sim}{E}_2 \right)$$

whereas for equation (2) superposition no longer holds:

$$J = \sigma' \left(E_1 + E_2 \right) + \sigma'' \left(E_1^2 + E_2^2 + 2E_1 E_2 \right) + \ldots . \tag{3}$$

Consequently, if the fields $\underset{\sim}{E}_1$ and $\underset{\sim}{E}_2$ are of the form

$$\underset{\sim}{E}_1 = \underset{\sim}{E}_{01} e^{j\omega_1 t} \quad \text{and} \quad \underset{\sim}{E}_2 = \underset{\sim}{E}_{02} e^{j\omega_2 t}$$

harmonic generation, in equation (3), will occur (Shaub, 1965).

If relation (2) describes the behavior of a given material, then under small electric fields, and if the condition

$$\sigma' \gg \sigma'' \gg \sigma'''$$

[1] MKS units are used in this paper.

holds, the response will be linear. Clearly, for sufficiently large E fields,

$$\sigma'' E^2 \sim \sigma' E$$

and the non-linearities will appear.

However, intense electric fields are not the only possible cause of non-linearities. Non-linear behavior may also be observed at small electric fields in insulators and semiconductors in contact with metallic electrodes.

Contact effects have been discussed in relation to insulators and semiconductors by Mott and Gurney (1950), Frank and Simmons (1967) and others. Simmons (1971) has reviewed the three types of contacts that may arise in metal-insulator-metal and metal-semiconductor-metal systems: ohmic, blocking and neutral. Once an ohmic or blocking contact is established, linear and non-linear behavior may be obtained for the same metal-insulator-metal system depending on the voltage applied. Furthermore, a contact that in a given voltage region is ohmic may, at different voltages, become blocking and viceversa. A space charge is often found at the metal-insulator or metal-semiconductor interface; it plays a central role in the contact properties.

Consequently, the possibility exists of observing similar phenomena in the case of rock specimens, which are either semiconductors or insulators, in contact with metallic electrodes.

Anderson and Keller (1964) established the existence of an upper limit for current density, up to which the behavior of a pyrite sample was linear. They used direct current in this determination. We have also used direct current in the experiments reported herein since we are looking for electrode effects as the origin of non-linearities; they will be most clearly shown under these conditions.

The measurements were performed with samples exposed to room

conditions although, for comparison purposes, a few were made at high vacuum conditions (i.e. 10^{-7} Torr). At room conditions the samples were , of course, subject to the effects of atmospheric moisture, which ranged from 20 to 45% relative humidity. A two-electrode system was used throughout the experiments.

The samples studied can be divided in two groups: argillaceous sandstone, granite, limestone and hematitic sandstone belong to the group hereafter called "resistive samples", and samples whose main constituents are galena and pyrite respectively belong to the "conductive samples".

NON-LINEARITIES: EXPERIMENTAL

The dc regulated power supply used was a Princeton Applied Research model TC-602CR. Total current and voltage in the sample were measured with two electrometers (Keithley, models 601 and 610B) of 10^{14} ohms input impedance. A two electrode system was used; Indium-Mercury electrodes were directly applied to the sample in each case and, as a result, a Maxwell-Wagner effect was observed when measuring the samples belonging to the resistive group (Alvarez, 1972). Transients occur when establishing or discontinuing dc excitations; the measurements reported were made after all transients had disappeared.

It has become common practice to report values of resistivity ρ, for rocks, derived from measurements of total current and voltage in the sample. When the sample geometry corresponds to parallel faces of area A and thickness d the relations

$$\frac{V}{I} = R = \rho \frac{d}{A}$$

are used to obtain ρ. This operation results in deriving a point property (i.e. $\rho(x, y, z)$ from the bulk properties of the sample (i.e. total I

and V). Clearly, this way of proceeding will be valid only if the field E in the sample is uniform. Further ahead we shall present experimental evidence showing the non-uniformity of the field on the surface of a sample. Consequently, we have tried to avoid the above operation wherever possible. The data is presented mainly as I-V or R-V plots (Figures Ia and b); the measured parameters were current and voltage in all cases. Since the sample geometries are given, one may obtain, if necessary, the sample resistivities from the resistance plots by making the assumption of uniform field in the sample; at any rate, they will differ only by the geometric factor d/A. Two plots of resistivity vs current density are included to allow for comparison with previous work (i.e. Anderson and Keller, 1964, and Scott and West, 1969).

In Figure 2a the total resistance R of a limestone sample of the dimensions shown is plotted against the total voltage across the sample. The shaded surface represents an electrode. For voltages of less than 5 volts a non-linear region is observed; linear behavior appears to occur for larger voltages. Notice that for V = 0.1 volts a negative value of R is obtained. This was due to current flowing in the direction opposite to that determined by the polarity of the applied voltage. The only way such an effect can be accounted for is by the existence of a polarization within the electrode-rock-electrode system, larger than and of opposite polarity to the one externally applied.

In Figure 2b data corresponding to a similar sample of limestone is plotted. The voltage goes from -8.0 to + 7.0 volts; in this case one electrode of the sample was constantly grounded while the other was varied from positive to negative voltages. The presence of a polarization within the electrode-rock-electrode system is again manifested by a zero current flow at a voltage of +0.18 volts. Correspondingly, there is

a non-zero current of -0.3×10^{-10} amp when the sample terminals are short-circuited.

The data in Figure 2b, is plotted as resistivity vs current density modulus in Figure 2c; according to the established criterion (Anderson and Keller, 1964), the resistivity varies non-linearly with current density. A discussion of these results and the way of plotting them is made below.

The fact that a voltage exists between the sample terminals when no excitation is applied constitutes an important difference with respect to the common meterials obeying Ohm's law; in these the current vs voltage characteristic is a straight line passing through the origin, whereas in the rock sample it is displaced from the origin (Figure 2b).

In Figure 3a the current-voltage characteristic (the scales of current and voltage are multiplied by arbitrary factors) of a material assumed to have such properties is used to model the behavior of the limestone sample. They show a voltage of 1 unit when the terminals of the model sample are open-circuited, and a current of -2 units when they are short-circuited. Other than the peculiarity of being displaced from the origin the characteristic is linear. Assuming that the geometry of such a sample is a unit cube we can obtain the resistivity vs current density plot (Figure 3b) corresponding to the characteristic in Figure 3a.

In Figure 3b there are two branches of resistivity values, denoted ρ^+ and ρ^- . Since resistivity is obtained by making the ratio V/I and multiplying by a geometric factor (in the present case 1), it will be positive for voltages $V > 1$ and $V < 0$, in which both V and I have the same sign; for the region $0 < V < 1$ the voltage is positive, but the current is negative, thus the resistivity will be negative. It is for this reason that we have been forced into defining negative resistances and resistivities. In common materials obeying Ohms' law this problem never arises.

For the same absolute value of current, in Figure 3a, there are two different values of voltage. Therefore there will be two different values of resistivity for each value of the current density modulus (Figure 3b). This is true up to a value of current density, approximately 100 times larger than the one corresponding to zero resistivity (i.e. to the current density J_o flowing when the sample is short-circuited.) Above such a value of current density the resistivity corresponds to that of the reciprocal slope of the characteristic (i.e. the actual resistivity).

Thus, a material with a linear I-V characteristic, displaced from the origin, gives rise to an apparent non-linear behavior when plotted as resistivity vs current density. The apparent non-linearities appear for values of the current density modulus $|J| < 100\ J_o$; whereas for $|J| > 100\ J_o$ the resistivity is linear.

In trying to determine non-linear behavior with dc excitations, it is important to establish whether or not the I-V characteristic of the rock sample is displaced from the origin; otherwise non-linear behavior may be inferred from resistivity vs current density plots for samples with linear I-V responses. Therefore, it seems more adequate to decide on the linearity of the rock response on the basis of I-V rather than ρ-J plots.

Returning to the results of the limestone sample one can observe (Figure 2b) the displacement from the origin plus an actual non-linear plot of the I-V characteristic. Figure 2c shows the behavior predicted from Figures 3a and 3b; except that at the higher current densities the ρ^+ and ρ^- values, although coincident, show a non-zero slope; this fact plus a distortion of the curve shapes with respect to the theoretical one (Figure 3b) arise from the non-linear behavior of the limestone sample.

Figure 4a shows the I-V plot corresponding to granite. A linear region, for $V > 3$ volts, and a non-linear region, for $V < 3$ volts, are obtained. Figure 4b, the corresponding R-V plot, suggests a non-linear region below 3 volts. Notice, however, that from Figure 4b alone one would not be able to discriminate between the increase in R, when V decreases, due to an actual non-linear effect or to that due to a displacement of the I-V characteristic from the origin.

The main difference of the granite data with respect to the limestone data is that the latter shows non-linear behavior throughout the voltage region analyzed, whereas the former presents a linear region from 3 to 8 volts.

The I-V plot corresponding to an argillaceous sandstone sample is presented in Figure 5. The characteristic is linear, and, in the scales plotted, appears not to be displaced from the origin.

In Figure 6 data corresponding to a muscovite schist sample plots as a straight line; the behavior is linear but there is a small displacement of the characteristic from the origin, towards the positive side of the current axis, contrasting with that of the limestone sample (Figure 2b), which intersected the current axis on the negative side. As a result, the resistance values will decrease, instead of increase as in the limestone sample, when zero voltage is approached from the positive side of the voltage axis.

Figures 7a and b correspond to the R-V plots of argillaceous sandstone and muscovite schist respectively. In Figure 7a a linear region seems to start at around one volt; for smaller voltages the decreasing R-values suggest a slight displacement from the origin of the I-V characteristic. This feature is masked in Figure 5 as a consequence of plotting

in the scales shown, which are too large for the smaller values.

The R-V plot for the muscovite schist (Figure 7b) gives no clear indication of linear behavior, contrasting with the obvious linearity shown by the same data when plotted as an I-V characteristic (Figure 6). This example underlines the importance of not relying on R-V or ρ-J plots alone to analyze the linearity of rock samples.

The points shown as crosses in a circle, in Figures 7a and b, were taken immediately after having applied the largest voltages to the samples (i.e. 9 volts for the limestone sample and 8 volts for the muscovite schist sample). In Figure 7a three such points delineate a behavior similar to the one observed in the case of limestone (Figure 2a), and in Figure 7b the corresponding point suggests a similar trend. This points out that a shifting of the I-V characteristics, from its original position, was brought about in each case by the application of the external voltage.

The change is thought to consist of a redistribution of charge carriers within the material, caused by the passage of current. However, the change is not permanent since the sample presents the peculiarity of recovering its original properties if no new excitations are applied in several hours. Zheludev (1971) discusses the factors that may produce redistribution of charge carriers in a material and their relation to the space charge accumulation usually accompanying it.

Figures 8a, b, c, and d correspond to a set of measurements on a hematitic sandstone sample. Figure 8a represents the typical response of a "resistive" rock sample, measured with a two-electrode system, when an external voltage V_0 that has been applied to the sample for some time is interrupted. The response consists of a "fast drop" in voltage (V_F) followed by a voltage

decay resembling an exponential function. This remaining voltage (V_R) decays to a small value (with respect to the magnitude of the applied excitation) within a few seconds, but seldom goes to zero, even after several hours of observation; it seems to correspond to the displacement from the origin of the I-V characteristics.

The measurements on the hematitic sandstone sample include a comparison of the total resistance of the sample, designated R_T (obtained as the ratio of the total applied voltage V_o to the total current I_T in the sample; Figure 8c), to the resistance R_F (Figure 8b) defined as the ratio of the voltage V_F (Figure 8a) to the total current I_T in the sample.

As can be appreciated from Figure 8b, there is a linear range for the resistance corresponding to the fast decay (R_F), starting between 3.0 volts and 4.0 volts, whereas the total resistance (R_T) in Figure 8c, shows a non-linear behavior up to 9.0 volts. Below 3.0 volts R_F becomes non-linear; the negative value of R_F at V=0.5 volts requires additional description: when the excitation was interrupted, an <u>increase</u> in voltage took place (i.e. instead of the usual fast decaying voltage, there was a fast increment); it was defined as negative V_F. This increase was followed by the usual decay. The measurement was repeated at least four times and the response was reproducible. Figure 8d shows the I-V characteristic obtained for the hematitic sandstone. Non-linearity is observed below 3 volts; above 3 volts the behavior is linear. The I-V characteristic shows a displacement of +1.0 volt from the origin. On the basis of further verifications, a value of +0.5 volts seems more adequate than the +1.0 volt value obtained in these measurements. The value of +0.5 volts was obtained after periods of several weeks of not subjecting the sample to voltage excitations. Observation times ranging from a few minutes to half an hour were necessary to insure

that steady state was attained when obtaining the data of Figures 8b, c, and d. It appears that this hematitic sandstone sample requires much longer periods, than the other resistive samples analyzed, to return to its normal state after voltage excitations have been applied to it. Periods of around one hour necessary to attain equilibrium conditions have also been reported in ac measurements (Scott and West, 1969).

A discussion of a schematic model shall be made in relation to the results of Figures 8a, b, c, and d, which may help to understand the origin of the non-linearities. One may think of the two decay regions in the voltage response as due to two different relaxation mechanisms, corresponding to at least two different species of charge carriers having a marked difference in relaxation times. The fast decay is similar to that of samples in which electronic conduction predominates, whereas the slow decay resembles ionic diffusion characterized by low mobilities.

Although the latter mechanism may account for displacements of the I-V characteristic arising from the application of external excitations[2], it cannot account for the displacements observed when the sample has not been subjected to voltage excitations at all, or when the sample is not excited in periods of several days: these need to be explained in terms of a mechanism of different origin.

Information on the same type of hematitic sandstone reported elsewhere (Alvarez, 1971) shows that the magnitude of the fast voltage decay (V_F), attributed to electronic conduction in this model, tends to zero when the atmospheric moisture content is reduced, by evacuation, in the sample; eventually, in a vacuum of around 10^{-7} Torr, V_F becomes zero. At this time the decay voltage V_R equals the applied voltage V_o, since $V_F = 0$.

[2] See explanation related to the crossed circles in Figures 7a and b.

In terms of the model under discussion, $V_F = 0$ implies that the electronic conduction mechanism has been supressed, leaving only the low-mobility charge carriers to conduct current through the sample. But since the water has been removed from the sample the low-mobility carriers cannot be moving in an aqueous electrolytic medium, which leaves only the possibility of such ions moving through the solid sample matrix (i.e. they travel through the minerals forming the rock). One may conclude, therefore, that the exponential-like decay V_R (Figure 8a) is associated with properties of the minerals forming the rock.

When exposing the sample to atmospheric moisture, after evacuation, the fast decay voltage V_F reappears in the rock response. This and related observations led the author (Alvarez, 1971) to suggest that water molecules adsorbed on resistive samples induce radical changes in their surface conductivity by forcing an electronic-type conduction in the sample surface. Consequently, in the model presently discussed, the fast decay voltage attributed to electronic conduction should be related to surface conduction in the sample.

One would expect fast relaxation times associated with electronic-type conduction, as well as a linear response of current vs voltage. The former feature is readily observed, although the term "fast relaxation" is taken here as relative to the relaxation time of the voltage V_R, which is often of less than 10 seconds. The linear response seems to be supported by the linearity, above 3 volts, of the plot in Figure 8b, which coincides with the linear region of the I-V characteristic (Figure 8d).

However, it would be more proper to decide on the linearity of R_F by obtaining the current associated only with V_F, which may be labeled I_F, and plot the I_F-V_F characteristic. At the time the measurements were made we did not have means of obtaining I_F and thus the total current I_T had to be used. The main differences between the I_F- V_F and the I_T- V_F plots are expected to take

place at voltages of values around the magnitude of the voltage shift from the origin (i.e. around +1.0 volt for the data in Figure 8d).

Summarizing the discussion on the hematitic sandstone sample, and the schematic model of conduction proposed to explain its response, we have that: (1) there is a linear region above 3 volts and a non-linear region below such a voltage; (2) a fast decaying voltage (V_F) is associated to surface conduction; (3) a slowly decaying voltage (V_R) is associated with conduction through the rock matrix, and (4) there is a persistent polarization voltage obtained when the sample has not been excited, that corresponds to the displacement of the I-V characteristic from the origin.

In addition, evidence of the presence of the polarization voltage mentioned in point (4) above was obtained when the sample was in a high vacuum: the currents flowing with forward and reversed polarities were different. From this fact follows that, whatever the mechanism responsible for such a polarization, it does not depend on the presence of water in the sample.

The discussion of the resistive group of samples brings about a common feature present in all of them, namely the displacement of the I-V characteristics from the origin. We found that this feature may give rise to apparent non-linear behavior if R-V or ρ-J plots of the data are made, but that the problem does not appear if the I-V characteristic is considered; from it, actual linear or non-linear behavior can be most properly inferred.

The possibility of observing non-linear behavior at low voltages in rocks in contact with metallic electrodes is confirmed by the I-V plots of limestone, granite and hematitic sandstone.

In the introductory discussion it was mentioned that non-linear behavior at low-voltages has been observed in relation to metal-insulator-metal or

metal-semiconductor-metal systems, and that space charge accumulations play an important role in the contact properties.

By analogy with such observations we propose that, in resistive rock samples in contact with metallic electrodes, the displacement of the I-V characteristics from the origin is due to space charge accumulations within the electrode-sample-electrode system.

The spatial charge accumulations would give rise to the non-linearities in the case of the limestone, granite and hematitic sandstone samples. The linear behavior manifested by the argillaceous sandstone and the muscovite schist samples is not necessarily in disagreement with the presence of spatial charges since, as pointed out previously, contact effects can give rise to linear or non-linear behavior depending on the type of contact (ohmic, blocking or neutral) established between the metallic electrode and the sample, as well as on the magnitude of the applied voltage. Changes in the type of contact induced by the latter may be responsible for the transitions from non-linear to linear behavior in the granite and hematitic sandstone samples.

Assuming that the displacement of the I-V characteristics from the origin is due to space charge accumulations, one can infer the existence of the latter, at high vacuum conditions, from the evidence of polarization voltages obtained for the hematitic sandstone sample. This fact is of importance since it rules out the possibility of non-linearities arising from aqueous electrolyte-electrode effects (i.e. the sample is extremely dry at high vacuum conditions) thereby supporting the hypothesis of the non-linearities being due to electrode-sample matrix effects.

At any rate, electrode-sample effects are expected to be proportional to the magnitude of the difference between the sample conductivity and the electrodes' conductivity.[3] From the data for galena and pyrite, presented below, one observes that the contrast in conductivity between the metallic electrodes and the sample is at least five orders of magnitude smaller for galena and pyrite than for the samples of the resistive group. Consequently, much smaller effects arising from the metal-sample interface are expected for the conductive samples than for the resistive ones.

Figures 9a and b correspond to samples of the semiconductors galena and pyrite (i.e. "good"conductors). As expected, the responses were linear. The experiments were not carried to higher voltages due to the low resistance of the samples which demanded larger than available currents; in any event the region of interest was the one around zero volts. Their responses to dc excitation voltages did not show the slow-decay region characteristic of resistive samples (Figure 8a). The fast decay V_F was equal to the applied excitation V_o and therefore V_R was zero for these samples; consequently the response to square pulses were square pulses for voltage and current. No variations of these responses were observed when the pyrite sample was evacuated to 10^{-7} Torr.

A formal proof of the hypothesis established above would require: (1) establishing the nature of the contact for each sample at different voltages and (2) obtaining positive evidence of space charges in the electrode-sample interface. As of now we have been unable to determine the former; the latter is discussed in the next section.

3 The problem of the contrast in electrical properties between two media in relation to conduction phenomena has been previously analyzed (Alvarez, 1972).

SURFACE VOLTAGE DISTRIBUTION

The purposes of the experiment to be described next was to determine the effect of the metallic contacts on a resistive sample. If the properties of the metal-sample interface differ from those of the bulk of the sample, the voltage distribution in the electrode vicinity should manifest the difference.

Figure 10 shows the schematic arrangement used in the experiment. The rock sample was a hematitic sandstone as the one used for the measurement reported in Figure 8. Indium-Mercury amalgam electrodes were used; one of them was constantly grounded while the other was polarized to + 4.9 volts; at times this electrode was floating or short-circuited to ground depending on the requirements of our observations. A micro-electrode with a platinum tip exposed five microns was used to determine the voltage with respect to ground at points (X, Y) on the sample surface. All measurements were performed at dc when transients had disappeared. Readings were taken at separations of tenths of a millimeter when close to the electrodes and by a millimeter elsewhere. Y was kept constant while X-traverses were made between electrodes, then Y was incremented by a millimeter and the process repeated.

The sample average dimensions were X = 24 mm, Y = 19 mm, and Z = 14 mm; the measurements were performed on 8 lines (i.e. Y = 0 through 7) covering somewhat less than half the surface of the sample. Figures 11a, b, c, and d show the voltage values along four different lines; Y = 0 corresponds to the edge of the sample.

The effect of the electrode-sample interface is manifested, at the positive electrode, by a voltage drop of around 1.7 volts occurring within a tenth of a millimeter from the electrode for Y = 0 and Y = 1.0 mm, and a voltage drop

of 0.3 volts and 0.7 volts within the same distance occurs for Y = 4.0 mm and Y = 6.0 mm respectively. At the grounded electrode a similar effect is observed; when going from the grounded electrode into the sample a "peak" is formed by a sharp increase followed by a decrease in voltage. Subsequently the average voltage rises when X decreases.

From the data in Figures IIa, b, c, and d, and recalling that those voltages correspond to stationary flow of direct current (i.e. the displacement current was zero when the measurements were taken), one can use the relation

$$\nabla^2 V = -\frac{\rho}{\varepsilon} = -\frac{(n_+ - n_-)e}{\varepsilon}$$

N. ed

ε = epsilon

to obtain information about the charge distribution in the sample. The concentrations (or charge densities) of positive and negative charge carriers at a given point are designated n_+ and n_-; ε is the dielectric permittivity of the sample at the same point and e is the magnitude of the electron charge. Although there is insufficient information to apply the above relation properly (i.e. we do not know ε locally) we can draw some general conclusions from it.

The large voltage drop close to the positive electrode corresponds to an accumulation of negative charge in its vicinity; that is $n_- > n_+$ in this region, while close to the grounded electrode a concentration of positive charge (i.e. $n_+ > n_-$) is observed. Along any line there is evidence of charge concentrations given by the increases and decreases in voltage over the average voltage slope. These reflect the inhomogeneous character of the sample, for in order to have steady state conditions in an inhomogeneous sample it is necessary that charge accumulations occur at the interfaces between regions of different electrical properties (Alvarez, 1972).

Since

$$J_x = -\sigma \frac{\partial V}{\partial x} = const.$$

there is obviously an inverse relationship between the slope of the voltage and the value of the conductivity within two points separated by a distance Δx. Therefore, associated to the space charge concentrations there are decreases in conductivity. The total current in the steady state was $I = 1.9 \times 10^{-5}$ amp; the intensity of the electric field varies roughly from 1 volt/cm to 170 volts/cm, thus variations of two orders of magnitude are observed between the average value of conductivity in the bulk of the sample and the regions close to the electrodes.

In Figure 12, contours of the voltage values are presented; the lines show the equipotentials on the surface of the sample. The non-uniformity of the electric field is evident. A word of caution is due regarding the contouring of the data: along Y-lines there are small vertical bars which show the actual points at which the measurements were taken; in order to obtain the equipotentials a linear variation of voltage was assumed between any two neighboring points. It is apparent that this is not a rigorous way of proceeding: suppose that, in the present case, measurements were taken every other point and, assuming there is a linear variation of voltage between them, predict the values at intermediate points; clearly there will be places in which the predicted value and the actually determined one will show large differences. In spite of this inaccurate assumption the general trends of voltage variation will manifest themselves when sufficient points are determined. In the case presently dealt with, closer sampling of the surface would modify the details of the contouring but the general trends would remain the same.

Earlier it was mentioned that deriving resistivity values from the total current, total voltage, and geometry of the sample in the case of measurements made with a two-electrode system (with parallel electrodes) was valid if the field E in the sample was uniform. The evidence presented above shows that assuming uniformity of the field may lead to a gross simplification of the actual conditions. Furthermore, it appears that by so doing essential information, that may help in explaining phenomena as the non-linearities, is lost.

Incidentally, the type of resistivity values that would be obtained with a four-electrode system, having the same current electrodes and a separation of a few millimeters in the voltage electrodes, can be inferred from the data in Figure 12. The values of resistivity thus obtained evidently depend on position and would show scatter if various electrode separations were tried along the same line.

CONCLUSIONS

Non-linear behavior at voltages of less than 10 volts was observed for limestone, granite and hematitic sandstone samples in contact with metallic electrodes; argillaceous sandstone, muscovite schist, galena and pyrite showed linear behavior. All of the resistive samples showed a displacement of the I-V characteristics from the origin, while the two samples of the conductive group did not.

Experimental determination of the voltage distribution on a sample surface showed the existence of space charge concentrations on the electrodes' vicinity. This fact strengthens further the hypothesis of non-linear behavior being due to contact effects.

Evidence of space charge accumulation in a hematitic sandstone sample at high vacuum conditions indicates that aqueous electrolyte-electrode effects are not the only possible cause of non-linearities. It was pointed out that interfacial phenomena were expected to be proportional to the magnitude of the difference between the sample conductivity and the electrodes' conductivity.

The use of dc excitation was suggested as the most effective way of observing electrode effects. Results obtained with a two-electrode system and dc excitation are relevant, in the context of our discussion, to measurements performed with four-electrode systems and ac excitations. A brief discussion in this respect closes the section.

In a four-electrode system there are contact effects between the sample and the electrolyte due to their different electrical properties (i.e. the electrolyte <u>is</u> the electrode). On the basis of the high conductivity contrast

between a sample and the electrolyte one may expect interfacial phenomena similar to the one reported in this work, in lieu of or in addition to eletrochemical phenomena occurring at the interfaces.

Studies on synthetic ores using ac excitations have shown decreasing resistivities when the current density increases (McEuen et al, 1959; Scott and West, 1969), indicating the existence of non-linearities in rock-electrolyte systems. Furthermore, the presence of a bias voltage has been commonly observed by various researchers when measuring with ac excitations; it corresponds to the displacement of the I-V characteristics, at dc, that we have reported. In particular Scott and West, 1969, indicate that when measuring at (ac) equilibrium conditions a bias remained in their potential measuring circuit. They offer no explanation for the presence of such a bias, but it has to be attributed to electrolyte-sample effects since measurements with a four-electrode system preclude the possibility of electrode-sample effects.

Thus, interfacial phenomena, non-linear effects and shifting of the I-V characteristics seem to be common features in two- and four-electrode systems, when either dc or ac excitations are used.

ACKNOWLEDGEMENTS

The author wishes to acknowledge H.F. Morrison for valuable criticisms of the manuscript..

Acknowledgements are due to the Consejo Nacional de Ciencia y Tecnología, México and to the National Aeronautics and Space Administration for financial support in the development of this research.

REFERENCES

Alvarez, R., 1971, Effects of atmospheric moisture in rock resistivity: (Abstract) AGU Transactions, v. 52, p. 918, Paper presented at the 1971 Fall Annual Meeting, San Francisco.

_____, 1972, Electrical conduction phenomena in rocks: Ph.D. thesis, University of California, Berkeley.

Anderson, L.A. and Keller, G.V., 1964, A Study in induced polarization: Geophysics, v. 29, p. 848.

Frank, R.I. and Simmons, J.G., 1966, Space-charge effects on emission-limited current flow in insulators: J. Appl. Phys., v. 38, p. 832.

Katsube, T.J. and Collett, L.S., 1972, Electrical non-linear phenomenon in rocks: Paper presented at the Symposium on the electrical Parameters of Rocks, Univ. of Utah, Salt Lake City. March 15-17, 1972.

Madden, T.R. and Marshall, D.J., 1959, Electrode and membrane polarization: AEC report RME-3157.

McEuen, R.B., Berg, Jr., J.W., and Cook, K.L., 1959, Electrical properties of synthetic metalliferous ore: Geophysics, v. 24, p. 510.

Mott, N.F. and Gurney, R.W., 1950, Electronic processes in ionic crystals: Oxford, Clarendon Press.

Scott, W.J. and West, G.F., 1969, Induced polarization of synthetic, high-resistivity rocks containing disseminated sulfides: Geophysics, v. 34, p. 87.

Shaub Yu, B., 1965, Use of the non-linear conductivity effect in rocks for electrical prospecting: Izv. Phys. Solid Earth, no. 6, English ed., p. 409.

_____, 1969, On the uses of the effects of nonlinear electrical conductivity in the detection of disseminated sulfide ores: Izv. Phys. Solid Earth, no. 1, English ed., p. 53

_____, and Ivanov, V.A., 1971, Experimental discrimination of sulfide ores and graphites by the use of the effects of non-linear electrical conductivity: Izv. Phys. Solid Earth, no. 3, English ed., p. 222.

Shaw, M. and Remick, A.E., 1950, The nature of polarization capacity and polarization resistance, Part I: J. Electrochem. Soc., v. 97, no. 10, p. 324.

Simmons, J.G., 1971, DC conduction in thin films: London, Mills and Boon Ltd.

Zheludev, I.S., 1971, Physics of crystalline dielectrics: v. 2, New York, Plenum.

Zonge, K.L., Personal communication

TABLE OF FIGURES

Fig. 4. (a) I-V characteristic of a granite sample. The non-linear region appears below 3 volts, above this voltage the behavior is linear. The displacement from the origin is not appreciable in the scales used. (b) The corresponding R-V plot agrees with the I-V characteristic showing linear and non-linear behavior in the same voltage regions.

Fig. 5. The I-V plot of an argillaceous sandstone sample shows linear behavior; in the scales shown it appears not to be displaced from the origin.

Fig. 6. The I-V plot of a muscovite schist sample shows linear behavior, a displacement from the origin towards the positive side of the current axis can be appreciated in the scales used.

Fig. 7. (a) R-V plot of the data in Figure 5 showing the effect of the displacement of the I-V characteristic towards the positive side of the current axis. It is manifested as a decreasing resistance when the zero voltage is approached from positive values. The points shown as a cross in a circle were obtained immediately after the 9 volts excitation was applied to the sample. They indicate that an additional displacement of the I-V characteristic took place after application of the maximum voltage. (b) R-V plot of the data in Figure 6 gives no clear indication of linear behavior contrasting with the information given by the I-V characteristic. The point shown as a cross in a circle was obtained immediately after exciting the sample with 8 volts. However the sample recovers its original values if no new excitations are applied in several hours.

Fig. 8. (a) Response of a resistive-type rock sample upon interruption of an externally applied voltage V_o ; V_F and V_R are the magnitudes of the "fast" and "slow" decays. (b) Ratio of V_F to the total current in the sample, (c) Ratio of the total voltage to the total current in the sample. (d) Current vs voltage characteristic showing a displacement of + 1.0 volt from the origin. Non-linear behavior is shown below 3

volts, above this voltage the characteristic is linear.

Fig. 9. R-V responses of (a) galena and (b) pyrite. Both show linear behavior.

Fig. 10. Schematic set-up for the determination of the voltage distribution in the surface of a sample. The micro-electrode traverses the lines taking voltage readings at points (X, Y) when a constant current is flowing.

Fig. 11. Voltage values as a function of distance X for a hematitic sandstone sample. (a) Y = 0, (b) Y = 1.0 mm, (c) Y = 4.0 mm, and (d) Y = 6.0 mm.

Fig. 12. Equipotentials on the surface of a hematitic sandstone sample showing the non-uniformity of the electric field when a constant current flows.

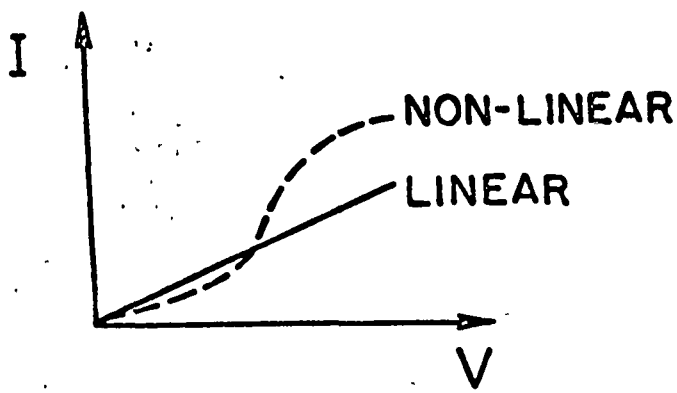

(a)

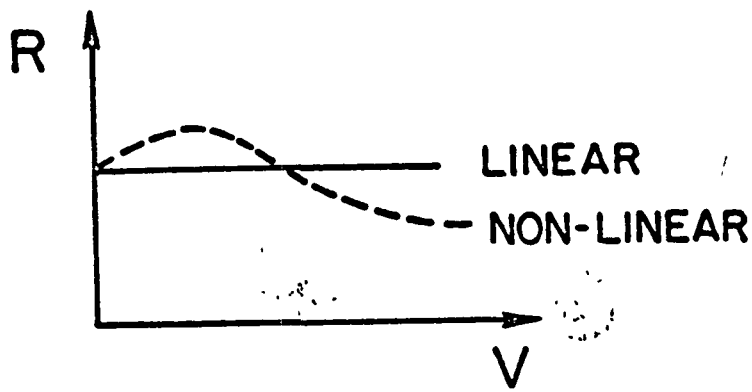

(b)

Fig. 1 ALVAREZ

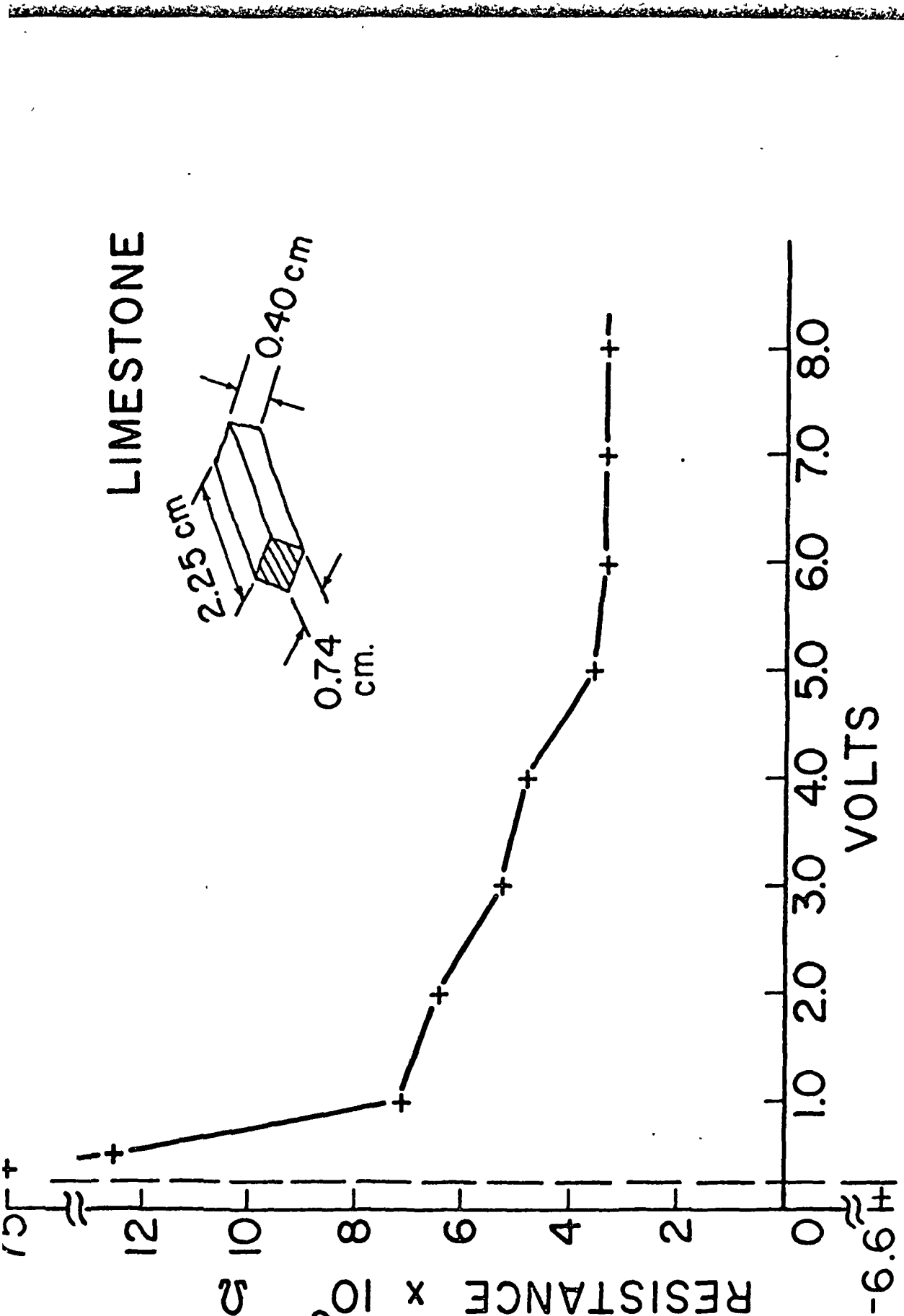
LIMESTONE
0.40 cm
2.25 cm
0.74 cm.
RESISTANCE x 10^8 Ω
VOLTS
0
1.0
2.0
3.0
4.0
5.0
6.0
7.0
8.0
2
4
6
8
10
12

Fig. 2 (a)

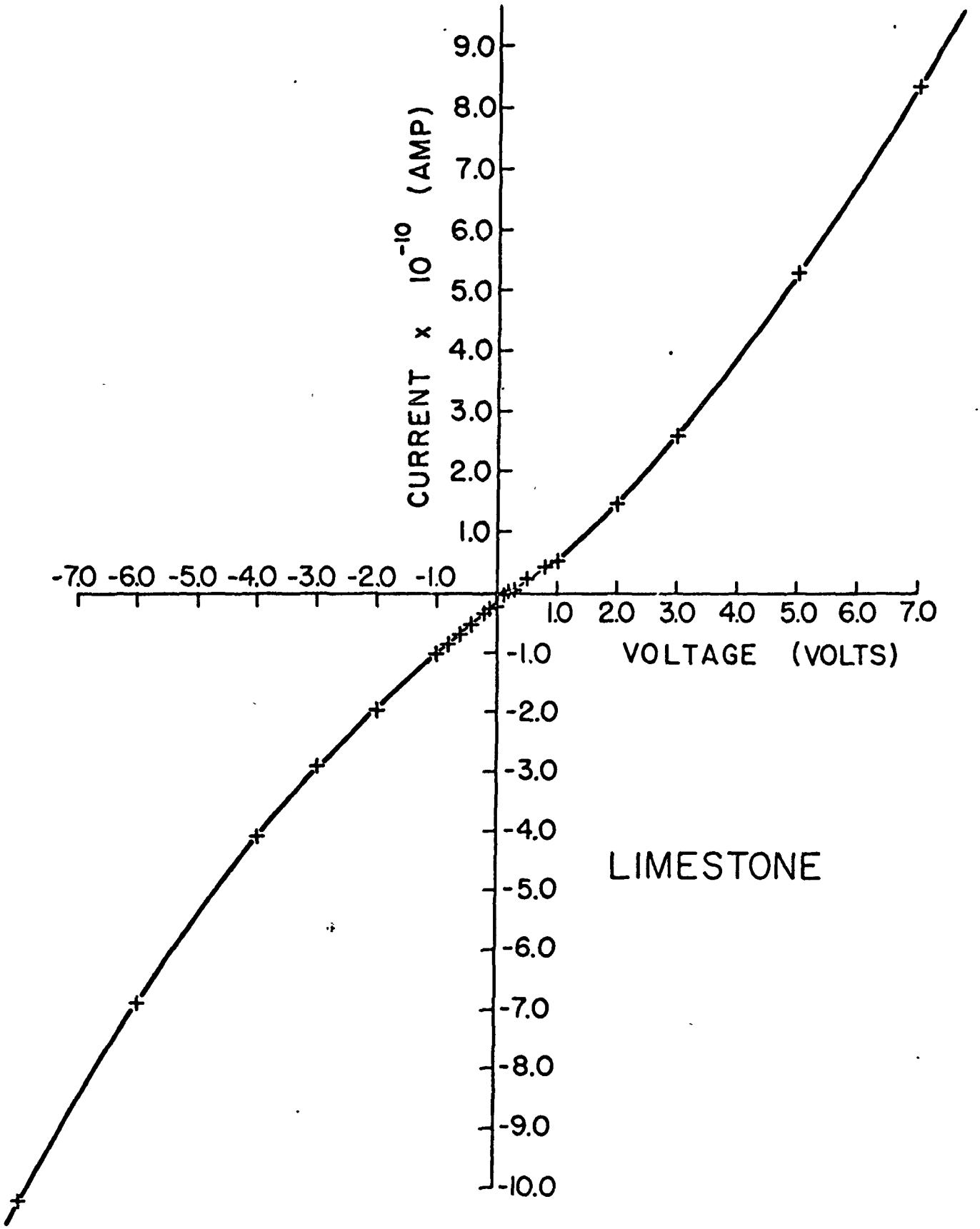
CURRENT x 10^{-10} (AMP)
9.0
8.0
7.0
6.0
5.0
4.0
3.0
2.0
1.0
-1.0
-2.0
-3.0
-4.0
-5.0
-6.0
-7.0
-8.0
-9.0
-10.0
-7.0 -6.0 -5.0 -4.0 -3.0 -2.0 -1.0
1.0 2.0 3.0 4.0 5.0 6.0 7.0
VOLTAGE (VOLTS)
LIMESTONE

Fig. 2 (b)

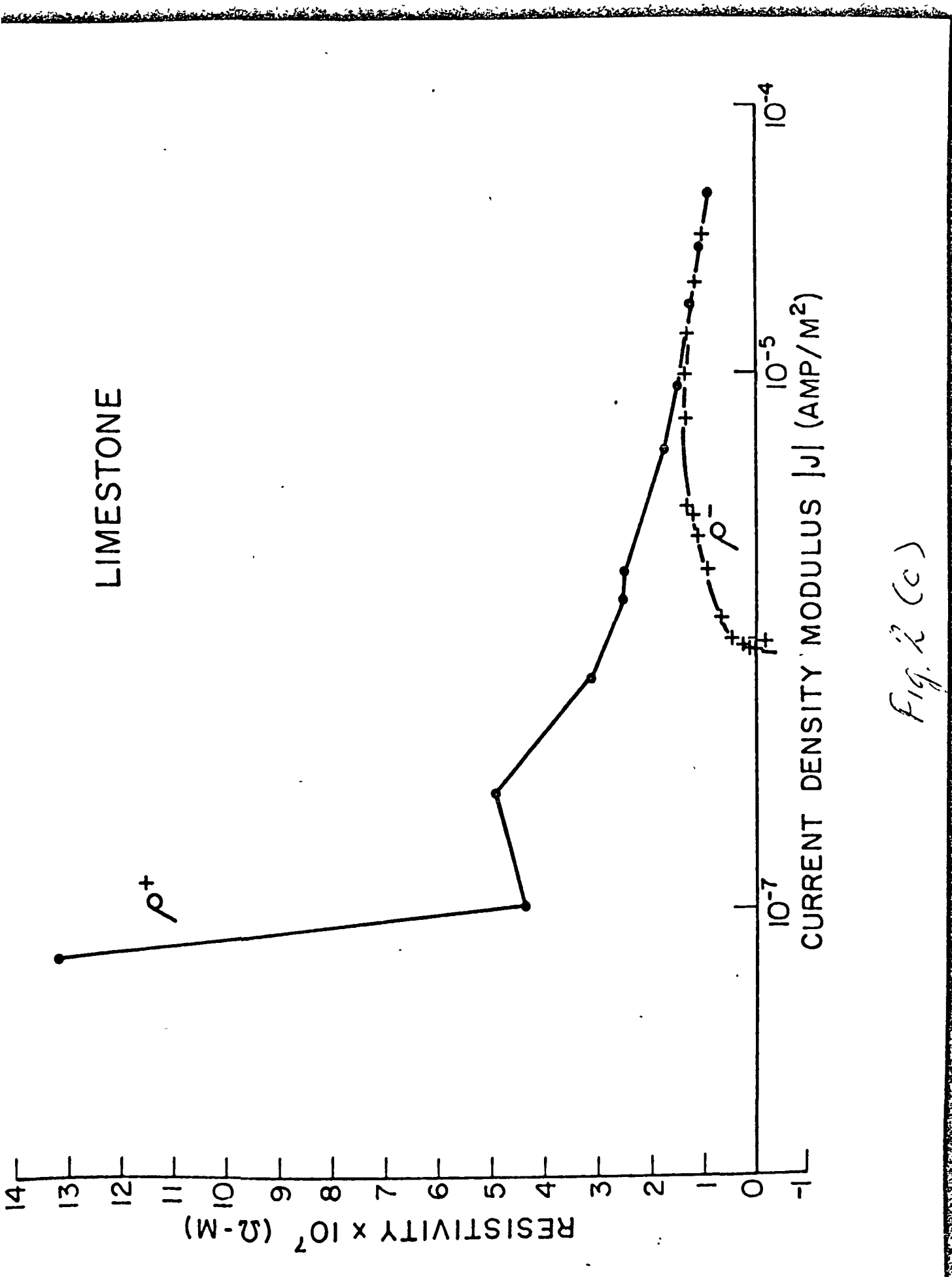
LIMESTONE
RESISTIVITY x 10⁷ (Ω-M)
CURRENT DENSITY MODULUS |J| (AMP/M²)
ρ+
ρ−
14
13
12
11
10
9
8
7
6
5
4
3
2
1
0
-1
10⁻⁷
10⁻⁵
10⁻⁴

Fig. 2 (c)

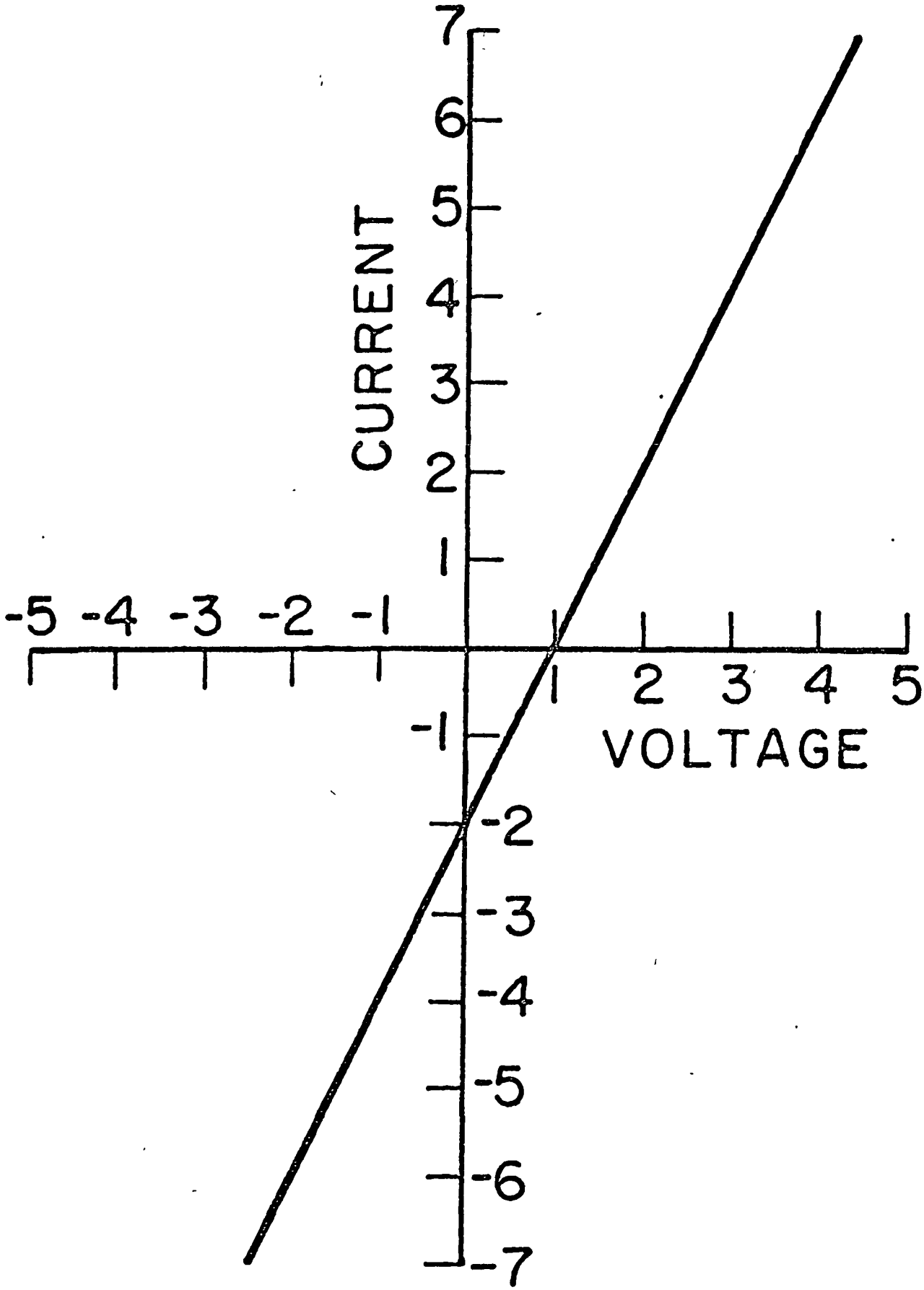

Fig. 3 (a)

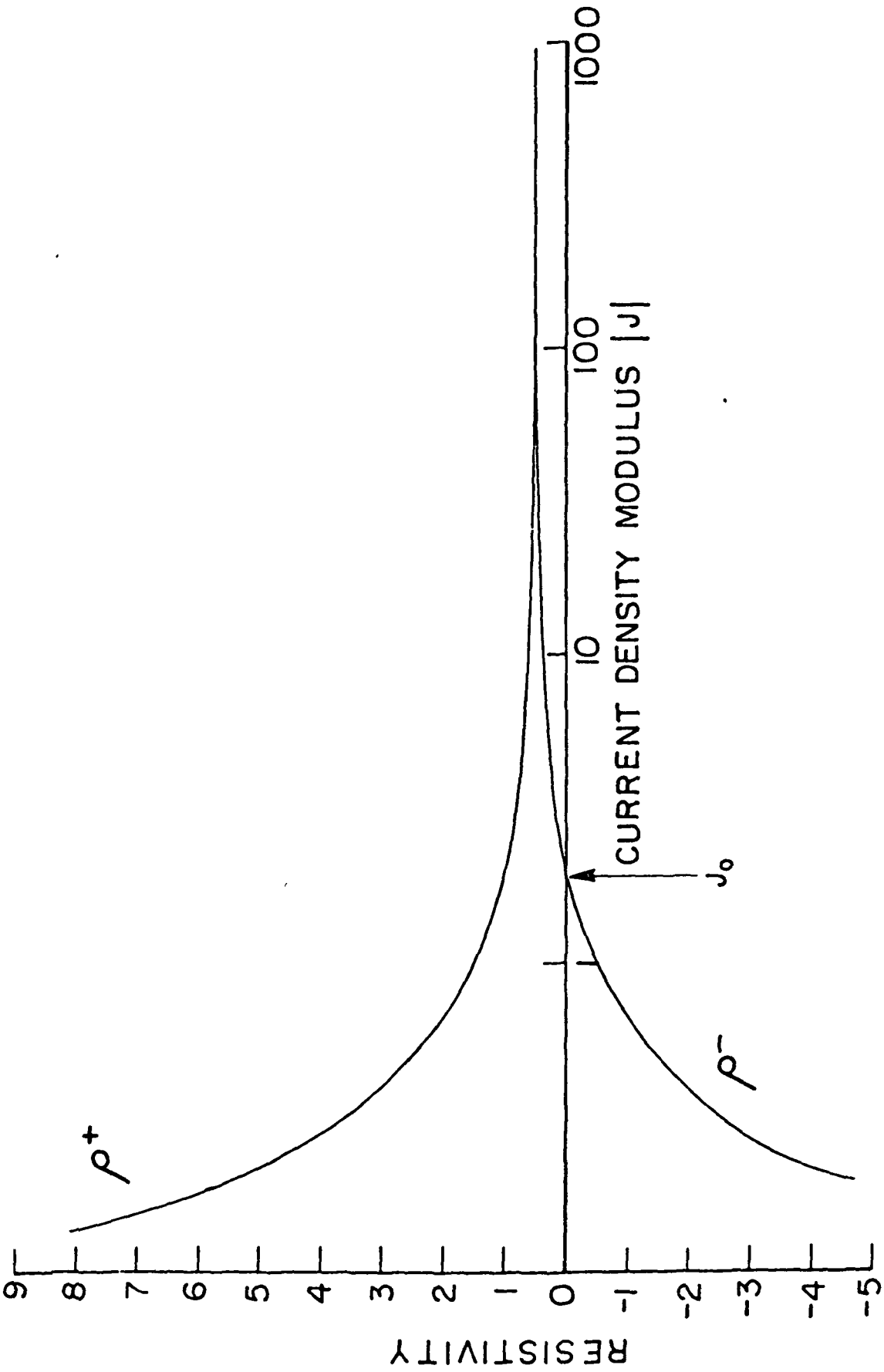
RESISTIVITY
9
8
7
6
5
4
3
2
1
0
-1
-2
-3
-4
-5
CURRENT DENSITY MODULUS |J|
1000
100
10
1
J_0
ρ^+
ρ^-

Fig. 3(b)

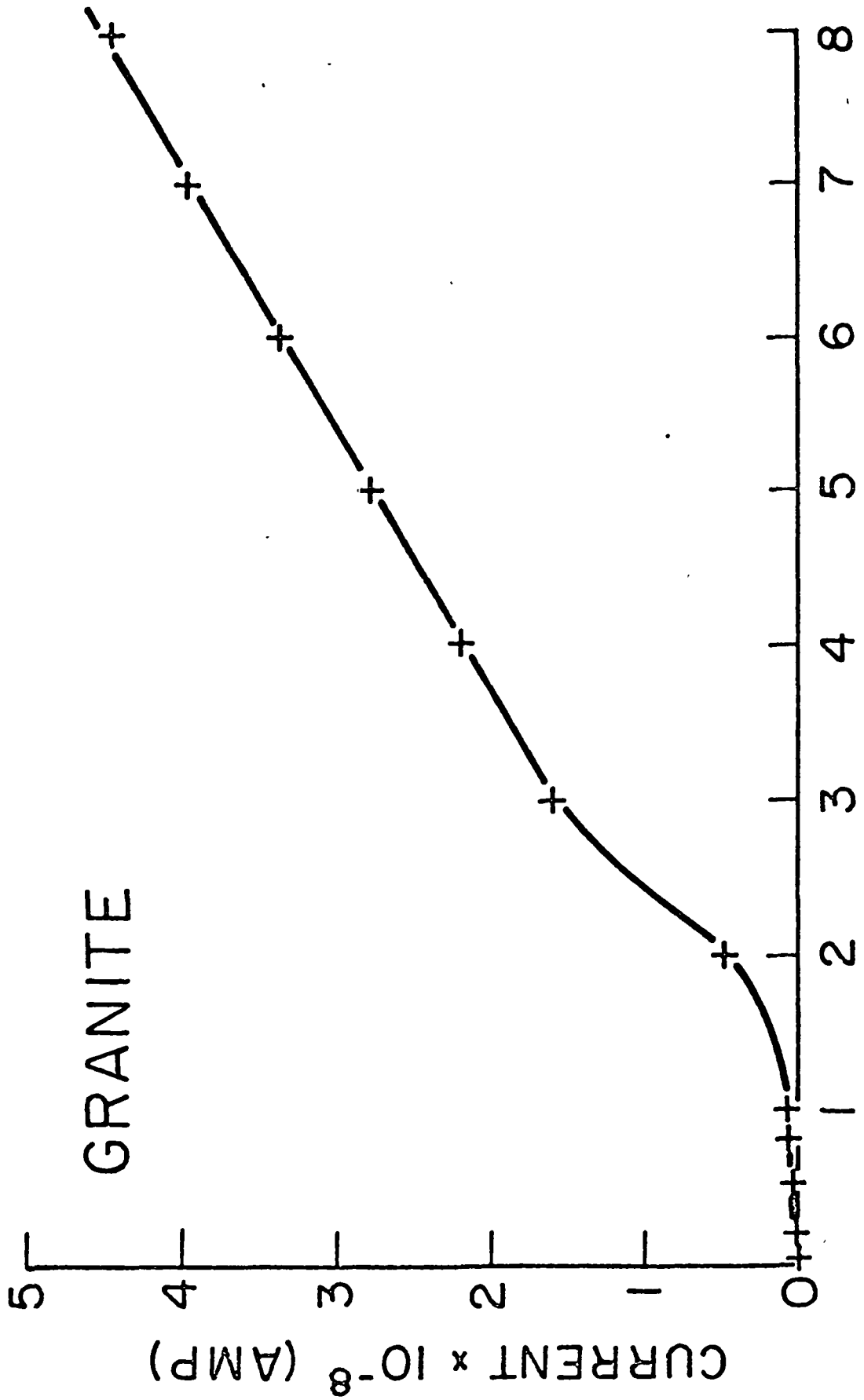

Fig. 4 (a)

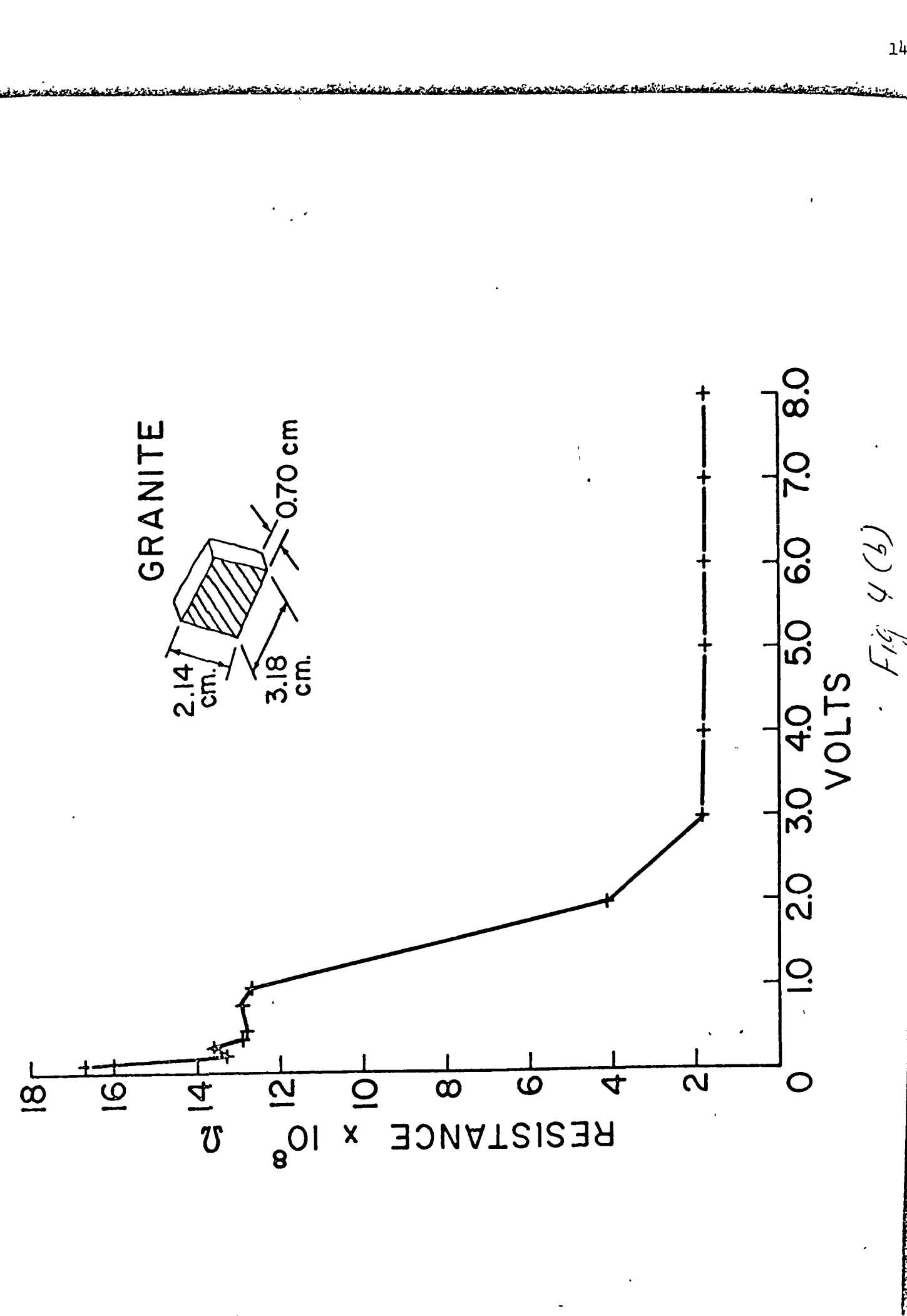
GRANITE
0.70 cm
2.14 cm.
3.18 cm.
RESISTANCE x 10^8 Ω
18
16
14
12
10
8
6
4
2
0
1.0
2.0
3.0
4.0
5.0
6.0
7.0
8.0
VOLTS

Fig. 4 (b)

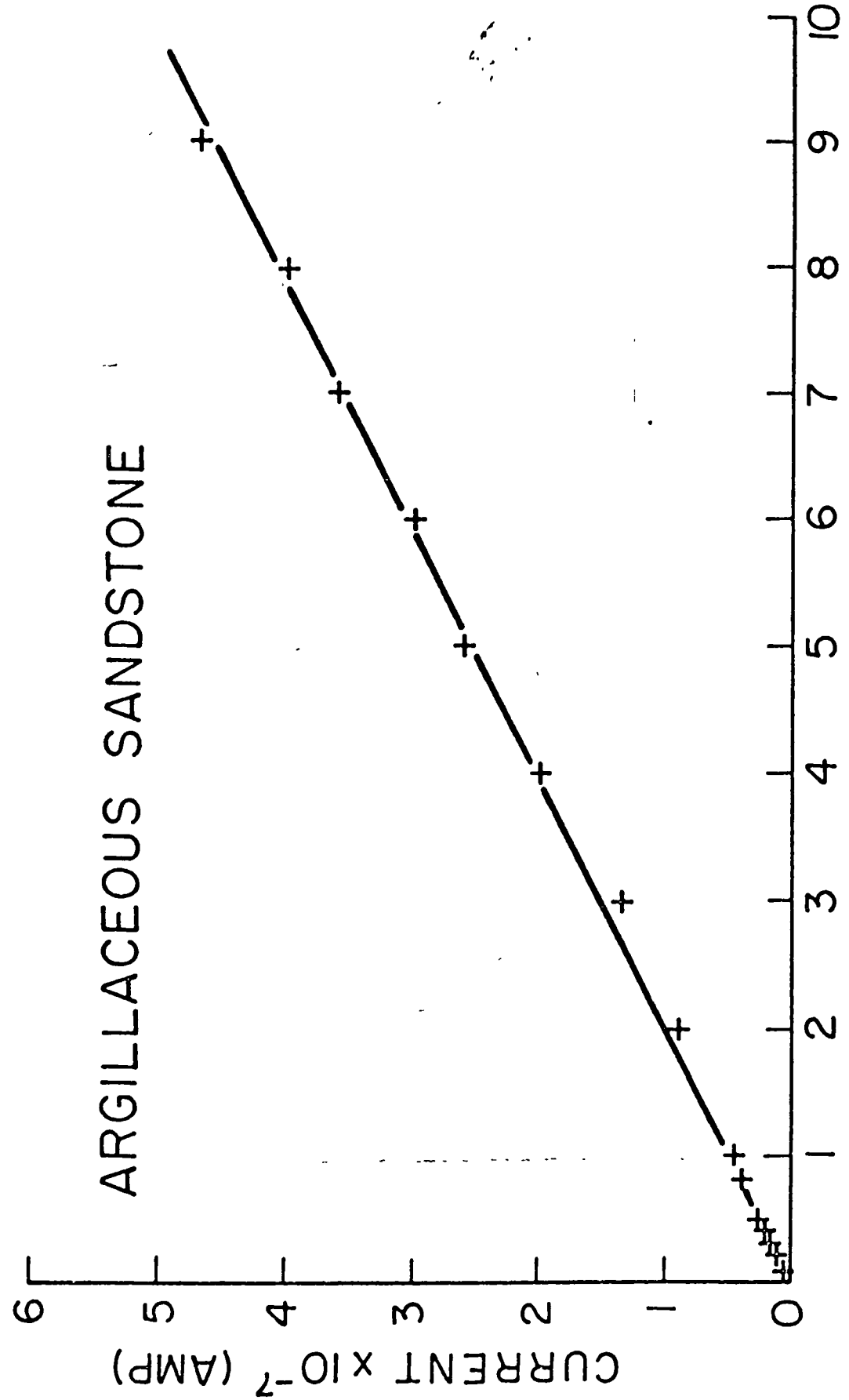
ARGILLACEOUS SANDSTONE
CURRENT x 10⁻⁷ (AMP)
VOLTAGE (VOLTS)
0
1
2
3
4
5
6
1
2
3
4
5
6
7
8
9
10

Fig. 5

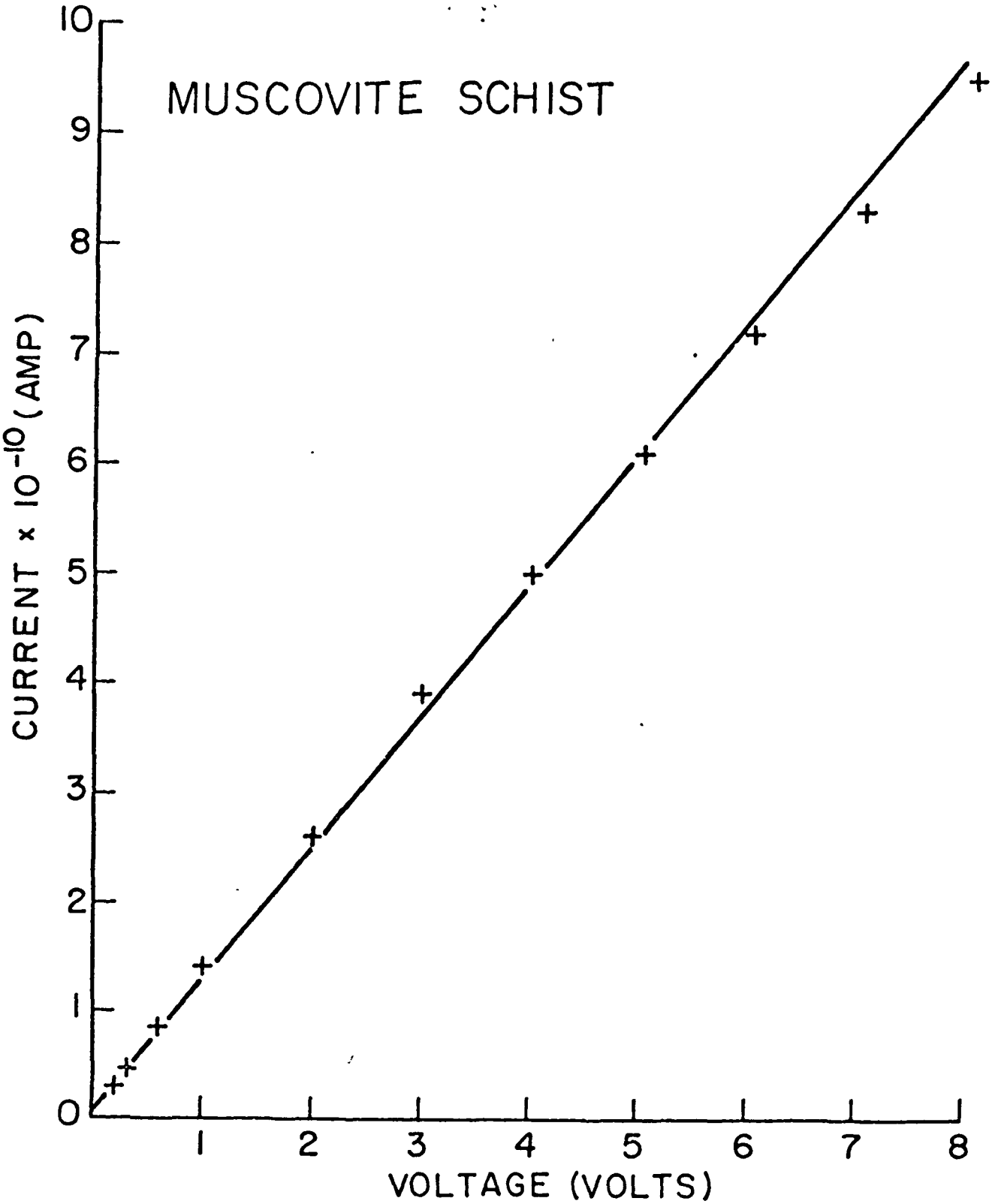
MUSCOVITE SCHIST
CURRENT x 10⁻¹⁰ (AMP)
VOLTAGE (VOLTS)
0
1
2
3
4
5
6
7
8
9
10

Fig. 6

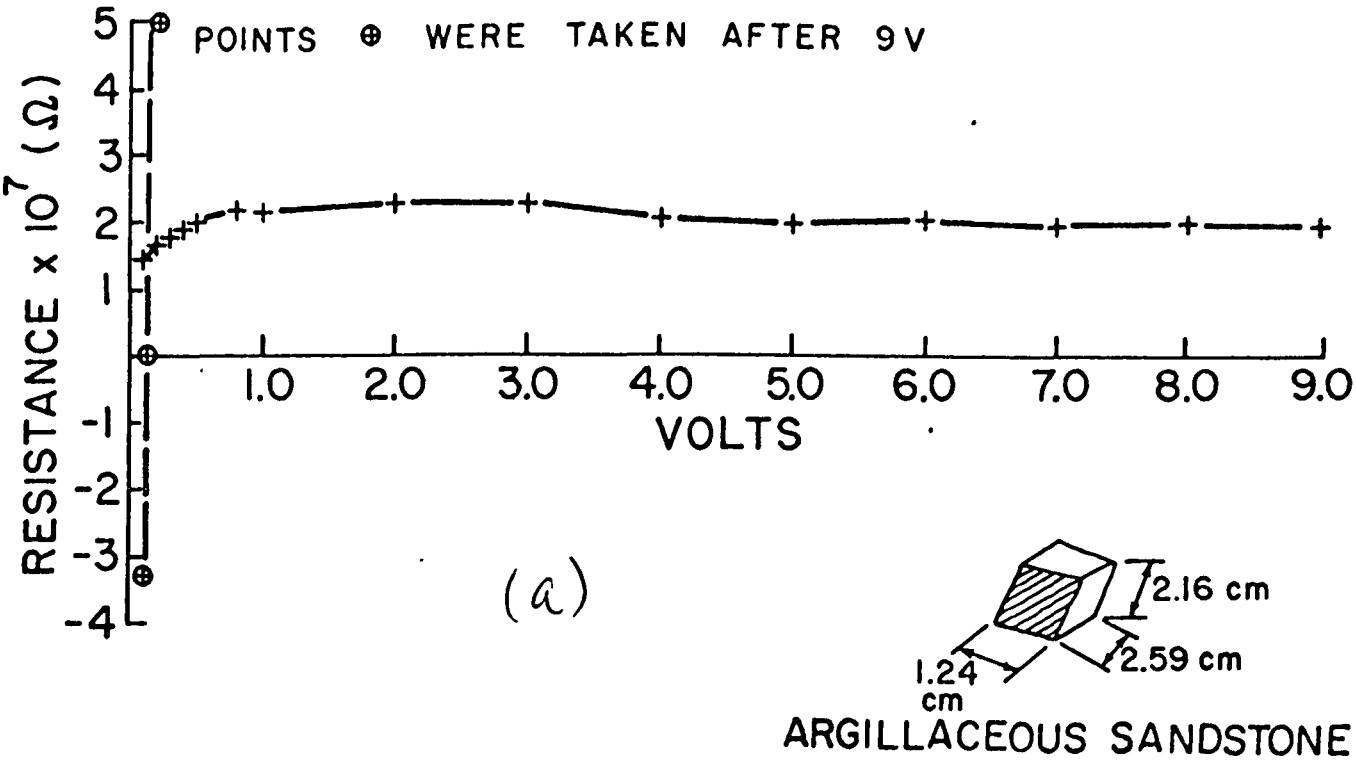
POINTS ⊕ WERE TAKEN AFTER 9 V
RESISTANCE x 10^7 (Ω)
5
4
3
2
1
-1
-2
-3
-4
1.0
2.0
3.0
4.0
5.0
6.0
7.0
8.0
9.0
VOLTS
(a)
2.16 cm
2.59 cm
1.24 cm
ARGILLACEOUS SANDSTONE

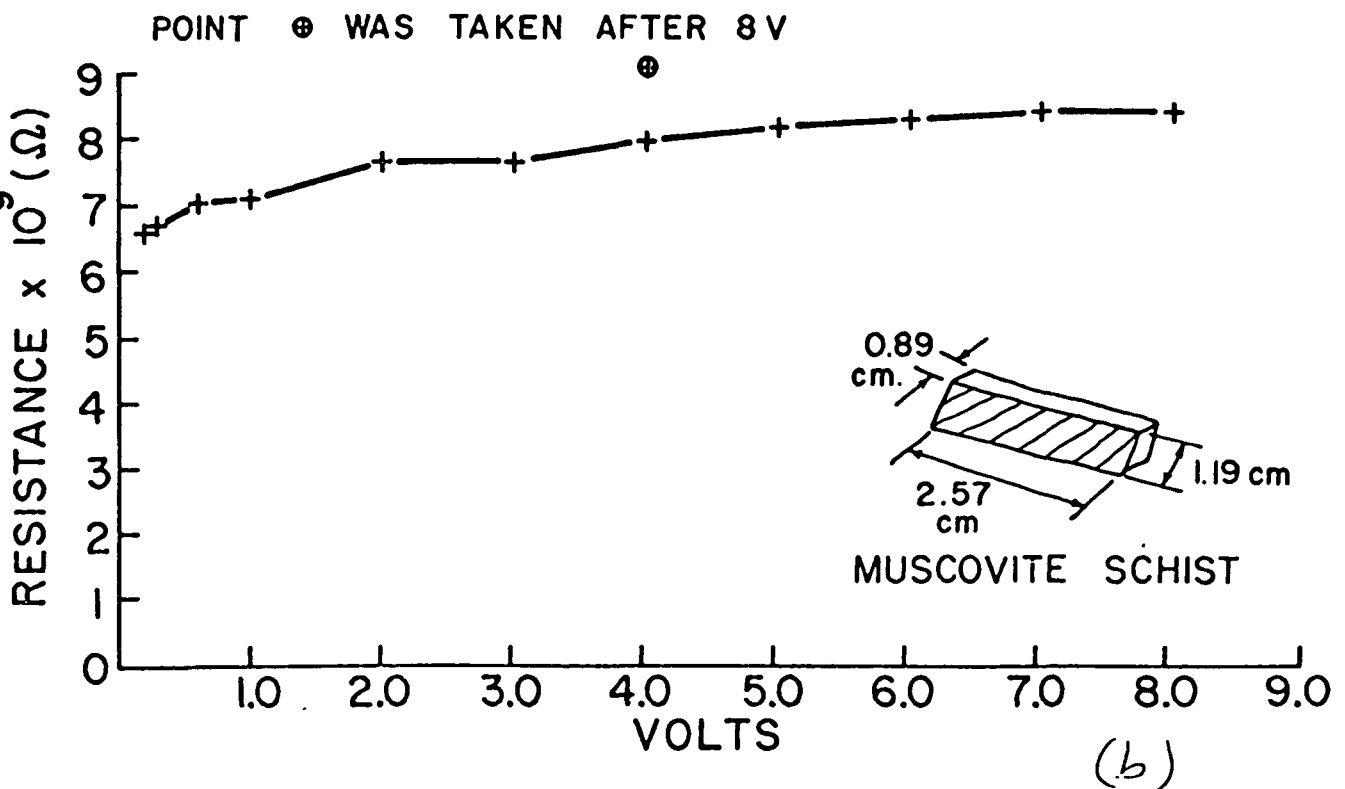
POINT ⊕ WAS TAKEN AFTER 8 V
RESISTANCE x 10^9 (Ω)
9
8
7
6
5
4
3
2
1
0
1.0
2.0
3.0
4.0
5.0
6.0
7.0
8.0
9.0
VOLTS
(b)
0.89 cm.
1.19 cm
2.57 cm
MUSCOVITE SCHIST

Fig. 7

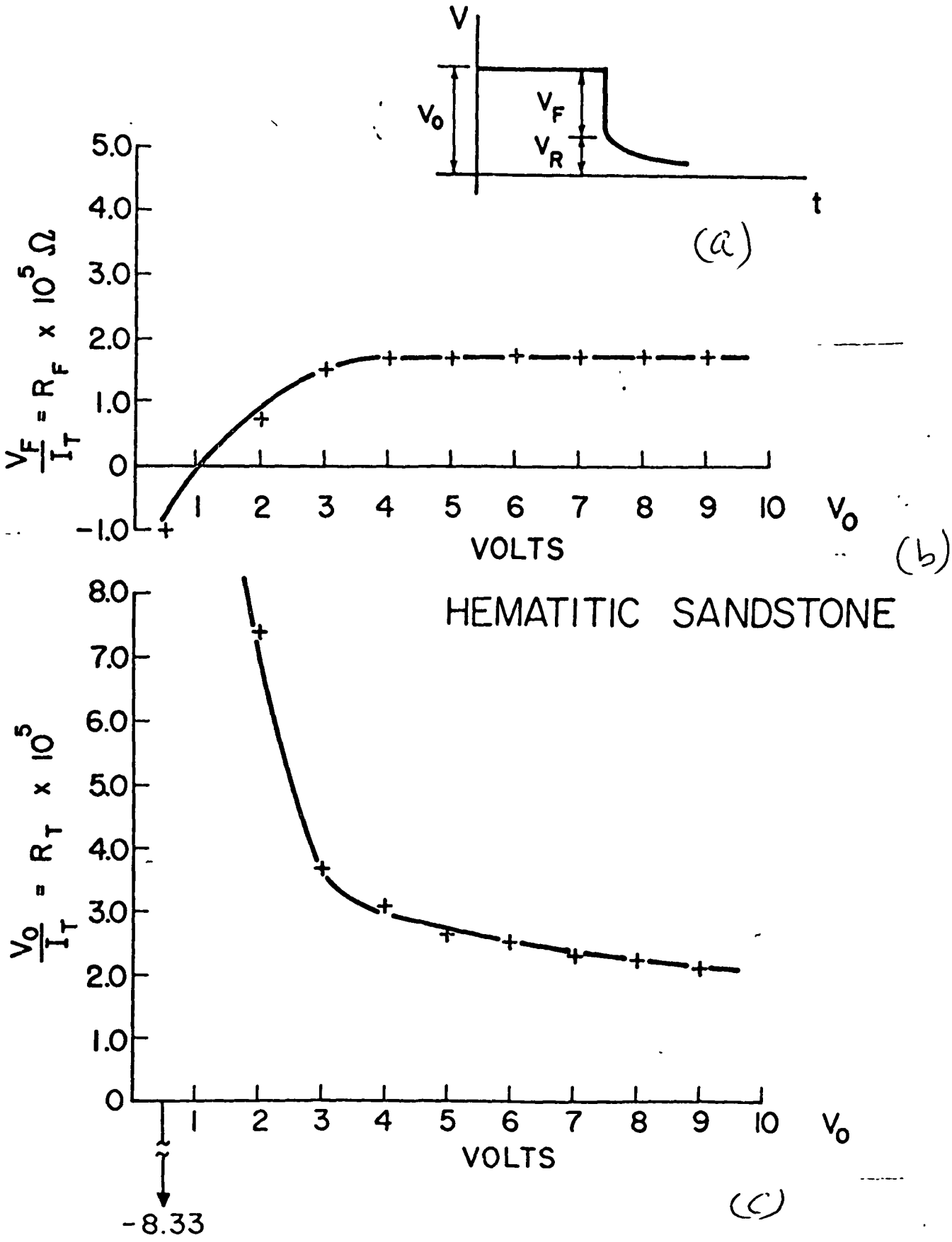
V
V_0
V_F
V_R
t
(a)
5.0
4.0
3.0
2.0
1.0
0
-1.0
$\frac{V_F}{I_T} = R_F \times 10^5 \Omega$
1 2 3 4 5 6 7 8 9 10 V_0
VOLTS
(b)
HEMATITIC SANDSTONE
8.0
7.0
6.0
5.0
4.0
3.0
2.0
1.0
0
$\frac{V_0}{I_T} = R_T \times 10^5$
1 2 3 4 5 6 7 8 9 10 V_0
VOLTS
-8.33
(c)

Fig. 8

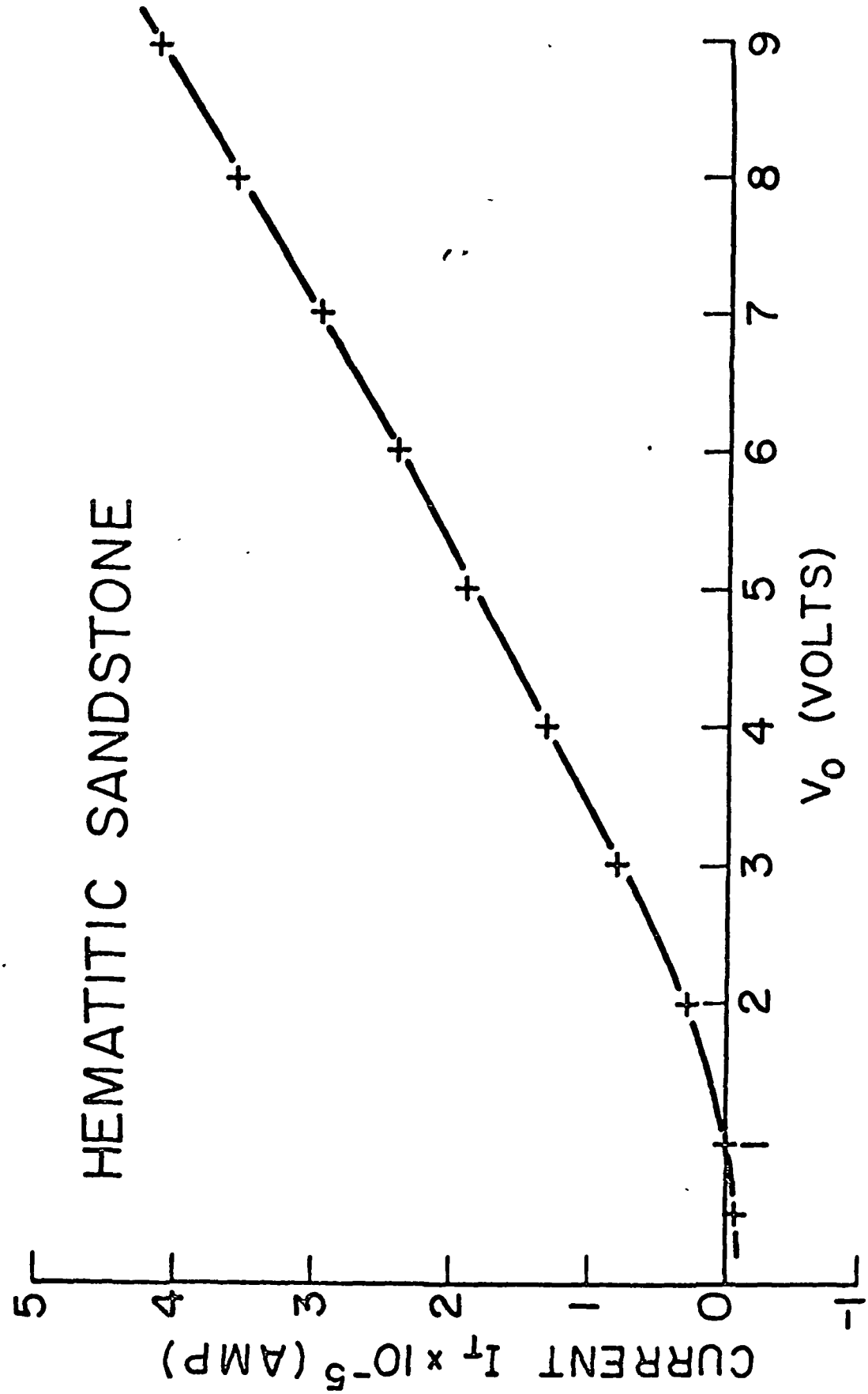
HEMATITIC SANDSTONE
CURRENT $I_T \times 10^{-5}$ (AMP)
5
4
3
2
1
0
-1
V_0 (VOLTS)
1
2
3
4
5
6
7
8
9

Fig. 8 (d)

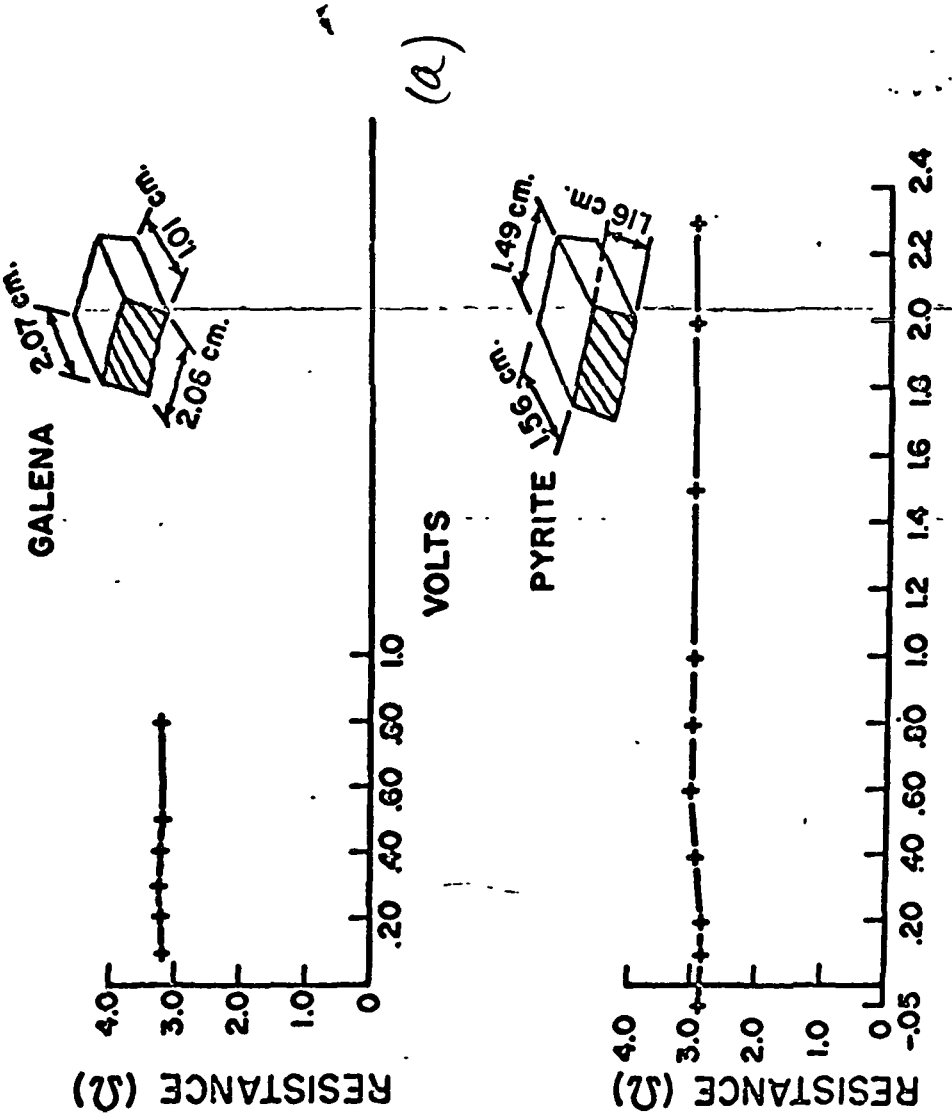

FIG. 9 ALVAREZ

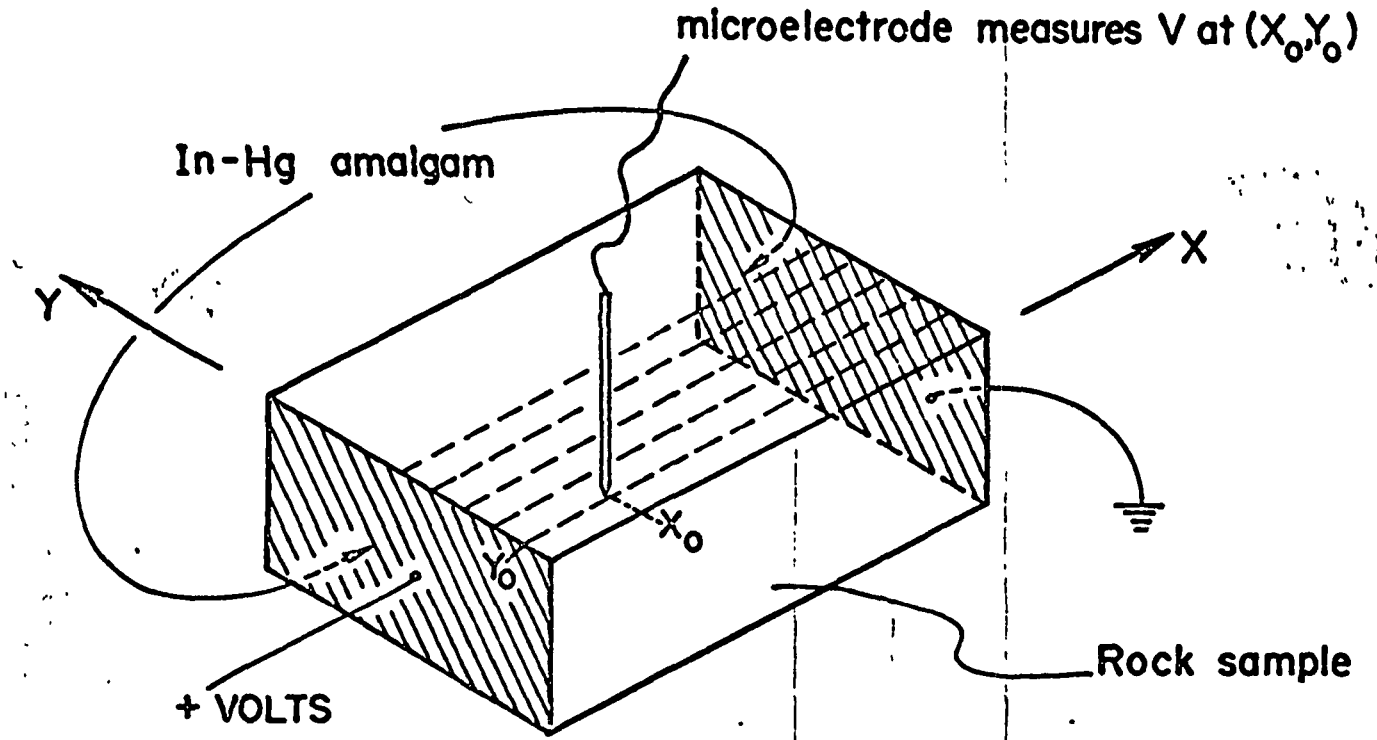

FIG. 10 ALVAREZ

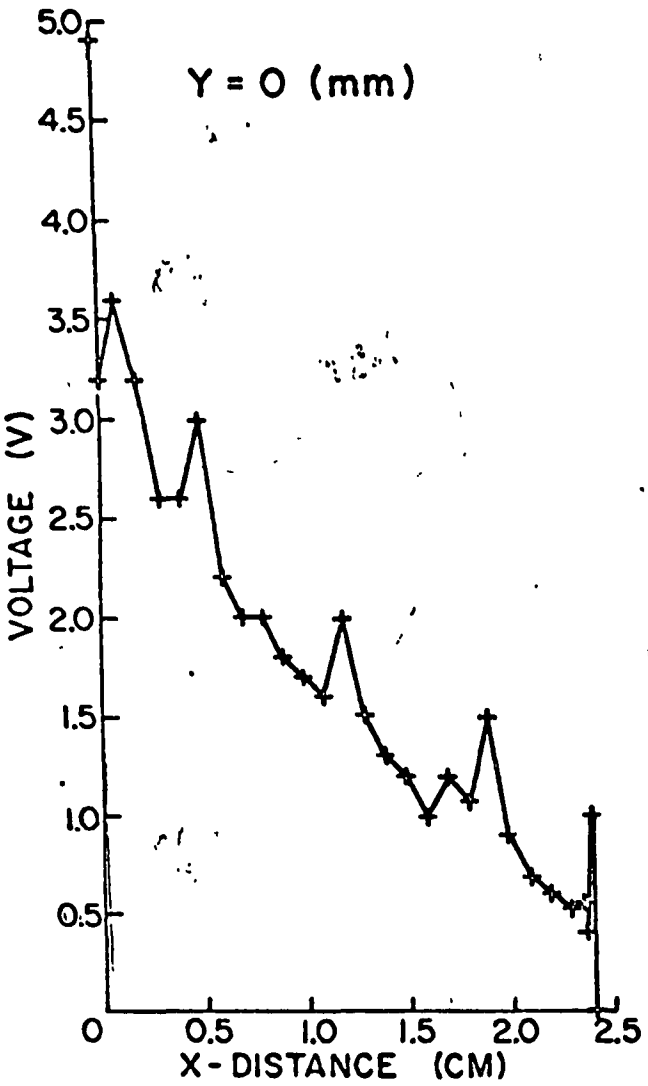
Y = 0 (mm)
VOLTAGE (V)
5.0
4.5
4.0
3.5
3.0
2.5
2.0
1.5
1.0
0.5
0
0.5
1.0
1.5
2.0
2.5
X-DISTANCE (CM)

(a)

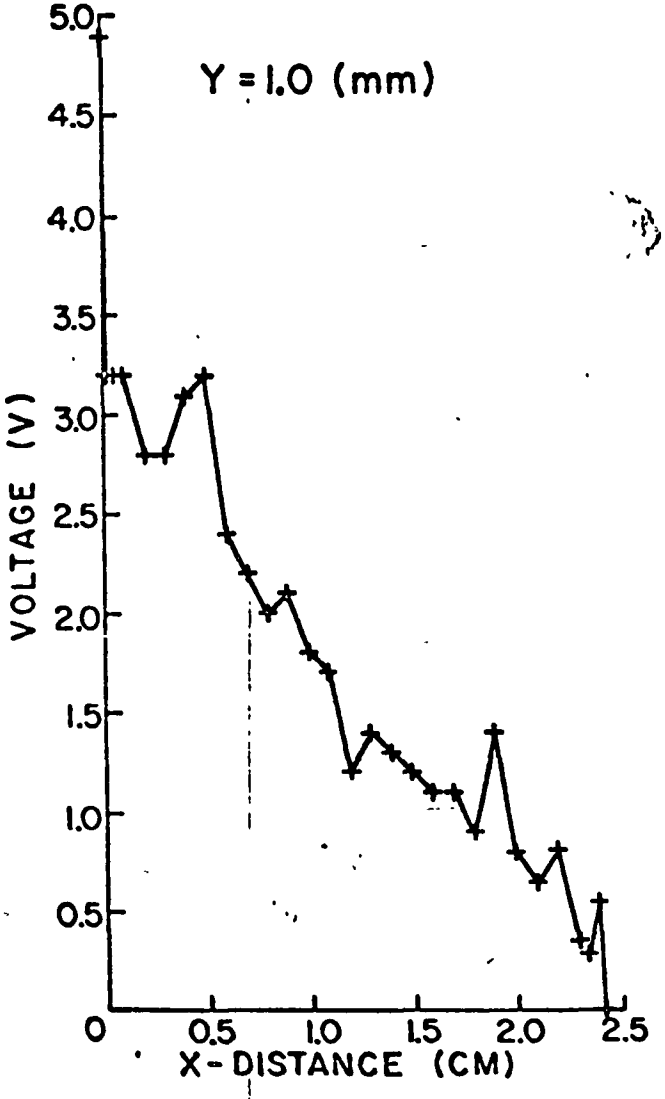
Y = 1.0 (mm)
VOLTAGE (V)
5.0
4.5
4.0
3.5
3.0
2.5
2.0
1.5
1.0
0.5
0
0.5
1.0
1.5
2.0
2.5
X-DISTANCE (CM)

(b)

FIG, 11

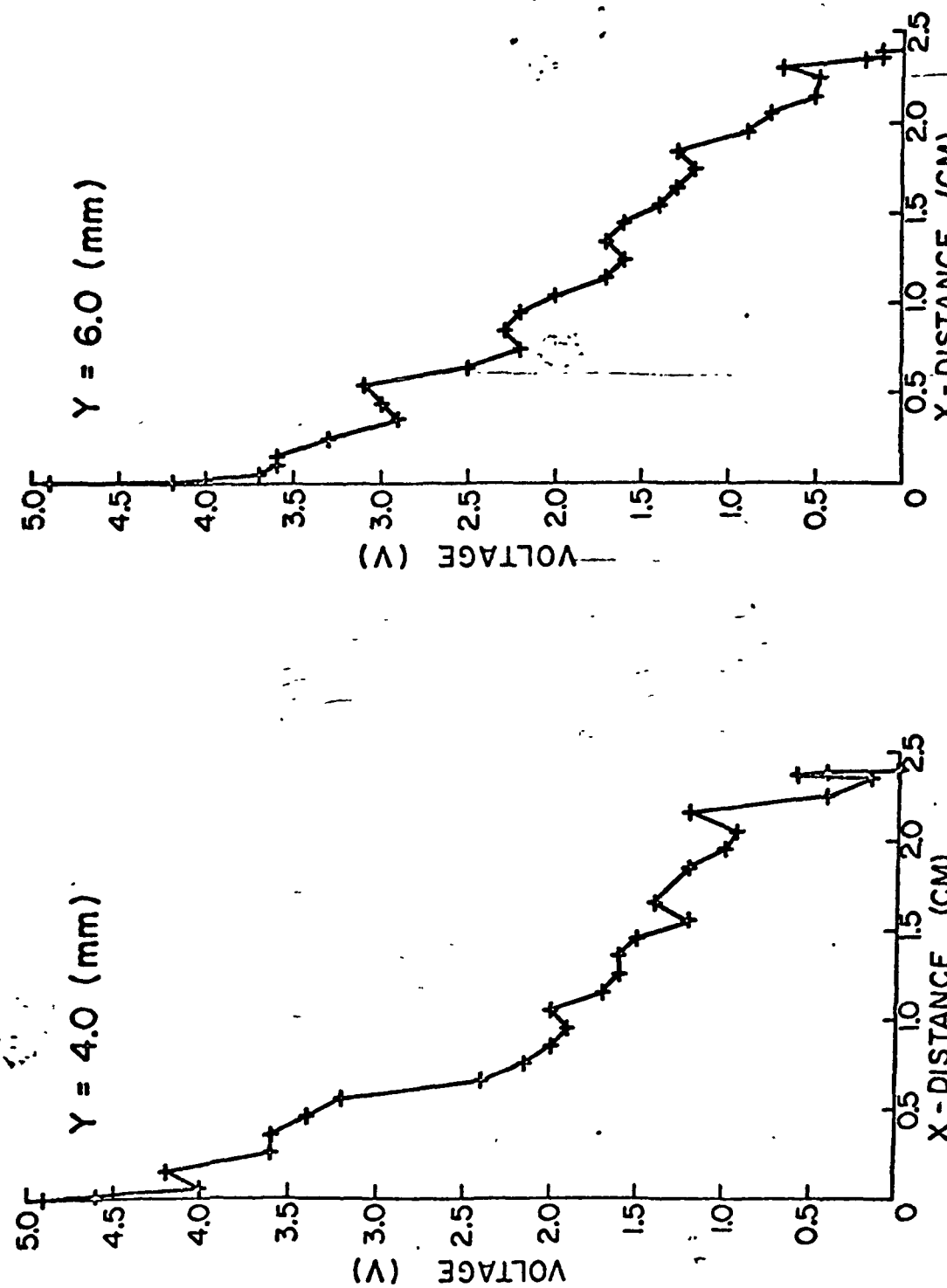
Y = 6.0 (mm)
VOLTAGE (V)
X - DISTANCE (CM)
(d)
Y = 4.0 (mm)
VOLTAGE (V)
X - DISTANCE (CM)
(c)

FIG. 11

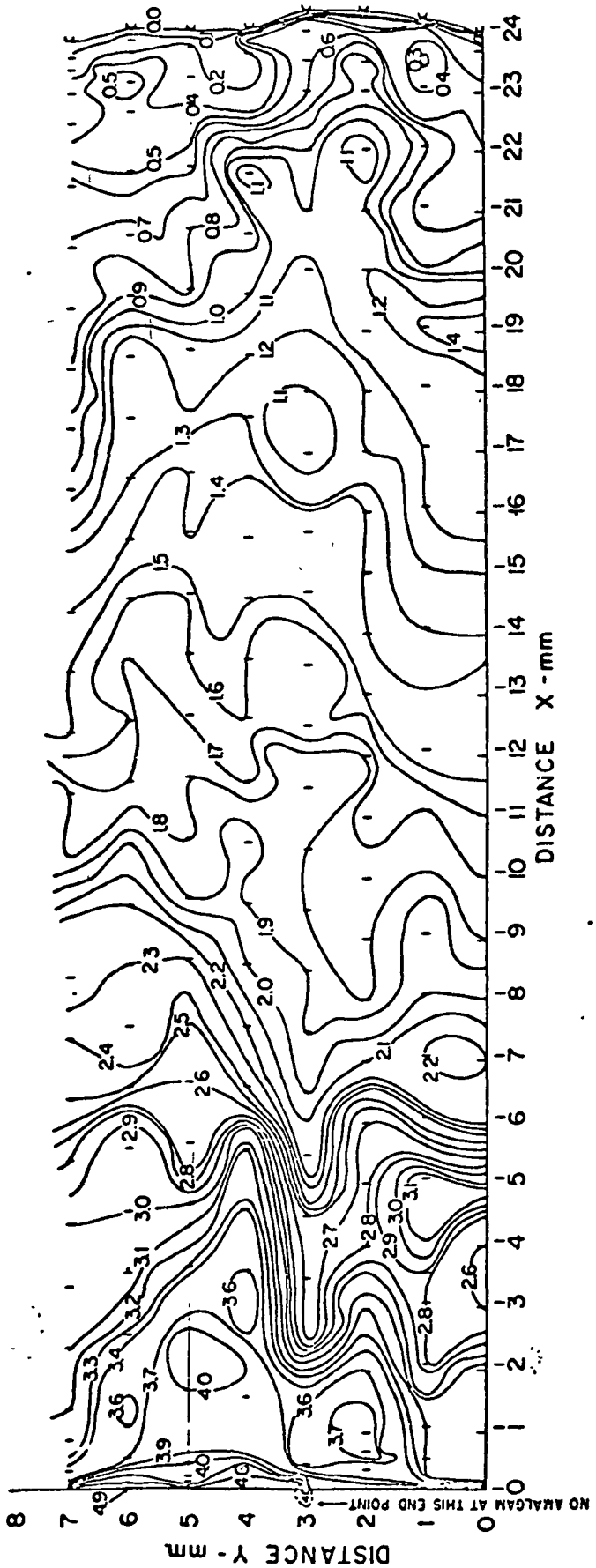

FIG, 12